1973

Growth And Radiation Survival Characteristics Of Cells In An In Vitro Tumor Model

Ralph Edward Durand

NATIONAL LIBRARY OF CANADA

CANADIAN THESES ON MICROFILM

BIBLIOTHÈQUE NATIONALE DU CANADA

THÈSES CANADIENNES SUR MICROFILM

NL-101(1/66)

GROWTH AND RADIATION SURVIVAL CHARACTERISTICS OF CELLS IN AN *IN VITRO* TUMOR MODEL

by

Ralph Edward Durand
Department of Biophysics

Submitted in partial fulfillment
of the requirements for the degree of
Doctor of Philosophy

Faculty of Graduate Studies
The University of Western Ontario
London, Canada
November 1972

ACKNOWLEDGEMENTS

The complexity and variety of the experiments described in this thesis obviously required a multiplicity of talents and several pairs of hands. The author is deeply grateful to all those who contributed in this work: to Drs. I. G. Walker and N. R. Sinclair who acted as advisors for the project; to Mr. E. C. Stroude for continued maintenance of the laboratory, supplies and equipment as well as for the histological preparations; to Dr. Bob Clattenburg for the transmission electron microscopy; to Dr. L. Johnson for the scanning electron microscopy; to Mr. John Drew for helpful discussions on computer programming, and to Mrs. Marion Alderson for preparing many of the drawings.

Special recognition is due Dr. Robert M. Sutherland who acted as chief advisor for the project.

The research was supported by the Ontario Cancer Foundation, and was carried out in the Radiobiology section of the London Clinic.

TABLE OF CONTENTS

	page
CERTIFICATE OF EXAMINATION	ii
ACKNOWLEDGEMENTS	iii
TABLE OF CONTENTS	iv
LIST OF FIGURES	vii
LIST OF TABLES	xi
ABSTRACT	xii
CHAPTER I. GENERAL INTRODUCTION	1
CHAPTER II. INTERCELLULAR CONTACT AND RADIATION SURVIVAL	6
2.1 Introduction	6
2.2 Growth and Morphology of Spheroids ..	7
2.2.1 Introduction	7
2.2.2 Methods of single cell monolayer and spheroid growth ...	7
2.2.3 Results	10
2.2.4 Summary	26
2.3 Radiation Survival of Cells in Contact	29
2.3.1 Introduction	29
2.3.2 Methods of irradiation and survival assay	29
2.3.3 Results	33
2.3.4 Summary	66
2.4 Discussion	66

CHAPTER III. CELL CYCLE REDISTRIBUTION AND RADIATION SURVIVAL 73

3.1 Introduction 73

3.2 Cell Cycle Redistribution in the Spheroid 74

3.2.1 Introduction 74

3.2.2 Methods of assessing cell cycle position in the spheroids 75

3.2.3 Results 77

3.2.4 Summary 92

3.3 Radiation Survival and Intercellular Contact at Different Stages of the Cell Cycle 95

3.3.1 Introduction 95

3.3.2 Methods of synchronizing small spheroids 96

3.3.3 Results 97

3.3.4 Summary 123

3.4 Discussion 123

CHAPTER IV. HYPOXIC CELLS AND RADIATION SURVIVAL 129

4.1 Introduction 129

4.2 Hypoxic Cells in the Spheroid 132

4.2.1 Introduction 132

4.2.2 Methods of spheroid growth under low oxygen tensions and hypoxic cell visualization .. 132

4.2.3 Results 134

4.2.4 Summary 150

4.3 Radiation Survival and Hypoxic Cells 150

4.3.1 Introduction 150

4.3.2 Methods of irradiation of large spheroids 151

4.3.3 Results 151

4.3.4 Summary 170

4.4 Discussion 173

CHAPTER V. GENERAL DISCUSSION 178

SUMMARY 188

BIBLIOGRAPHY 190

APPENDIX 1. THE CONTINUOUS CULTURING APPARATUS 214

APPENDIX 2. SURVIVAL CRITERIA AND SURVIVAL CURVE ANALYSIS 219

APPENDIX 3. CELLULAR RECOVERY FROM SUBLETHAL DAMAGE 231

APPENDIX 4. OXYGEN IN SPHEROIDS 241

VITA 259

LIST OF FIGURES

Figure	Description	Page
2.1	Gross morphological features of cells on petri dishes or in spheroids	12
2.2	Spheroid growth as a function of time	15
2.3	Scanning electron micrograph of the spheroid surface	19
2.4	Photomicrograph of sections through spheroids of different sizes	22
2.5	Electron micrograph of cells in different regions of the spheroid	25
2.6	Specialized cell junctions in the spheroid seen with the electron microscope	28
2.7	Survival of V79-171b Chinese hamster cells grown on plates and irradiated in air or nitrogen	35
2.8	Comparison of survival of single cells and day 1 spheroids irradiated in air or nitrogen	38
2.9	Survival of cells from spheroids trypsinized before irradiation	41
2.10	Survival of spheroid cells trypsinized at various times before irradiation ..	44
2.11	Kinetics of aggregation of cells into spheroids and radiation survival during the aggregation procedure	47
2.12	Survival of cells grown on petri dishes for various times	50
2.13	Relative multiplicity and radiation survival of cells regrowing from a day 8 monolayer culture	53

2.14	Survival of cells grown as day 1 spheroids or on petri dishes and irradiated at 4°C	57
2.15	Survival of cells from day 1 spheroids as a function of treatment at different temperatures	60
2.16	Survival of day 1 spheroids plated intact, or trypsinized to respread the cells after plating	65
3.1	Photomicrograph of autoradiographic sections of spheroids exposed to ^{3}H-thymidine for 48 hours	79
3.2	Mitotic and labelling indices of spheroids as a function of age	84
3.3	Mitotic and labelling indices of cells regrowing from a large spheroid during the regrowth interval	87
3.4	Cell size distributions and DNA and RNA content in cells grown as spheroid cells, or on petri dishes	89
3.5	Photomicrograph of ^{3}H-thymidine labelled spheroid	94
3.6	Survival of cells from spheroids of various sizes irradiated in air	99
3.7	Survival of irradiated, non-S phase cells of spheroids of various sizes ..	102
3.8	Multiplicity and radiation survival of cells regrowing from a large spheroid	105
3.9	Characterization of colcemid-synchronized day 1 spheroids	108
3.10	Radiation survival of single cells from plates or of day 1 spheroid synchronized cells at various stages of the cell cycle	113
3.11	Recovery of day 1 spheroid or single cells from sublethal damage	116

3.12	Recovery of synchronous cells from plates after irradiation	119
3.13	Theoretical synthesis of two-component survival curve	122
4.1	Photomicrograph of morphological organization of the C3HBA mouse mammary carcinoma	136
4.2	Photomicrograph of a human lung metastases	139
4.3	Growth of large spheroids under metabolite deprivation	142
4.4	Demonstration of hypoxic cells in a photomicrograph prepared by autoradiographic labelling of hypoxic cells .	146
4.5	Photomicrograph of a section from a very large spheroid	149
4.6	Radiation survival of spheroids developing hypoxic cells	154
4.7	Radiation survival of large spheroids under conditions of reduced oxygen and reduced temperature	156
4.8	Radiation survival of a large spheroid in comparison to single cells growing on petri dishes	160
4.9	Survival of cells from spheroids irradiated in nitrogen, with S-phase cells selectively removed after the irradiation	163
4.10	Survival of either non-S cells or all cells from large spheroids irradiated at 37°C or at 24°C	166
4.11	Specific sensitization of hypoxic cells using PNAP	169
4.12	Theoretical synthesis of multicomponent survival curves of large spheroids	172

A1.1	Schematic diagram of the continuous culturing apparatus	216
A2.1	Survival curve parameters	222
A2.2	Survival of mixed cell populations ...	227
A3.1	Recovery from sublethal radiation damage at 37°C and 24°C	234
A3.2	Theoretical derivation of recovery ...	238
A4.1	Oxygen concentrations in spheroids at different spheroid densities	250
A4.2	Oxygen concentrations in spheroids under typical irradiation conditions .	253
A4.3	Oxygen concentrations in spheroids under crowded irradiation, or high dose rate irradiation conditions	256

LIST OF TABLES

Table	Description	Page
1	Thickness of viable rim of cells in spheroids under different growth conditions	143
2	Summary of survival curve parameters .	174
3	Symbols and units for oxygen diffusion calculations	243

ABSTRACT

The crowded growth conditions, altered blood supply and lack of growth regulation of many solid tumors produces a cell population heterogeneous in morphology, proliferation kinetics, oxygenation and nutrition. The influence of these factors on cell growth and radiation survival characteristics can easily be studied using an *in vitro* suspension culturing technique that produces multicellular 'spheroids' of complexity intermediate to standard cell cultures and animal tumors. Spheroids of V79-171b Chinese hamster cells had growth kinetics similar to many solid tumors, and a decreasing growth fraction and accumulation of a partially synchronous, internal population of pre-DNA synthesis cells (hereafter called G_0 cells) were demonstrated autoradiographically and with a microfluorometer. Development of central necrosis was dependent on available metabolites, and under optimal conditions of nutrition the viable rim of cells was found to vary as the square root of oxygen concentration, in agreement with theoretical predictions. Electron microscopy showed that 'close' and 'tight' junctions developed, as did intercellular contacts similar to desmosomes.

Irradiated spheroids were reduced to single cells by trypsinization, and survival was assayed by colony

formation. Cells grown in contact for as little as one day developed a higher capacity for accumulation of sublethal radiation damage as reflected by survival curves with extrapolation numbers (and hence survival at large doses) increased by 15-fold. These small spheroids were demonstrated to contain exponentially growing, well oxygenated cells, and could be synchronized by exposure to colcemid. Irradiation of synchronized spheroids showed that the contact effects were variable through the cell cycle, and that recovery from sublethal radiation damage was maximum at late S phase. The G_0 population that developed in larger spheroids was found to be relatively radiosensitive, as were early G_1 phase synchronous spheroids. However, in very large spheroids, the internal G_0 cells became hypoxic and thus highly radioresistant. Large spheroids thus contained cells in three subpopulations which could be selectively studied by killing cycling S phase cells with hydroxyurea, or by varying the fraction of hypoxic cells by changing the oxygen tension in the growth medium, varying the temperature to alter oxygen consumption, reoxygenating the cells by reducing the spheroid to single cells, or by specific sensitization of the hypoxic cells with electron affinic chemicals.

Spheroids thus contain cells growing under conditions of oxygenation, nutrition and intercellular contact

similar to many solid *in vivo* tumors. In addition, the ability to maintain precise growth and irradiation conditions plus the fact that survival of individual cells can be studied suggest that spheroids provide a tumor model of unique potential for determining proliferation and survival characteristics of therapeutically treated or untreated cells.

I. GENERAL INTRODUCTION

Clinical treatment of cancer patients has developed empirically, and the appropriate treatment of the individual patient is now largely a matter of judgement based on the related experience of the treating physicians. One of the more common treatments, radiotherapy, is also one of the most empirical. This is not a recent development, as the observations of tissue injury that resulted from ignorance of the biological effects of X-rays likely contributed as much to the development of early radiotherapy as did actual controlled experiments. Although the vast advances that have since been made in radiotherapy may be considered to be proof of the value of the empirical approach, they also demonstrate its inherent limitations. Recent advances have been mainly technological, that is, development of machines having beams of more densely ionizing or higher energy radiation. Lack of purely scientific progress has, however, led many prominent therapists to speculate that radiotherapy may have reached an impasse (Revesz 1968, Mitchell 1968) which will be overcome only when more rational treatments can be initiated, based on an analytical understanding of biological effects of radiation at the cellular level.

In the past, experimental radiotherapy has been

largely restricted to the study of only a few types of malignancies in rodents, such as lymphoma and leukemia cells, and tumors either growing in ascites fluid or as solid carcinomas, hepatomas, or sarcomas. Survival of individual normal or tumor cells after treatment has been assayed in the animal by many techniques (Hewitt and Wilson 1959, Till and McCulloch 1961, Kember 1963, Bush and Bruce 1965, Withers 1966, Withers and Elkind 1969 and 1970, Lindop 1970, Potten and Chase 1970), but the procedures involved were rather laborious and time consuming. Unfortunately, tumor cell responses to radiotherapy can be altered by many factors, including host-cell immune reactions, systemic responses of the host, assimilation or dissimilation of nutritive or toxic materials or both, cellular interactions, changes in cell cycle times or distributions, and variations in local oxygen tensions or concentrations of other modifying agents. Whether or not a tumor can be 'cured' by radiation thus reflects the net contribution of all these factors rather than the biological effect of the radiation alone on the individual cell *in situ*.

Quantitative assessment of cellular survival after exposure to radiation *in vitro* was first demonstrated by Puck and Marcus (1956). Extensive reviews of the radio-

biology (Elkind and Whitmore 1967, Fabricant 1972) and the radiation biochemistry (Okada 1970) of mammalian cells *in vitro* are now available. There are numerous advantages to *in vitro* systems, in that cells can be maintained in a more or less ideal environment, free from immunological and other host-induced interactions. Oxygenation and local concentrations of other agents which may modify radiation response can be precisely controlled, and experiments can be performed relatively easily, economically, and rapidly.

The use of *in vitro* systems, despite the obvious advantages, is limited by the lack of complexity. As an example, suppose that malignant cells growing *in vivo* in ascites fluid could be grown equally well in suspension *in vitro*, under similar conditions of cell crowding and nutrition. Analysis of cell survival after radiation exposure would define the cellular response under each growth condition, and comparison of the responses would provide insight into the immunological and systemic contributions of the host during the radiation treatment. Although comparison of the results obtained *in vitro* and *in vivo* would be valuable and enlightening in the previous instance, one can hardly rationalize the extrapolation of data obtained with single cells *in vitro* to the case of a solid tumor *in vivo*. Most solid tumors are thought to

be composed of cells in at least two distinct states of markedly different responses to radiation (Thomlinson and Gray 1955, Tannock 1968 and 1970): cells with adequate nutrients which are actively proliferating; and cells more distant to the blood supply which proliferate more slowly due to deprivation of essential metabolites including, at large distances, oxygen.

Approximation of these conditions for in vitro experimentation has usually been achieved by growing cells under ideal conditions until treatment, and then abruptly subjecting the cells to synchronizing agents or oxygen-free atmospheres. Growth of cells to confluence, where normal cell multiplication is inhibited even in the presence of adequate nutrients, may be the best in vitro simulation of solid tumors that can be obtained with conventional cell culturing techniques (Hahn et al 1968, Berry et al 1970). Unfortunately, even confluent monolayers may still lack at least three important features of the in vivo solid tumor: extensive, three-dimensional intercellular contact; interaction of populations of cells cycling with different generation times; and gradual spontaneous development of differing metabolic environments due to diffusion limitations.

An in vitro system of increased complexity, in which cells are grown as three-dimensional colonies in semi-

solid medium (Dalen and Burki 1971, Shinohara and Okada 1972), or in normal medium in suspension culture as multicellular 'spheroids' (Sutherland et al 1971) may provide potentially useful *in vitro* models of some solid tumors. Spheroids are particularly attractive, as they have been demonstrated to have a morphological resemblance to some nodular carcinomas (Sutherland et al 1971), grow in a comparable manner (Inch et al 1970), and exhibit a multicomponent radiation survival curve similar to many *in vivo* tumors (Sutherland et al 1970).

The remaining chapters of this thesis demonstrate that the spheroid represents a model which allows better analysis of the biological effects of radiation at the cellular level for cells grown in a tumor-like environment, thus providing a possible system which may contribute to the development of a more rational basis for optimizing radiotherapy and possibly chemotherapy procedures. Chapter II contains evidence that the spheroids grow with cells close enough together to form intercellular junctions, and the effects of this close contact on survival after irradiation is examined. Development of a slowly-cycling population of cells and their survival after irradiation are shown in Chapter III, and Chapter IV demonstrates that highly radioresistant hypoxic cells develop spontaneously in large spheroids.

II. INTERCELLULAR CONTACT AND RADIATION SURVIVAL

2.1 Introduction

The first and most apparent difference between spheroids and conventional tissue culture systems is the fact that spheroid cells grow under conditions of extensive three-dimensional intercellular contact, which more closely simulates that of organized tissues. Although multicellular structures *in vitro* have previously been grown to determine cellular aggregation rates (Moscona 1961, Moskowitz 1963 and 1964) and their correlation with malignancy (Dodson 1966, Halpern et al 1966), the first recognition that such aggregates might serve as potentially valuable models of nodular carcinomas was made by Sutherland et al (1971).

It is extremely difficult to predict the effects of intercellular contact *per se* on the radiosensitivity of mammalian cells. A basic premise of cellular radiobiology has been the concept that cells survive radiation independently, that is, they are not influenced by neighboring cells (reviewed in Elkind and Whitmore 1967). However, results obtained by Froese (1967) and Aoyama and Rixon (1967) suggest that irradiated cells may be influenced by neighboring cells during the post-irradiation period. In addition, it is well known that cells

in organized tissues *in vivo* often have an increased survival after radiation in comparison to similar cells irradiated after growth *in vitro* (Alper 1972, Hornsey 1972a and 1972b). Hornsey has recently reviewed this phenomenon (1972b), where she also indicated the consequences of these observations to radiotherapy. Spheroids can be grown under culturing conditions where only physical geometry differs from normal growth of single cells on petri dishes, thus providing a system where intercellular contact effects on radiation survival can be easily studied.

2.2 Growth and Morphology of Spheroids

2.2.1 Introduction

The remainder of this section will present evidence that multicellular spheroids do in fact provide a reasonable model of cells in organized tissues (in terms of intercellular contact), and, as such, might be expected to respond to radiation in a manner similar to many organized tissues *in vivo*.

2.2.2 Methods of single cell monolayer and spheroid growth

All results presented in this thesis have been obtained with only one established line of cells, the non-malignant V79-171 strain of Chinese hamster lung cells.

This particular line was obtained from Dr. W. K. Sinclair and was subcloned twice in this laboratory, that is, the population was homogenized by selection and subsequent growth of a single cell (hence the line will be hereafter designated V79-171b). The cells were normally maintained by serial transplantation twice weekly, using Eagle's basal medium (BME) containing 1% L-glutamine (v/v), penicillin (100 I.U./ml) and streptomycin (.1 mgm/ml). Fetal calf serum (FCS) was also added depending upon the particular growth conditions required, and for most cases 15% (v/v) was used. All components of the medium were purchased from Grand Island Biological Company (GIBCO).

The cells were grown as monolayers attached to 100 mm Falcon plastic tissue culture dishes at 37°C in a humidified atmosphere of 3% CO_2 in air. Cells were typically removed from growth plates by aspiration of the growth medium, rinsing with warm (37°C) trypsin (GIBCO lyophilized 1:250) at a concentration of .25% in a citrate-saline buffer, and incubating in 4 ml of trypsin for an additional 8 minutes. The citrate-saline buffer (pH=7.3) was prepared by adding 10.0 gm KCl and 4.4 gm $Na_3C_6H_5O_7 \cdot H_2O$ to 1.0 liter of distilled water. Trypsinization was terminated by adding an equal quantity of whole medium (BME + FCS), and pipetting the cells gently up and down to give single cells. The multiplicity, or number of cells per

group, routinely obtained was 1.0 .

Spheroids were grown in spinner flasks (flasks with an internal magnetic stirring bar driven by an external magnet at about 180 rpm) in medium identical to normal growth medium with the exception that the serum was reduced in concentration to 5% (v/v). The spinner flasks were flushed with 3% CO_2 in air after adding the medium, and allowed to equilibrate to 37°C before adding cells. The initial inoculum of 10^4 cells/ml (except where specified otherwise) was prepared as for normal serial dilution of the stock cells. Fresh medium was typically added to the flask on the fourth day and every second day thereafter by allowing the spheroids to sediment to the bottom of the flask, aspirating off about 2/3 of the medium, and replacing it with fresh, warm medium. A detailed description of spheroid growth in the continuous culturing apparatus used for large experiments is given in Appendix 1.

Spheroids were counted or sized manually using an inverted microscope with a scale in the eyepiece. The size of a spheroid was determined by recording the diameter of the spheroid for two measurements at right angles, and then calculating the geometric mean diameter. After twenty or more spheroids were observed, the mean diameter of the population of spheroids was calculated.

Representative spheroids for light microscopy studies were fixed in phosphate-buffered formalin, dehydrated, and embedded in paraffin. Serial sections (5 microns thick) were cut and stained with hematoxylin and eosin. Spheroids were fixed for electron microscopy in 3.3% glutaraldehyde buffered to pH 7.2 with .1 M phosphate buffer. They were then postfixed in osmium tetroxide, dehydrated in a graded series of alcohols, and embedded in Epon. Thin sections were stained with uranyl acetate and lead citrate and examined with an AEI 6 electron microscope. Samples for scanning electron microscopy were fixed in 4% glutaraldehyde, vacuum dried, and coated with a gold-palladium (80-20) alloy prior to observation.

2.2.3 Results

The basic differences between the multicellular spheroid system and conventional monolayer growth of the V79-171b cell line are shown in figure 2.1 . Panel (a) shows the typical appearance of these cells growing on plates. In contrast, the spheroids of panels (b) to (f) have a highly ordered structure, with increasing homogeneity of size as the spheroids enlarged. The compactness of the spheroids is illustrated by the spheroid of figure 2.1f, which was .47 mm in diameter and contained about 10^5 cells. Large spheroids sedimented rapidly at unit gravity in the absence of agitation, whereas smaller spheroids and single cells sed-

FIGURE 2.1

Photomicrograph of Chinese hamster V79-171b cells growing as single cells on a petri dish (a) or as spheroids of increasing sizes (b) to (f).
Magnification: (a) X 185 ; (b) - (f) X 75

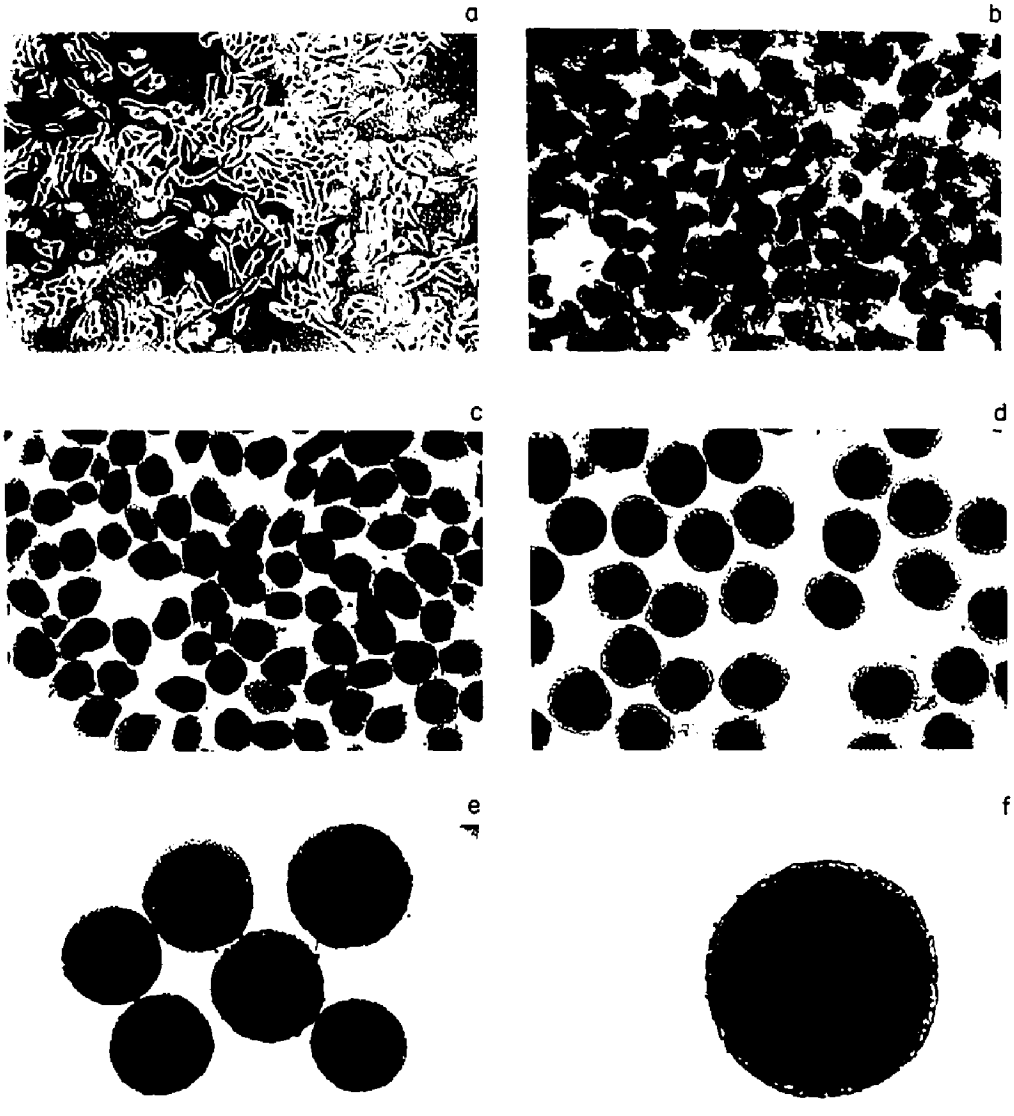
a
b
c
d
e
f

imented much more slowly. This provided a method of obtaining a very homogeneous population of spheroids, by allowing the larger spheroids to settle out, and removing the smaller ones in the supernatant. Even in the absence of this treatment or 'purification', fairly good homogeneity was apparent, especially at intermediate sizes as in panels (c) and (d).

Although no direct experiments on the degree of intercellular contact, or rather, the 'bonding-strength' of neighboring cells were performed, two conclusions could still be drawn on the basis of repeated microscopic observation. As seen in figure 2.1, very few single or unattached groups of cells were noted. In addition, when the spheroids were pipetted up and down or otherwise mechanically disturbed, little change in the number of free cells was noted. These observations indicated that the cells were very tightly held together.

A more quantitative description of spheroid growth for several experiments is shown in figure 2.2, where spheroid volume, spheroid diameter, or approximate cell number per spheroid was plotted as a function of time in culture. The approximate cell number per spheroid was calculated from the volume measurement, where it was assumed that a single cell had a diameter of 12 microns. This calculation was also found to agree well with the

FIGURE 2.2

Growth of multicellular spheroids as a function of time in culture. Error bars represent standard errors of the mean sizes. Different growth patterns were due to different initial numbers of cells/ml, and different feeding intervals.

Symbol	Initial Inoculum	Feeding Schedule
X	1.5×10^4	Daily +
●	10^4	2 days
o	2.0×10^4	2 days
■	10^4	Continuous

All experimental curves can be related to each of the three ordinates (see text).

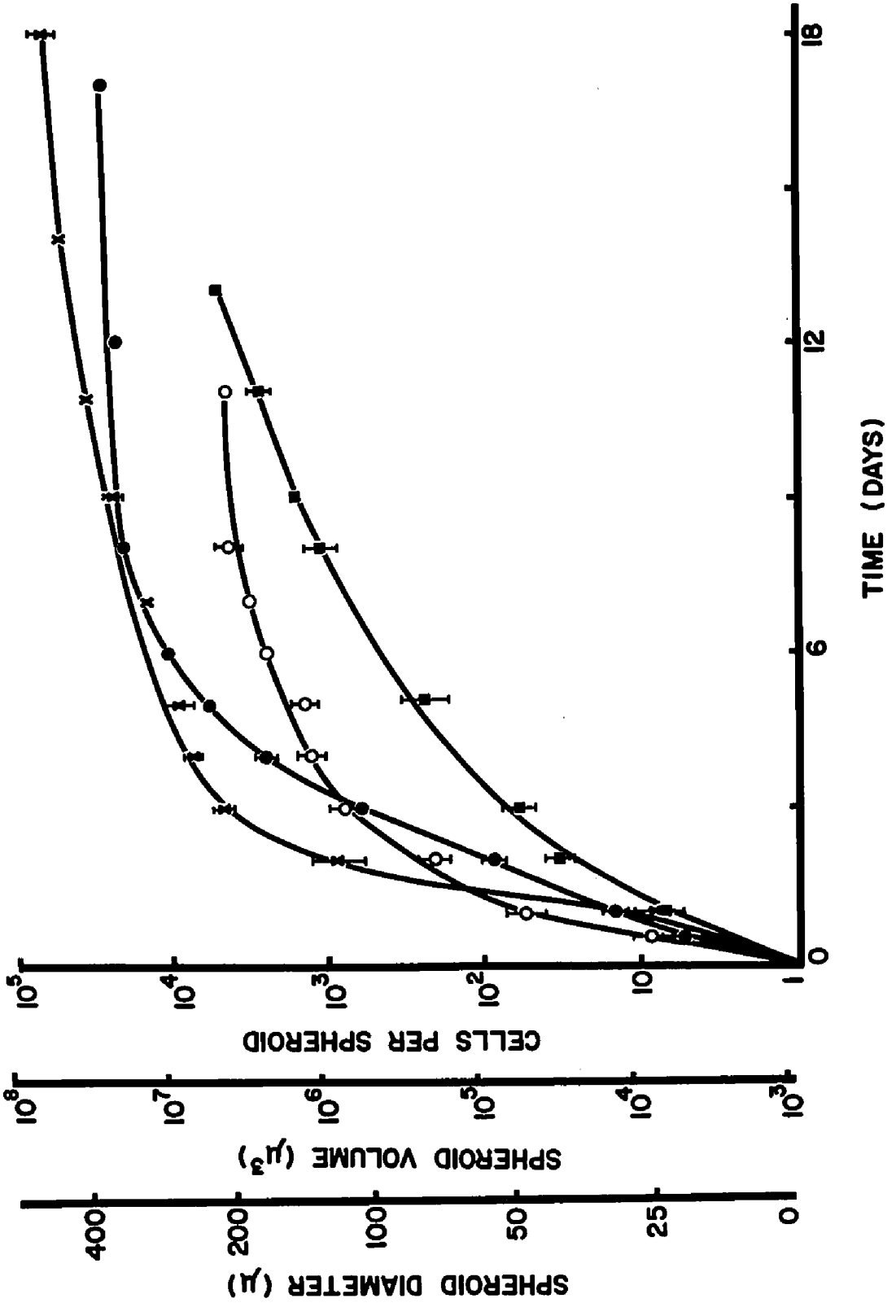
SPHEROID DIAMETER (μ)
0
25
50
100
200
400
SPHEROID VOLUME (μ³)
10³
10⁴
10⁵
10⁶
10⁷
10⁸
CELLS PER SPHEROID
1
10
10²
10³
10⁴
10⁵
0
6
12
18
TIME (DAYS)

actual number of cells counted electronically when a known number of spheroids of a given size were reduced to single cells by treatment with trypsin (see section 2.3.2).

Although the growth curves were obviously quantitatively different for the experiments, the qualitative features of an initial rapid growth followed by a retarded growth phase were common to all curves. The rapid initial increase in size could not be attributed to growth alone, as a spheroid typically increased its volume by a factor of 10 in the first 24 hours, whereas the number of cells/ml increased by no more than a factor of four. This suggested that the initial portion of the curves represented both growth and aggregation of cells. Other evidence for cellular aggregation is apparent from closer examination of figure 2.2, where spheroid size increased more rapidly initially when a higher initial number of cells was placed in the flask. It was also repeatedly observed that increasing the serum (FCS) concentration resulted in more initial aggregation, as did decreasing the speed of the spinner bar in the flasks, but detailed experiments to characterize these effects were not performed.

In the same way that the initial characteristics of the growth curves of figure 2.2 were determined almost

exclusively by the number of cells placed in the flasks, the later portions of the curve were primarily determined by the feeding schedule. For the one experiment in which the cells were fed daily or more often as required, the spheroids did not reach a growth plateau, but kept increasing in size over the entire course of the experiment as predicted theoretically for diffusion dependent growth (Burton 1966). Less frequent feeding reduced the comparative size of the spheroids, and was probably responsible for the apparent growth plateau in two of the curves of figure 2.2 (see also section 4.2.3).

The degree of intercellular contact necessary for spheroid growth can be visualized more easily in the scanning electron micrograph of figure 2.3 . Panel (a) shows that the cells were rigidly held in place. Higher magnification suggested that some of the external cells had fibroblastic characteristics, that is, they tended to spread over the surface of the spheroid much the same as single cells spread across a plate as in figure 2.1a.

The topology of the spheroid in panels (c) and (d) shows some interesting features. An apparent surface coat can be seen, which probably contributes to maintaining the spheroid structure. The external cells have occasional microprojections, and in panel (d) several microdepressions are also evident. Other culture tech-

FIGURE 2.3

Scanning electron micrograph of 380 micron diameter spheroid.

Magnification: (a) X 100 ; (b) X 1000 ; (c) X 500 ; (d) X 2000

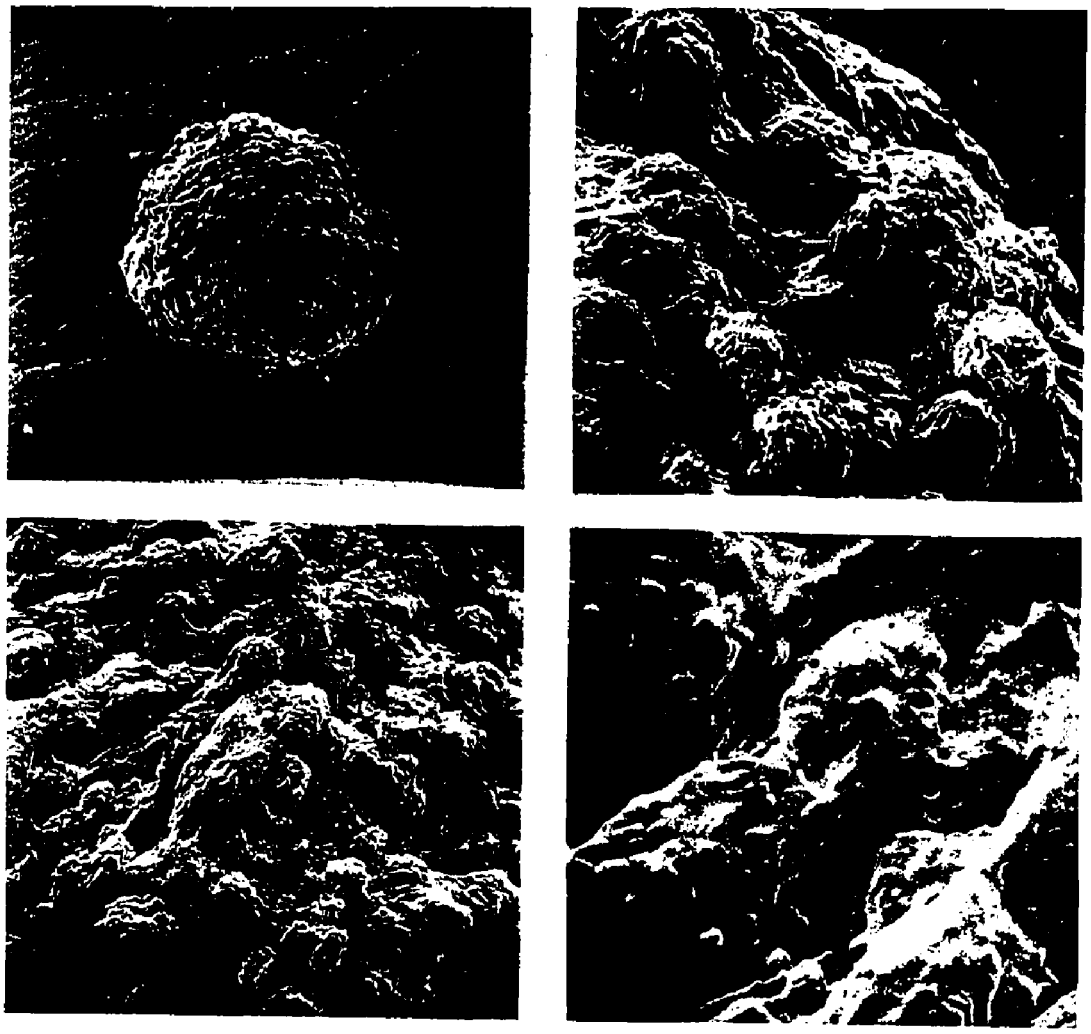

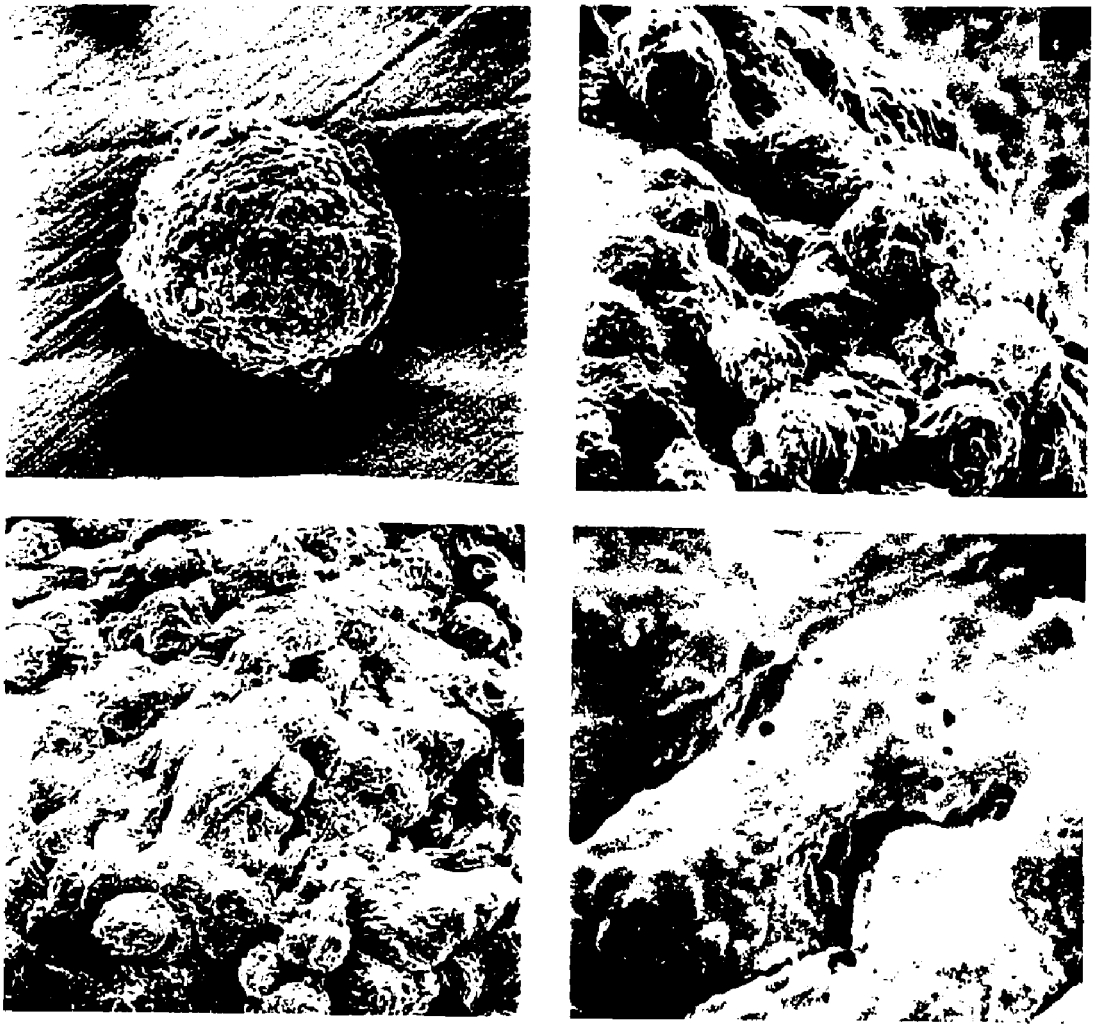

niques have produced aggregates of malignant cells (Dalen and Burki 1971) which, in contrast to figure 2.3, were extremely loose structures. Although those cells were forced to grow in close apposition, the contact apparent here was not seen under the other culturing conditions.

More structural detail can be seen in figure 2.4, which shows histological sections from three spheroids. Although the spheroids of figure 2.4 appear to be three spheroids of different sizes, the sections are in fact from three spheroids of essentially equal diameters. The smallest section was actually a peripheral section, while the larger sections were from more central regions of other spheroids as determined by following the same spheroid in several serial sections. Histological observation of numerous spheroids of various sizes has shown that these sections do, however, accurately represent sections from spheroids of various sizes.

Several features are apparent in the sections of figure 2.4 . The cells were tightly packed together, and examination of slides at higher magnification showed that intercellular material, probably a mucopolysaccharide substance, was found between many cells. Central necrosis developed gradually with time in culture, and quantitative experiments showed that necrosis first devel-

FIGURE 2.4

Photomicrograph of sections through three spheroids. Note progressive development of central necrosis, also fibroblastic external cells and lightly staining internal cells.

Magnification: X 165

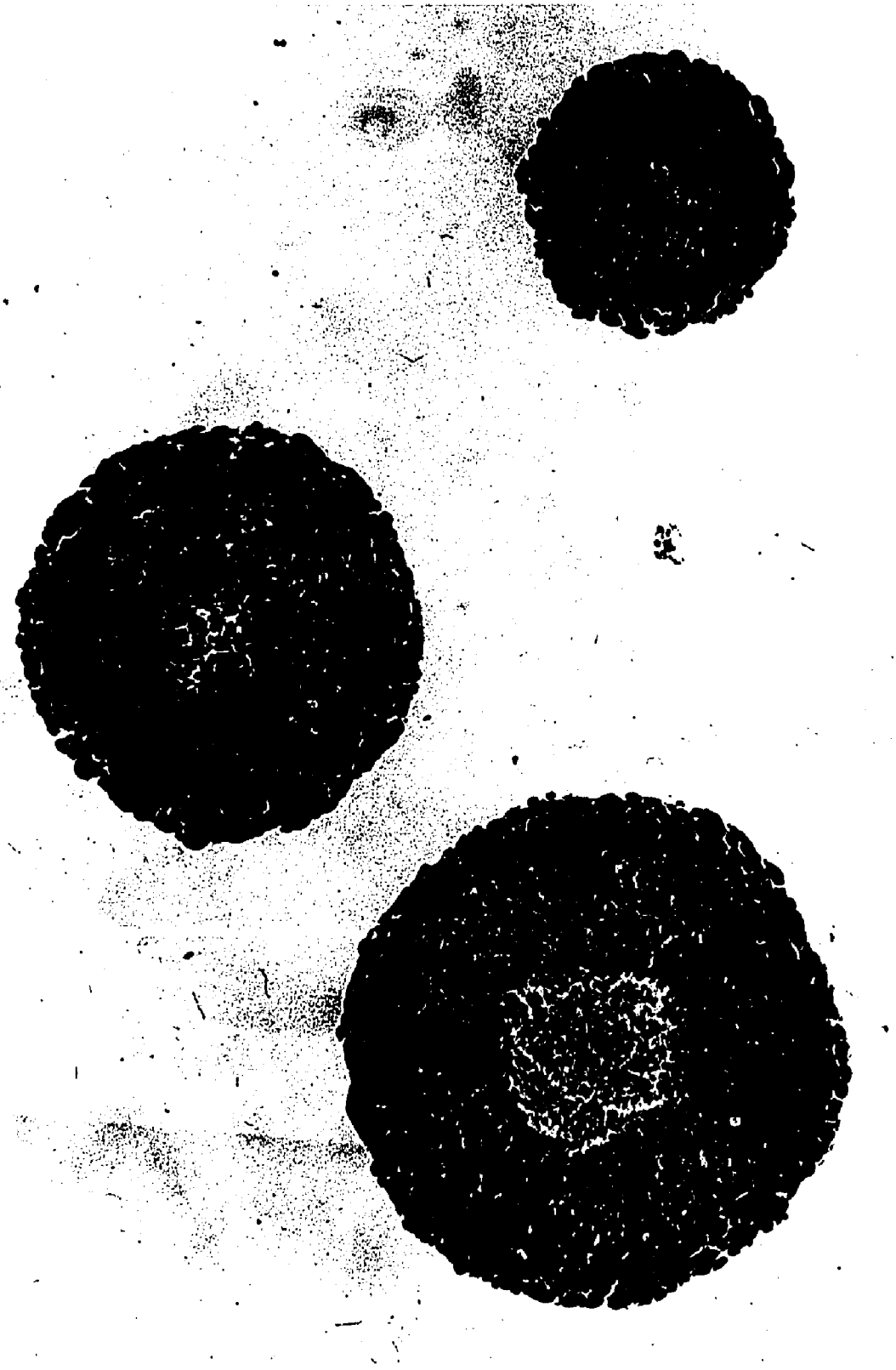

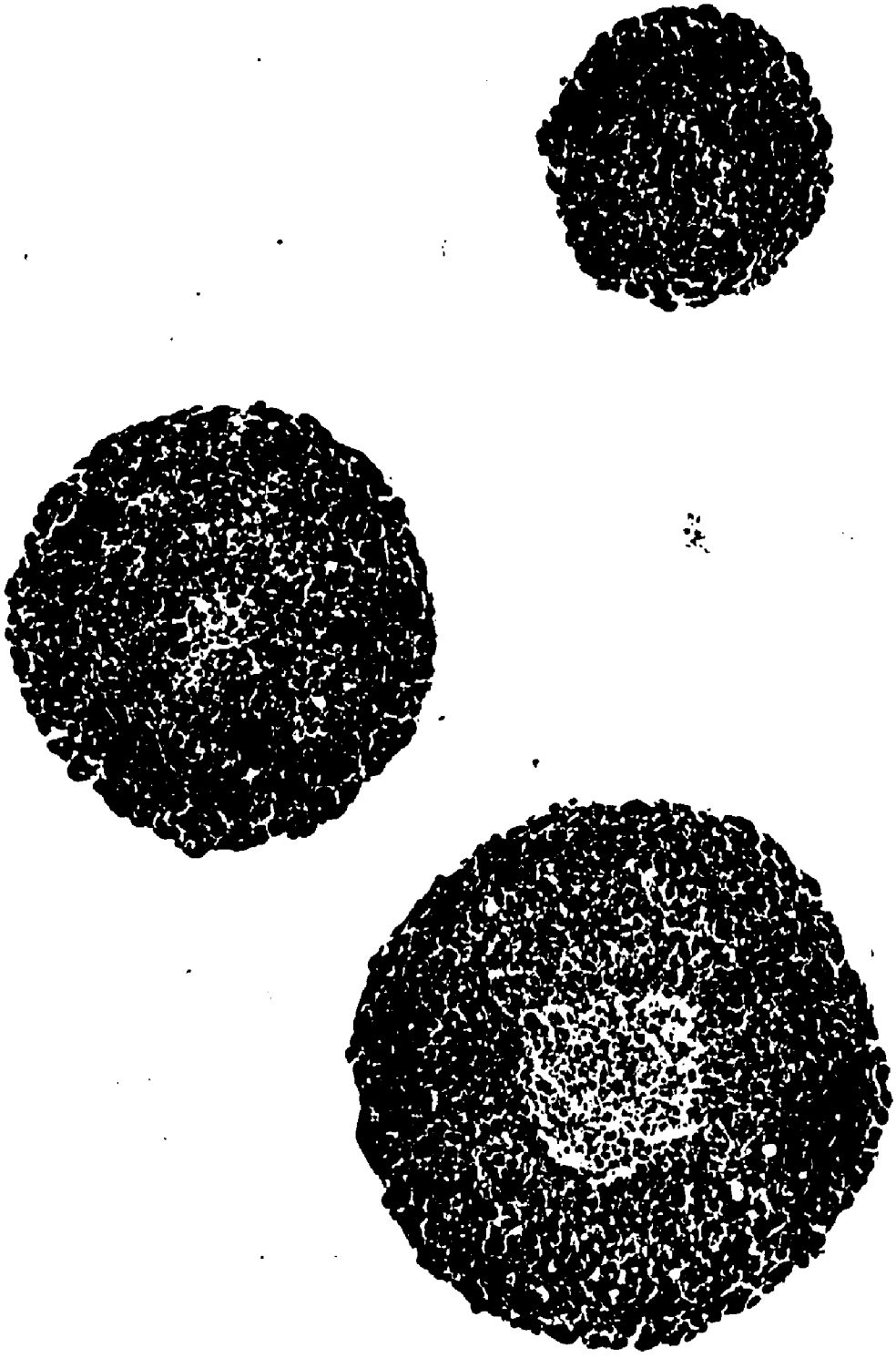

oped in spheroids of 250-360 microns in diameter, depending on their nutritional state. Quantitative experiments relating the appearance of central necrosis to various growth conditions are described in section 4.2.3 .

Many unique features of the spheroid can be seen in the electron micrographs of figure 2.5 . Cells near the periphery had relatively large intercellular spaces (figure 2.5a), whereas the internal cells (figure 2.5b) were more crowded and usually had electron dense material in the intercellular spaces. All cells appeared to be metabolically active with numerous mitochondria (m) and ribosomes, although the peripheral cells generally had more of these organelles and thus may have been somewhat more metabolically active.

Several characteristics were common to all cells of the spheroid. Vacuoles of various types (v) appeared in many cells, and became very abundant in cells bordering necrotic regions. Microprojections (p) were seen both on the external cell surfaces and in the intercellular areas between internal cells. Many of the cells appeared to be synthesizing some type of secretion product, which can be seen inside dilated endoplasmic reticulum (e) and may be related to the electron dense intercellular

FIGURE 2.5

Electron micrographs of (a) cells near the edge of a large spheroid, and (b) cells from an internal region. Dilated endoplasmic reticulum (e) containing an electron dense product can be seen in both sections, as can microprojections (p), various types of vacuoles (v), mitochondria (m), intercellular products (c) and areas of close contact (j). Magnification: X 4500

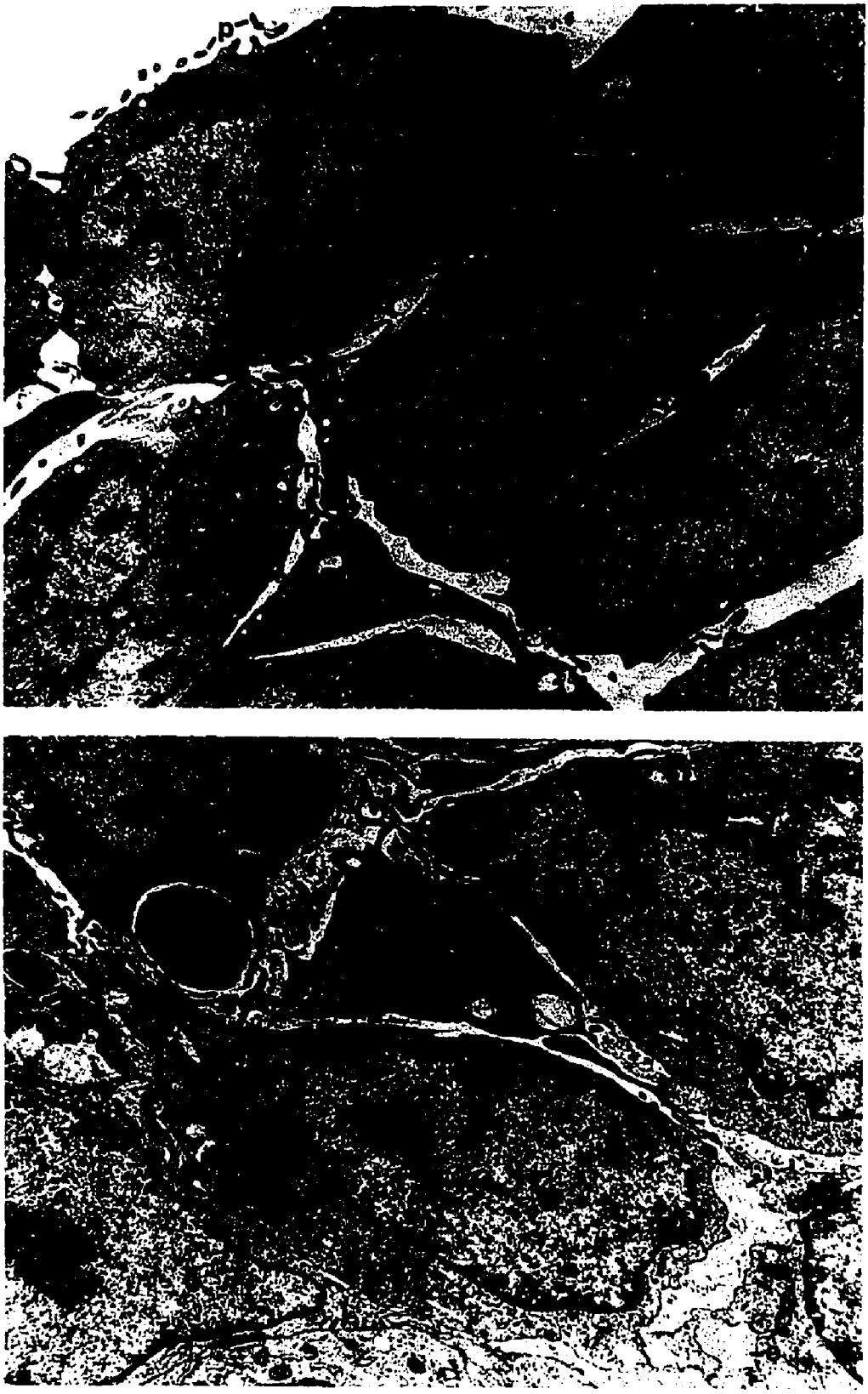

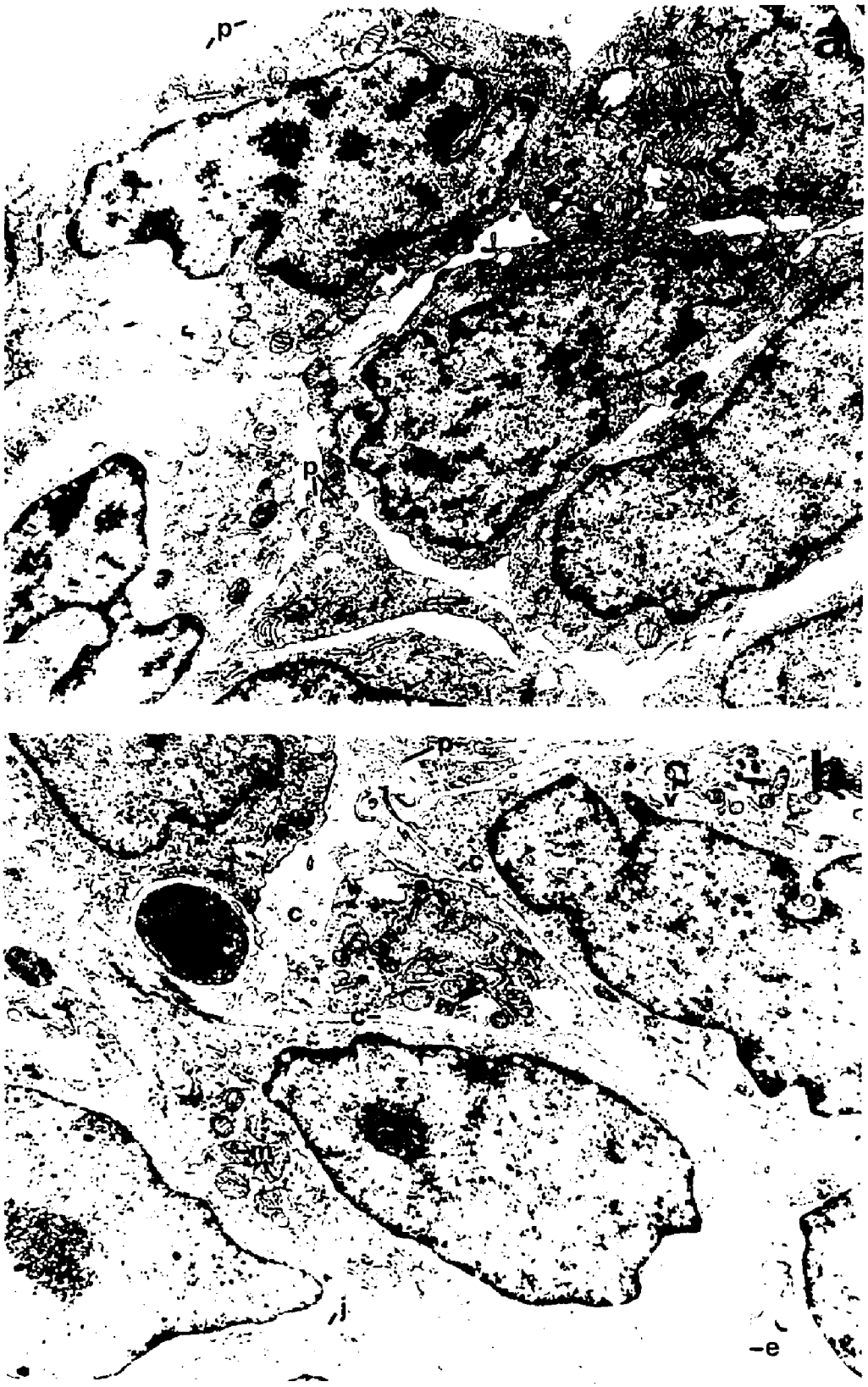
a
p
p
b
p
c
c
c
m
i
e

material (c).

In addition to the close contact illustrated in figures 2.3 and 2.4, specialized cell junctions occur between many cells. A few areas of close contact and possible junctions (j) are marked in figure 2.5, and figure 2.6 is a composite of some junctions that have been observed. In figure 2.6a, an area of very close contact between the external membranes can be seen, and in (b), an apparent fusion of the plasma membranes is shown. These junctions are similar to the classical 'close' and 'tight' junctions respectively (Ham 1970). A desmosome-like junction is seen in figure 2.6c, where electron-dense material appears to have accumulated in the cytoplasmic regions near the junction. Specialized junctions of these types were not common in the spheroid, and no attempt has yet been made to determine their frequency, or to determine possible differences in frequency with position in the spheroid or with spheroid age.

2.2.4 Summary

The previous figures emphasize the fact that each cell of the spheroid appears to be an integral part of an ordered structure, much as each cell in organized tissues <u>in vivo</u> contributes to that tissue's properties. In addition, the three dimensional contact found between the

FIGURE 2.6

Electron micrographs of specialized junctions occurring between cells of spheroids. An area of close contact can be seen in (a), and panel (b) shows a tight junction. A desmosome-like structure can be seen in panel (c), with electron dense material in the cytoplasm of each cell near the junction. Magnification: (a) X 40,000 ; (b) X 400,000 ; (c) X 800,000

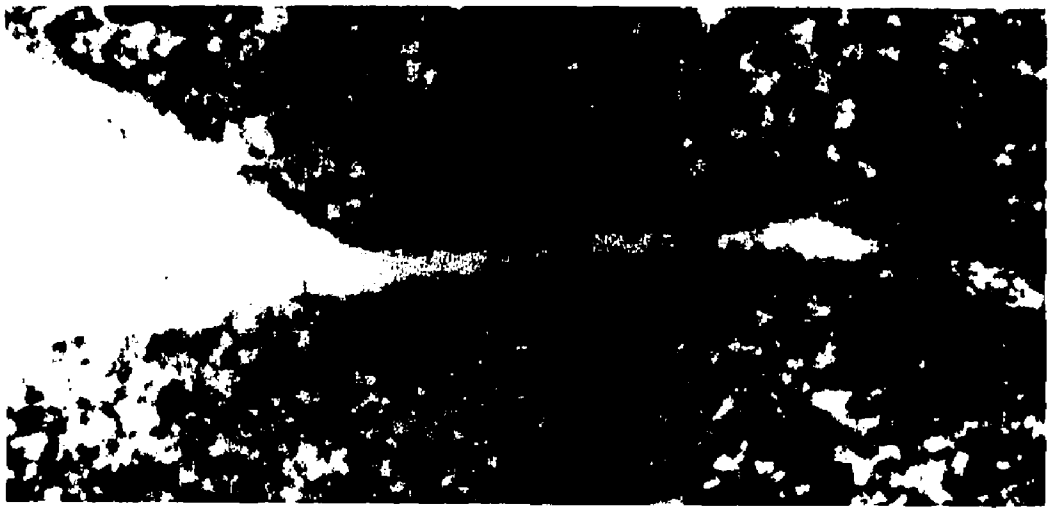

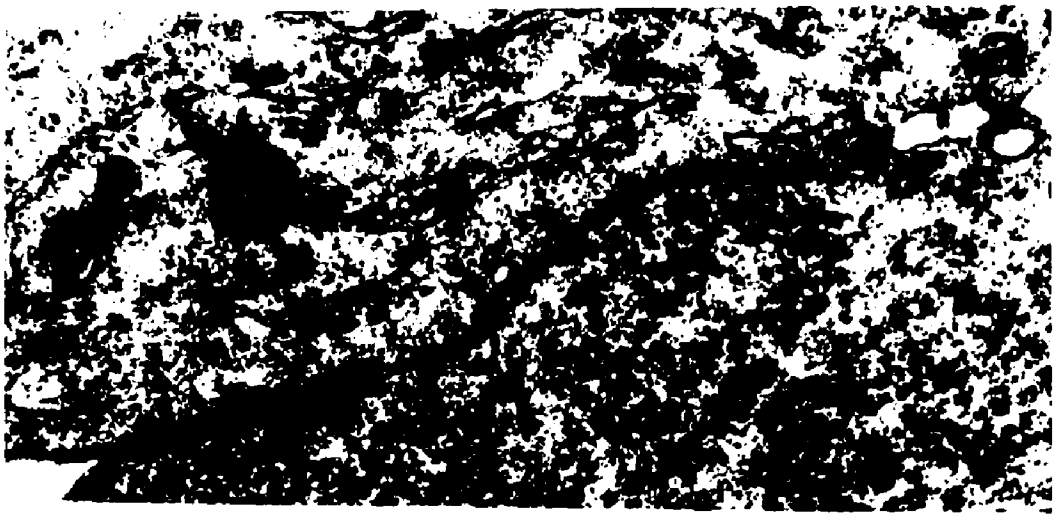

spheroid cells, which cannot be produced in conventional monolayer or suspension culturing systems, suggests that spheroids may simulate the intercellular contact of organized tissues to a greater extent than has previously been attainable.

2.3 Radiation Survival of Cells in Contact

2.3.1 Introduction

The extensive intercellular contact which was described in section 2.2 represents a major change in the cell's microenvironment, a change which might be reflected by modified survival after irradiation. Very small spheroids (8-15 cells) had growth rates and cell cycle distributions similar to exponentially growing single cells (see section 3.2), and as such, provided a system in which radiation survival changes were directly attributable to intercellular contact. This section contains evidence that intercellular contact in the spheroid does modify its radiation survival characteristics, and suggestions about possible mechanisms are presented.

2.3.2 Methods of irradiation and survival assay

Small spheroids were grown under standard conditions (see section 2.2.2) for 24 hours (day 1 spheroids), and removed as required from the culture flask. They were either centrifuged gently (400g) for 6 minutes and then

resuspended in complete fresh medium in glass vessels, or placed directly from the culture flask into 100 mm plastic petri dishes on a revolving carousel for irradiation. A water bath was used to control the temperature of the glass irradiation vessels, and humidified air containing 3% CO_2 was flushed through the vessels at a rate of .15 cfh (about 2 volume changes per minute). Anaerobic experiments were performed only in glass vessels (Chapman et al 1970), with the vessels flushed with humidified nitrogen plus 3% CO_2 at the above rate before and during the exposure. A ^{60}Co source with a dose rate of 100-175 rad/min was used for all irradiations, with the absorbed dose determined by lithium fluoride thermoluminescent powder intercalibrated with a Baldwin-Farmer secondary standard ionization chamber.

After the irradiation, the small spheroids were centrifuged and the supernatant was discarded. They were then reduced to single cells by resuspending the spheroids in 3 ml of 37°C trypsin (prepared as previously described in section 2.2.2) and transferred to 60mm dishes to which the cells would not attach (Lab Tek). These dishes were then placed on a rotary-action shaker at 37°C. After 8 minutes of gentle agitation, the dishes were removed, and a minimum of 3 ml of complete medium added to stop the trypsinization procedure. The cells

were then pipetted up and down gently to produce a suspension of single cells.

Cells were counted with a Celloscope electronic particle counter having an orifice opening of .1 mm; a threshold particle diameter of about 5 microns and an upper limit cutoff of about 30 micron were set electronically. The electronics of the counter were modified to increase its sensitivity and thus allow counting on scales increasing by factors of two from 6.25 particles per count to 200 particles per count. Although the instrument was unable to distinguish between cells and other particles of comparable sizes, comparison of electronic cell counts with those obtained manually with a hemocytometer confirmed that excellent agreement was possible.

When the cell concentration was determined, an appropriate dilution was made to ensure that 1.0 ml of cells added to replicate growth plates would produce about 250 colonies on each plate. Final counts were performed on the dilution of cells actually plated to increase accuracy.

Survival was assayed by manually counting visible colonies which were attached to the plates 8 days after irradiation. At the termination of this growth period, the medium was poured out of the plates, and 2 ml of .5% methylene blue added to the plates for 15 minutes. When

the colonies were sufficiently stained, the plates were gently washed with cold water and stacked to dry before counting. The statistical variation in plating and survival in each experiment was such that the standard errors of survival means were smaller than the plotting symbols unless otherwise indicated. Regression analysis was used to determine the terminal slopes of the survival curves, using a General Electric Mk I computer.

Control cells for all spheroid experiments refers to single cells in exponential growth from plates, which were treated identically to the spheroids with the exception that trypsinization occurred prior to irradiation. The centrifuging and resuspending procedures were not found to alter the multiplicity of either the spheroids or the single cells.

Single cells used for determining responses as a function of time after subculturing were initially pooled from several plates of exponentially growing cells, and 10^4 cells/ml were inoculated into enough growth plates to complete the 8-day experiments. Appropriate plates were irradiated on days 1, 2, 4, 6, and 8. After irradiation, the cells were removed from the plates by trypsinization, counted, and plated as for spheroid cells to determine survival.

2.3.3 Results

A complete description of survival criteria and survival curve generation and analysis is contained in Appendix 2. Standard survival curves for the V79-171b Chinese hamster cell line in exponential growth and irradiated under aerobic and anoxic conditions are shown in figure 2.7 . This is the conventional dose-effect curve, where survival is plotted on a logarithmic scale as a function of the radiation dose. Data from several experiments have been included to indicate the reproducibility of results generally obtainable, and the plotted survival points were always corrected for the plating efficiency (PE), or the fraction of the cells which formed colonies in the absence of radiation.

In the absence of oxygen, the survival curve was characterized by a mean lethal dose or D_o of 456 ± 16 rad, where the error represents the 95% confidence interval of the slope. The extrapolation number n was found to be 9.3 ± 2.9 . When the cells were irradiated in well-oxygenated conditions, the well-known 'oxygen effect' or enhancement of cell killing was observed, as the D_o was 168 ± 9 rad with n = 11.2 ± 1.1 . The extrapolation numbers were not significantly different under the two conditions, so the effect can be called 'dose modification', where the dose modifying factor (DMF)

FIGURE 2.7

Survival of exponentially growing V79-171b Chinese hamster cells grown on petri dishes and irradiated at 37°C in air or nitrogen (155 rad/min).

Symbol	PE	D_o	n
●	70-90%	168±9	11.2±1.1
X	60-80%	456±16	9.3±2.9

Data were pooled from several experiments. Uncertainties shown above are 95% confidence intervals.

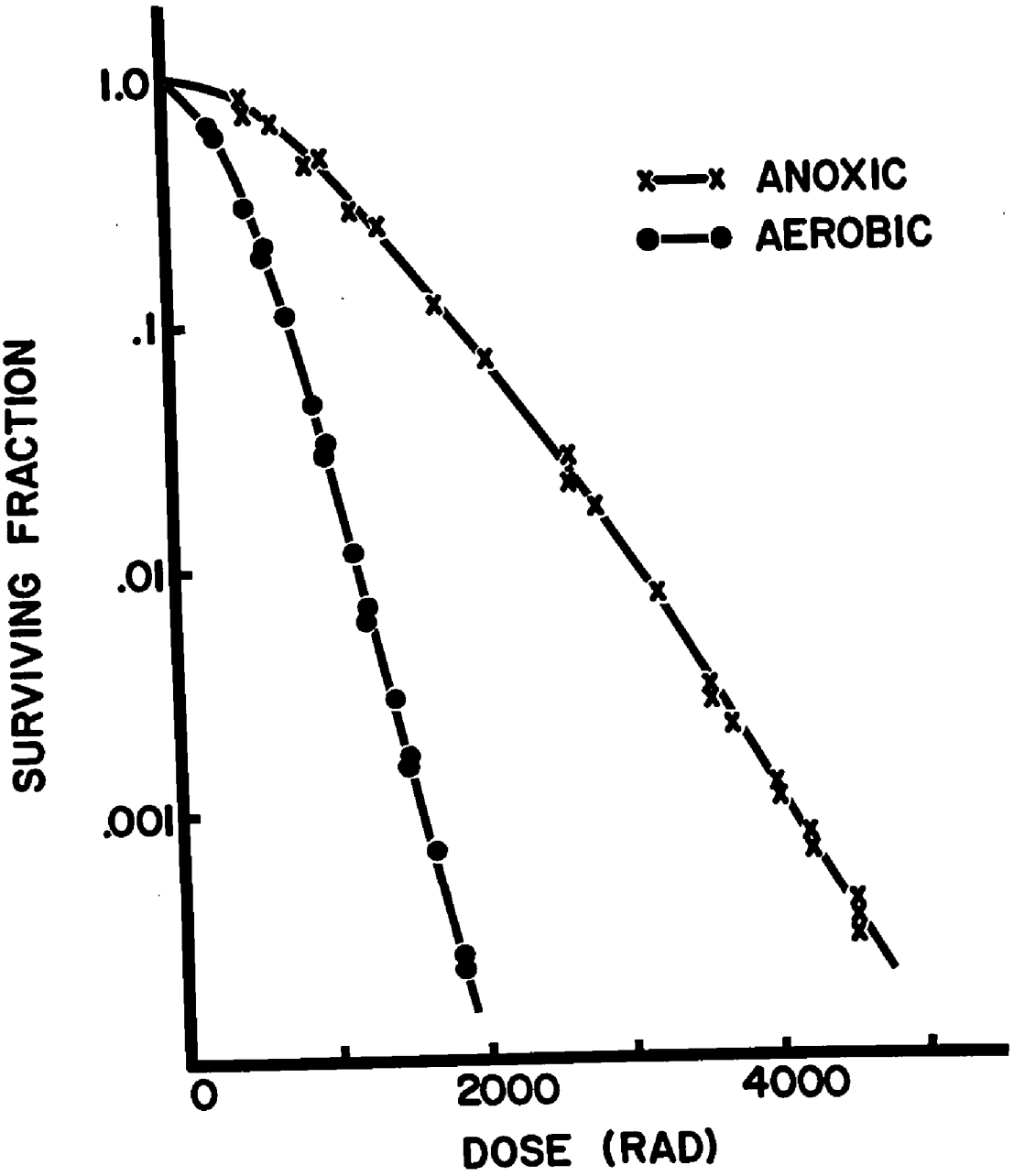
1.0
.1
.01
.001
SURVIVING FRACTION
ANOXIC
AEROBIC
0
2000
4000
DOSE (RAD)

or ratio of the D_o's was 2.7, well within the range of values normally observed for mammalian cells (Elkind and Whitmore 1967, Okada 1970, Fabrikant 1972).

The effect of intercellular contact on cell survival after irradiation can be seen in figures 2.8a and 2.8b. The data can immediately be compared with the single cell curves, since the small spheroids were irradiated intact, but were then reduced to single cells and the viability of these single cells was assayed. The curves obtained under aerobic conditions (a) for control cells and spheroids had D_o's of 171 ± 11 and 186 ± 14 rad respectively, while the corresponding curves for anoxic conditions had D_o's of 457 ± 30 and 491 ± 22 rad. This represented no significant change in radiosensitivity in either case. However, in air the extrapolation number increased from 9.4 for single cells to 152, and a similar increase of 11.2 to 164 was noted under anoxic conditions in panel (b). At high doses of radiation, survival was thus increased about 15-fold when the cells were grown and irradiated as spheroids, independent of the presence of oxygen during the irradiation procedure. Identical survival curves were also observed when the spheroids were irradiated at 37°C, and whether they were centrifuged and irradiated in glass vessels, or irradiated directly in plastic petri dishes (in air).

FIGURE 2.8

Survival of exponentially growing V79-171b Chinese hamster cells grown on petri dishes or as spheroids and irradiated at 24°C in air or N_2 (165 rad/min).

	Symbol	PE	D_o	n	D_q
(a)	●	35-50%	186±14	152±21	910
	o	75-85%	171±11	9.4±2.3	406
(b)	●	30-50%	491±22	164±33	2490
	o	65-82%	457±30	11.2±2.4	1100

Data were pooled from several experiments. Uncertainties shown above are 95% confidence intervals.

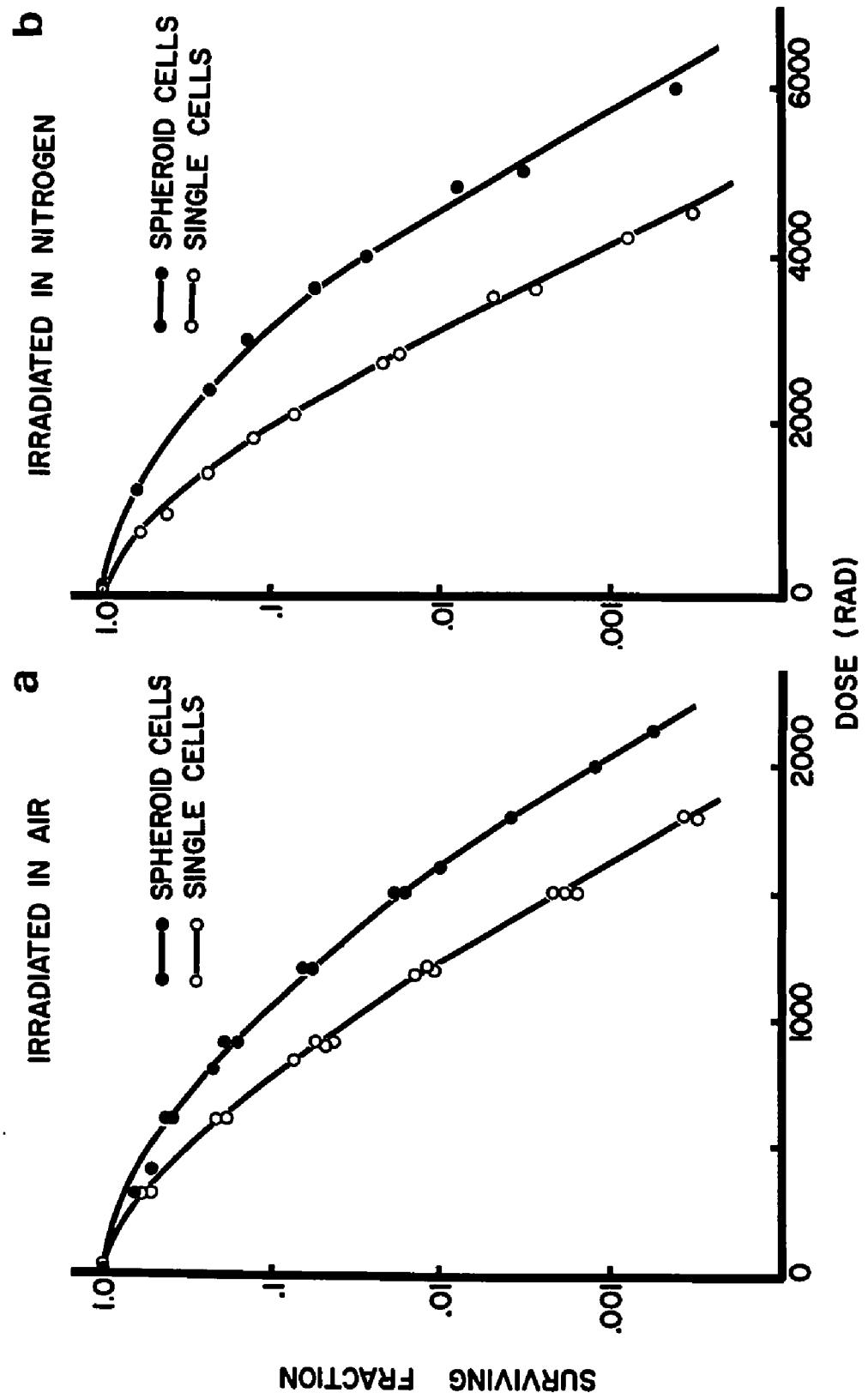
a
IRRADIATED IN AIR
SPHEROID CELLS
SINGLE CELLS
b
IRRADIATED IN NITROGEN
SPHEROID CELLS
SINGLE CELLS
SURVIVING FRACTION
1.0
.1
.01
.001
0
1000
2000
4000
6000
DOSE (RAD)

Plating efficiencies for cells from day 1 spheroids were typically in the range 35-65%. Although a higher PE would have been desirable, the reproducibility of the survival curves indicated that the low values were not a cause for excessive concern. Staining day 1 spheroids with vital stains (e.g. trypan blue) to determine cell viability on the basis of dye exclusion showed that the visible cells in the spheroids were all viable, but that single cells were often darkly stained. This probably indicates that only the viable cells aggregated into spheroids. Since the electronic cell counter counted all particles of the appropriate size, the number of non-viable single cells as well as any other particles would have been expected to lower the observed plating efficiencies. Typical experiments quantitating the numbers of single cells as a function of time are presented in this section (see figure 2.11).

If intercellular contact at the time of irradiation was the only requirement for the enhanced survival, it would be expected that cells grown as spheroids by conventional techniques, but irradiated after being reduced to single cells would have survival curves similar to the control cells. Figure 2.9 demonstrates that cells grown as spheroids, but separated into single cells immediately before being irradiated showed a survival intermediate to

FIGURE 2.9

Survival of cells grown as spheroids but trypsinized immediately (▲) or 1.5 hours (●) before irradiation at 24°C (165 rad/min). Broken curves represent survival of spheroids irradiated intact (upper) and of single cells grown on plates (lower).

Symbol	PE	D_o	n
▲	55%	181	32
●	61%	174	24

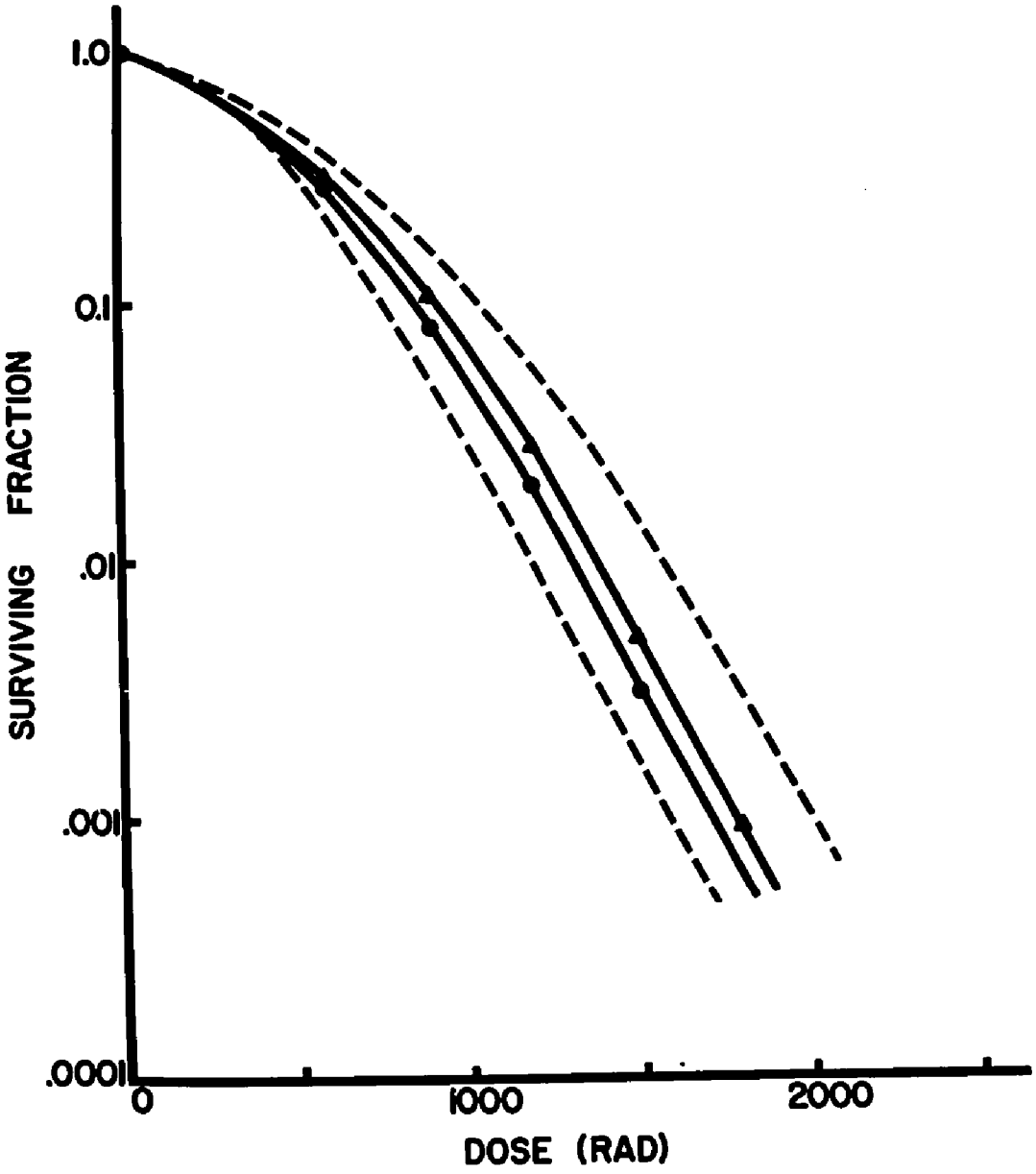
1.0
0.1
.01
.001
.0001
SURVIVING FRACTION
0
1000
2000
DOSE (RAD)

spheroids and control cells. A further survival decrease was observed when irradiation followed trypsinization and replating by 1.5 hours. This effect was found to be highly dependent on spheroid multiplicity for very small spheroids of <10 cells, as much smaller decreases in survival were noted when spheroids of lower multiplicity were pre-trypsinized (see also figure 2.11). The fact that survival was enhanced even when the spheroid cells were irradiated as individual cells suggested that an inherent capacity for increased accumulation of sublethal damage resulted from growth as spheroids.

The time required for loss of the enhanced capacity for accumulation of sublethal damage to become complete was determined and is shown in figure 2.10 . The extent of the immediate decrease in survival varied according to multiplicity for small spheroids as previously stated, but was generally similar to figure 2.10 where the survival of cells trypsinized and plated for colony formation at various times prior to irradiation is shown. When survival was corrected for the increasing cell numbers on the plates, it was found that survival after 1120 rad decreased to the same level as found for control cells after about 10 hours, or approximately the duration of one cell cycle.

FIGURE 2.10

Isodose (1120 rad) survival of spheroids trypsinized at various times prior to irradiation at 24°C (165 rad/min). The cells were placed in petri dishes at time 0, and incubated at 37°C until and after exposure. PE = 62%
The upper broken line represents the survival of spheroids irradiated intact; the lower broken line represents the survival of cells grown on petri dishes.

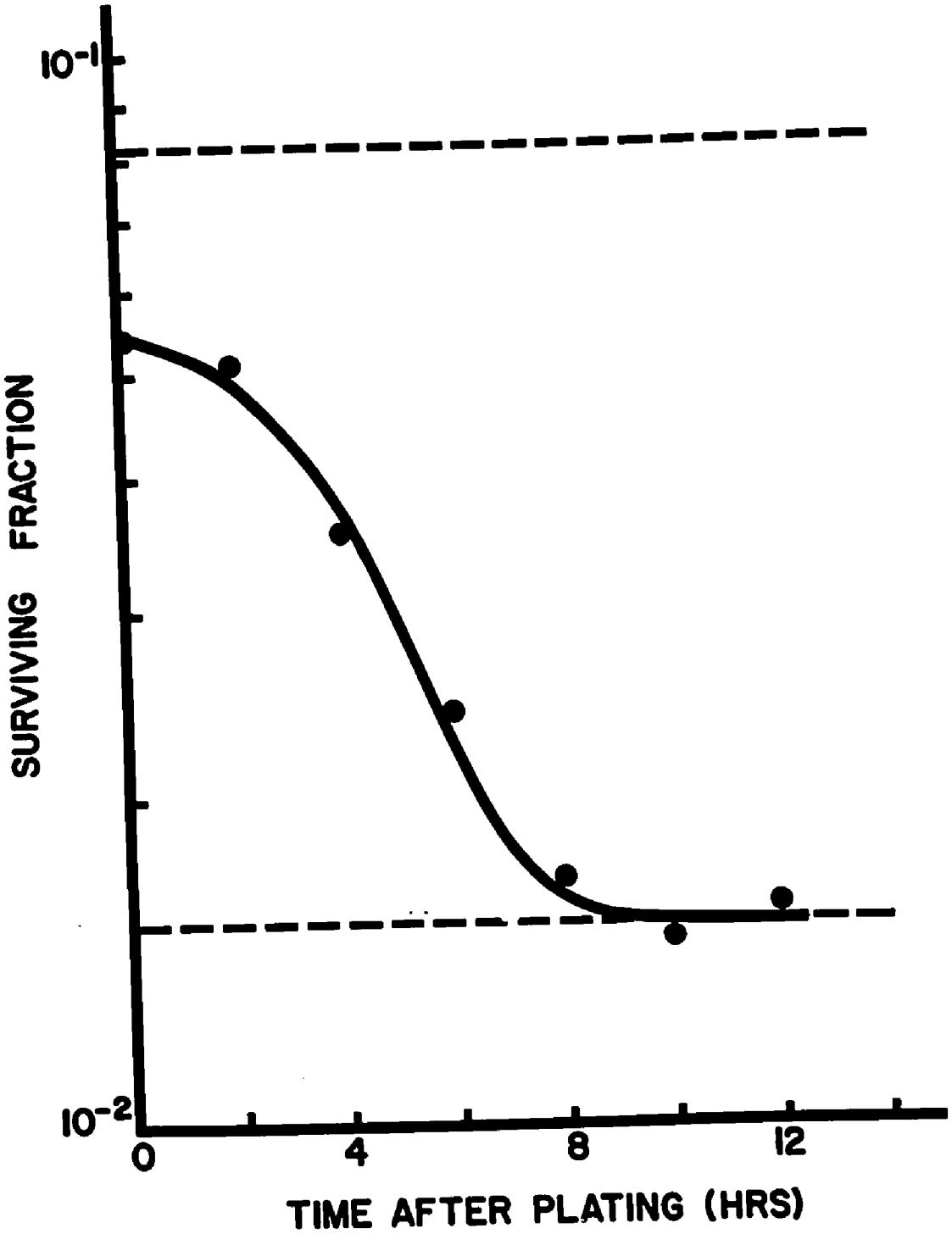
10^{-1}
10^{-2}
SURVIVING FRACTION
0
4
8
12
TIME AFTER PLATING (HRS)

The time required for development of this enhanced capacity for accumulation of sublethal radiation damage was investigated and the results are shown in figure 2.11 . Panel (a) shows the decrease of single cells in the culture as a function of time, and panel (b) the relative multiplicity of the spheroids (determined by comparison of electronic counts of whole and trypsinized spheroids). The large number of single cells tended to lower the average multiplicity, that is, most spheroids contained more than 10 cells after 12 hours. It was interesting to note that aggregation occurred mainly from 8 to 12 hours, and concurrently, survival following a dose of 1300 rad increased sharply. These results show that increased survival can be correlated directly with spheroid multiplicity. Apparently about one cell cycle was required for the cells to 'adapt' to the new environment, and to grow as spheroids.

The results presented in figures 2.10 and 2.11 thus suggest that cells grown in contact for periods longer than one cell cycle develop a capacity for increased accumulation of sublethal damage, and this capacity declines slowly over the first cell cycle after cells are separated. An additional capacity for accumulation of sublethal damage was observed when cells were in contact during the actual irradiation procedure.

FIGURE 2.11

Aggregation of single cells into spheroids, and cell survival after 1300 rad during the aggregation procedure.

(a) The percentage of single cells in the culture is plotted as a function of time.

(b) The average number of cells per spheroid, or the spheroid multiplicity as a function of time.

(c) Isodose (1300 rad) survival as a function of time in culture. Plating efficiency increased approximately linearly from 56% at 0 hours to 67% at 16 hours. Exposures were at 24°C at a dose rate of 135 rad/min.

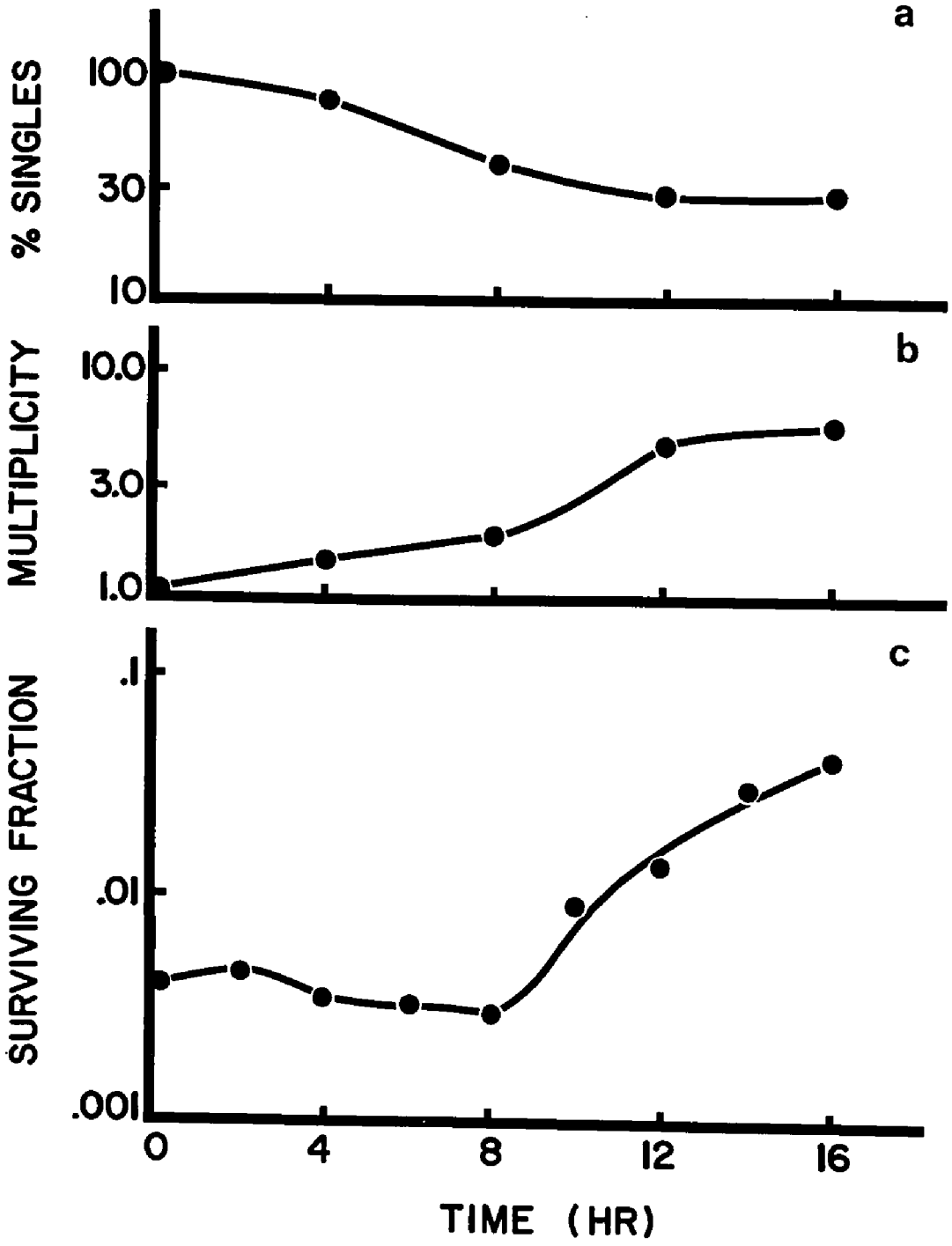
a
% SINGLES
100
30
10
b
MULTIPLICITY
10.0
3.0
1.0
c
SURVIVING FRACTION
.1
.01
.001
0
4
8
12
16
TIME (HR)

As cells increase in density in monolayer cultures, the intercellular contact which develops is thought to be at least partially responsible for the reduced growth rate observed. If intercellular contact was indeed responsible for the increased survival, even dense monolayer cultures might be expected to show a higher capacity for accumulation of sublethal radiation damage. The radiation survival characteristics of single cells on plates was thus studied, with the initial cell inoculum chosen to be identical to spheroid cultures (10^4 cells/ml). Growth and survival of such cells as a function of time in culture are shown in figure 2.12 . During the exponential growth phase, the cells doubled in number every 10.6 hours.

The radiation survival of cells after various periods of growth is shown in figures 2.12b to 2.12f, where the broken curves of the latter panels repeat the survival curve for exponentially growing cells as in panel (b). Although both day 1 and day 2 cells appeared to be in exponential growth from panel (a), there was an obvious decrease in survival even at this early stage of growth. At day 4, panel (d), the curve showed the characteristic response of a two-component cell population (see Appendix 2). The more resistant population represented an increased fraction by day 6, and became the

FIGURE 2.12

Growth and radiation survival of cells grown on petri dishes. Panel (a) shows total number of cells per plate as a function of time, where the initial cell number/plate was 10^5. Doubling time during exponential growth was 10.6 hours.
All irradiations were performed at 24°C at a dose rate of 124 rad/min. Broken curves in panels (c) through (f) represent survival of exponential cells as in panel (b).

Panel	PE	D_o	n	D_q
(b)	61%	174±21	12.1	436
(c)	63%	169±13	9.9	-
(d)	86%	202±17	11.9	-
(e)	65%	181±14	21.1	-
(f)	63%	195±16	30.5	664

Errors shown above represent 95% confidence intervals.

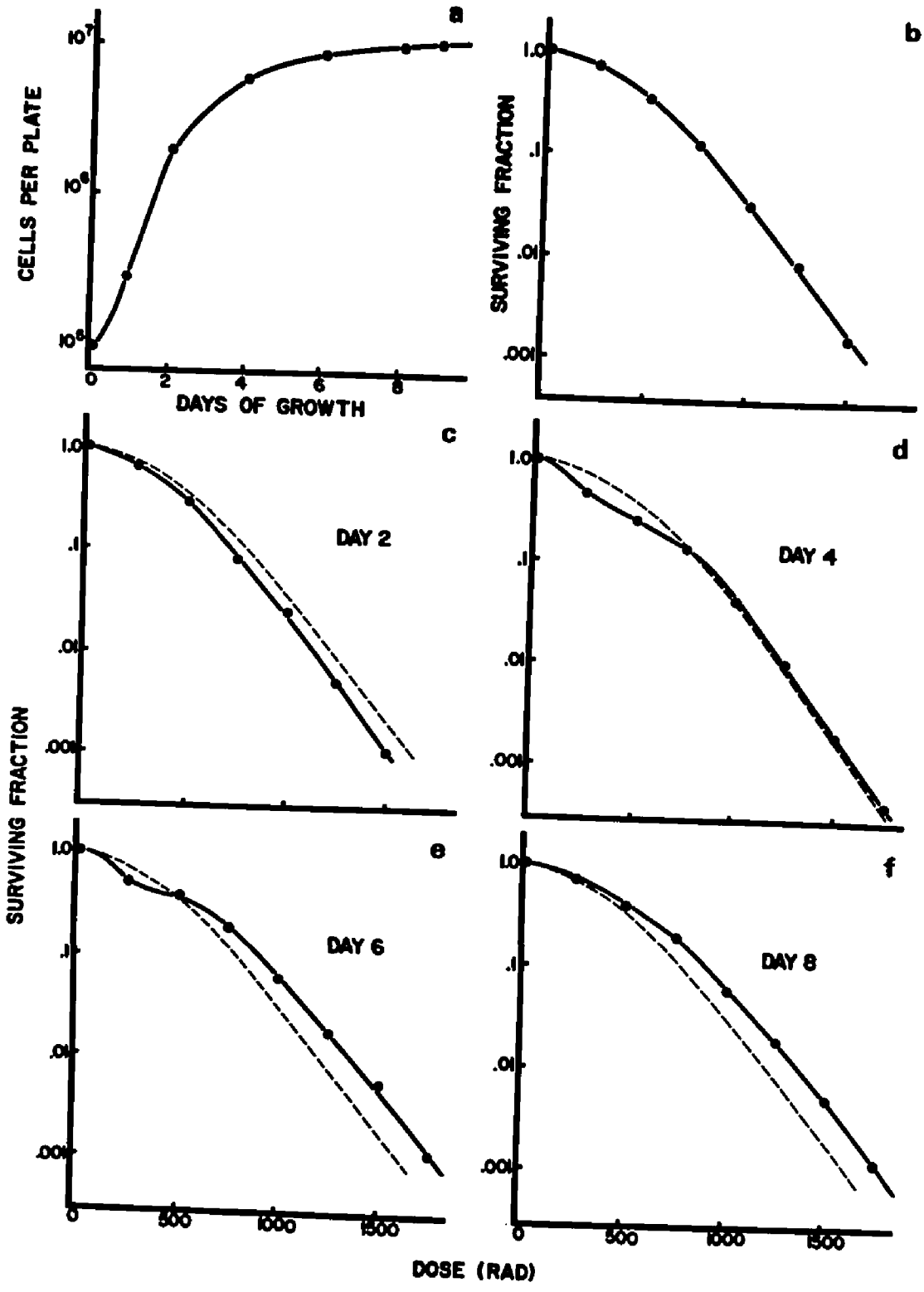
a
b
c
d
e
f
CELLS PER PLATE
DAYS OF GROWTH
SURVIVING FRACTION
DAY 2
DAY 4
DAY 6
DAY 8
DOSE (RAD)

only significant component by day 8 in panel (f). Comparison with the broken curve indicated that the plateau phase, contact inhibited cells had a radiosensitivity of 195 ± 16 rad, not significantly different that the 174 ± 21 rad of exponentially growing single cells. However, the extrapolation number increased from 12.2 to 30.5, a factor of 2.5 .

Since intercellular contact was a feature common to this system and the spheroid system at the times when increased accumulation of sublethal radiation damage was observed, the results of figure 2.12 provide additional evidence that intercellular contact does alter survival characteristics. Degree of contact may also be improtant, since the increase in n seen in the confluent cultures, a factor of about 3, is much smaller than the value of at least 15 seen for spheroids. One main difference between the two systems is that spheroids had cells that were cycling normally, while a majority of the confluent cells had stopped cycling and had accumulated at a relatively sensitive position in the cell cycle (Durand and Sutherland 1972).

Separation of the confluent cells prior to irradiation would be expected to decrease survival in a manner analogous to that seen for spheroid cells (figure 2.10). The results presented in figures 2.13a and 2.13b

FIGURE 2.13

Multiplicity and radiation survival of cells in regrowth, obtained from a day 8 plateau phase culture.

(a) Number of cells per microcolony, or multiplicity as a function of time after regrowth was initiated.

(b) Isodose (1250 rad) survival of cells incubated at 37°C before irradiation (126 rad/min; 24°C). Plating efficiency was 63%.

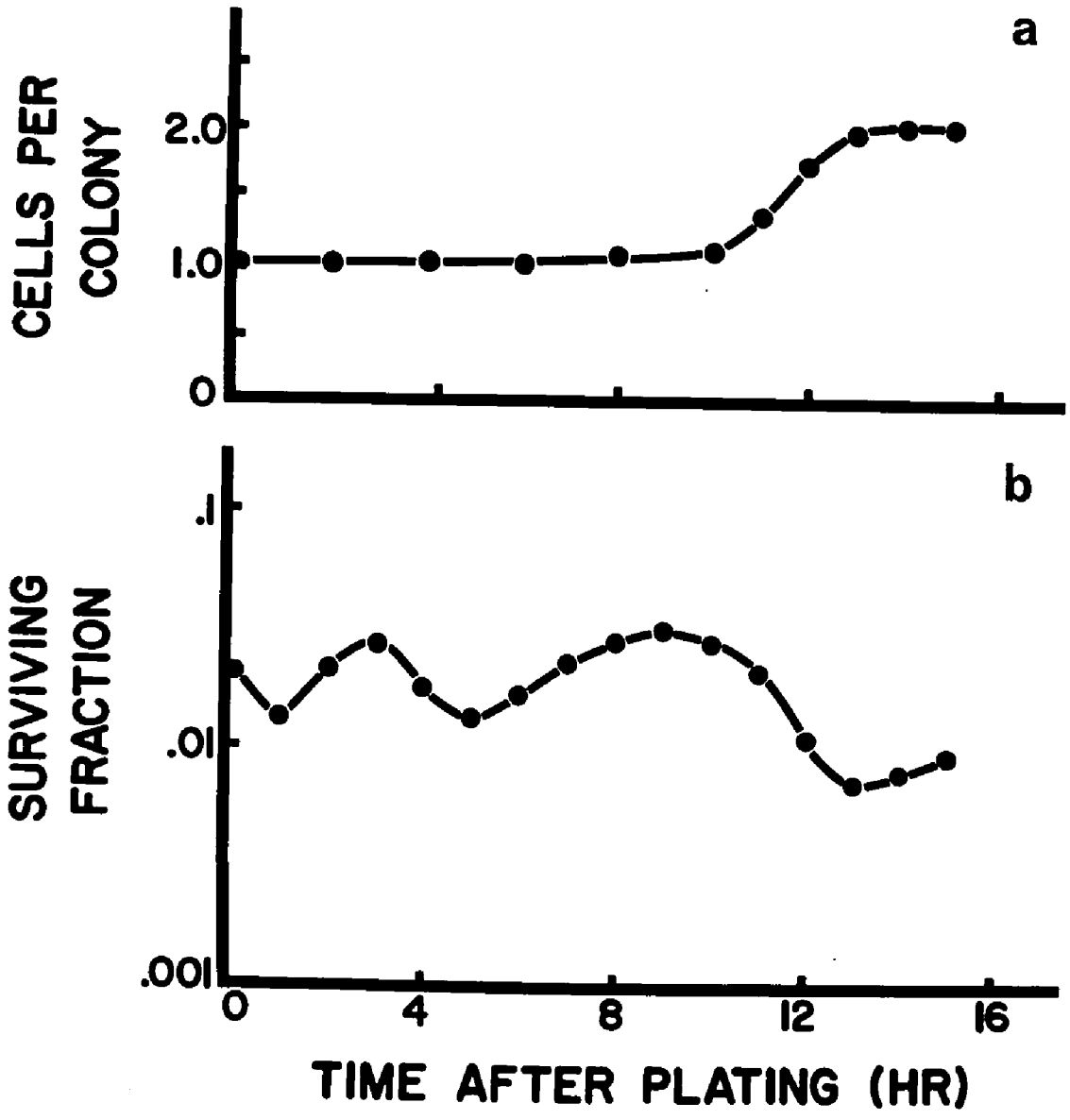
a
CELLS PER COLONY
2.0
1.0
0
b
SURVIVING FRACTION
.1
.01
.001
0
4
8
12
16
TIME AFTER PLATING (HR)

tend to confirm this suggestion, but an important difference from the previous case is immediately apparent in figure 2.13a. Cell number per colony does not increase exponentially with time as would be expected for normal asynchronous growth, but rather, no increase in cell number was seen for the first 10 hours after plating. The 'burst' of mitotic cells had to result from a partial synchrony in the population as previously suggested (Chapman et al 1970b, Ross and Sinclair 1972, Durand and Sutherland 1972).

The confluent cells accumulated at a position of relative radiosensitivity, so progression of the cells would be expected to mediate increased radiation survival. However, a survival decrease was noted immediately after separation of the sensitive plateau phase cells into single cells, despite the prediction that higher survival was expected. These results thus serve to strengthen the argument that intercellular contact between these cells does increase survival. It should also be noted that the most resistant survival noted in figure 2.13b, at the time when most of the cells were in late S phase (Sinclair and Morton 1966, Sinclair 1968), was no higher than the survival of the more sensitive confluent cells in contact.

The mechanism of this contact effect has yet to be elucidated. One method of determining whether enhanced accumulation of sublethal radiation damage was a metabolically active or passive phenomena was to reduce metabolic activity by lowering the temperature of the spheroids to 4°C. To accomplish this, the spheroids were removed from the culture flasks as required, and centrifuged at 4°C. Total time at 4°C before irradiation was 15 minutes, followed by a 15 minute irradiation procedure in a 4°C water bath. Trypsinization was also carried out on the mechanical agitator at 4°C, and a time of 15 minutes was found adequate to reduce the spheroids to single cells. The spheroids were then restored to normal conditions by adding warm, complete medium, counting and plating as usual. Similar treatment times and temperatures were adopted for control, single cells.

The survival curves obtained during the low temperature irradiation are shown in figure 2.14 . No effect was noted with single cells, since the D_o of 178 rad and n of 10.4 were similar to those usually obtained. However, the survival of the spheroid cells was significantly reduced, with a D_o of the usual 172 rad but with n reduced to about 17 (a factor of at least 8). This reduction in survival at large doses suggests that accumulation

FIGURE 2.14

Survival of cells grown as spheroids or on petri dishes and irradiated at 4°C in air (140 rad/min). Broken line indicates survival of spheroids irradiated at 24°C.

Symbol	PE	D_o	n
X	64%	178	10.4
●	52%	172	16.6

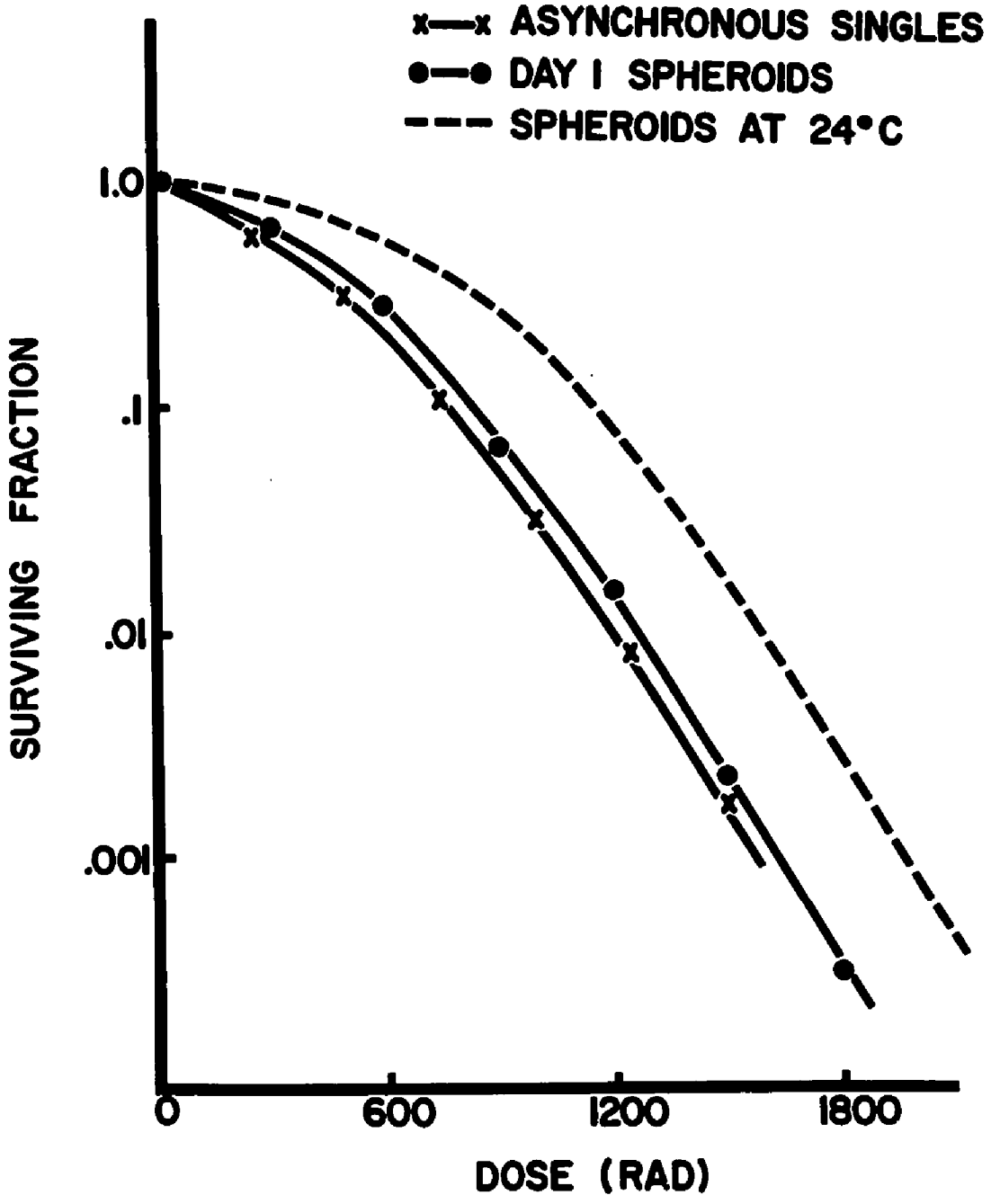
x—x ASYNCHRONOUS SINGLES
●—● DAY I SPHEROIDS
- - - SPHEROIDS AT 24°C
SURVIVING FRACTION
1.0
.1
.01
.001
0
600
1200
1800
DOSE (RAD)

of larger quantities of sublethal damage was, at least in part, a process that required active metabolism.

More information on the conditions required for minimal survival was obtained in an experiment designed to isolate the particular time at which reduced metabolic activity would decrease cellular survival in the spheroids. The irradiation procedure was divided into three parts of equal length, and all permutations of warm (37°C) and cold (4°C) conditions in the pre-exposure, exposure and post-exposure periods were investigated. Temperatures were held constant with water baths, so rapid changes of temperature were possible at the boundaries of each time period. The results of one of several experiments are shown in figure 2.15 . This figure has been plotted differently than most, with survival represented as a function of treatment condition for only one dose, 1750 rad. The temperature at which each treatment was carried out is indicated by the different lines. Survival was maximum when the spheroids were held at 37°C before, during and after the exposure, and was minimum when the spheroids were warm before exposure, but irradiated and trypsinized at 4°C.

In general, the results from figure 2.15 can be placed in three groups. Maximum survival was seen when the spheroids remained under optimal growth conditions at 37°C. However, when the spheroids were cooled prior to

FIGURE 2.15

Isodose (1750 rad) survival of day 1 spheroids as a function of pre-, post-, and exposure temperature. Temperatures were maintained by water baths, allowing rapid temperature changes at the boundaries. Spheroids trypsinized at 37°C had PE = 69%; at 4°C the PE = 78%. The dose rate was 135 rad/min. Standard errors of the means for survival points were omitted for clarity, but were less than ±10% of the plotted values.

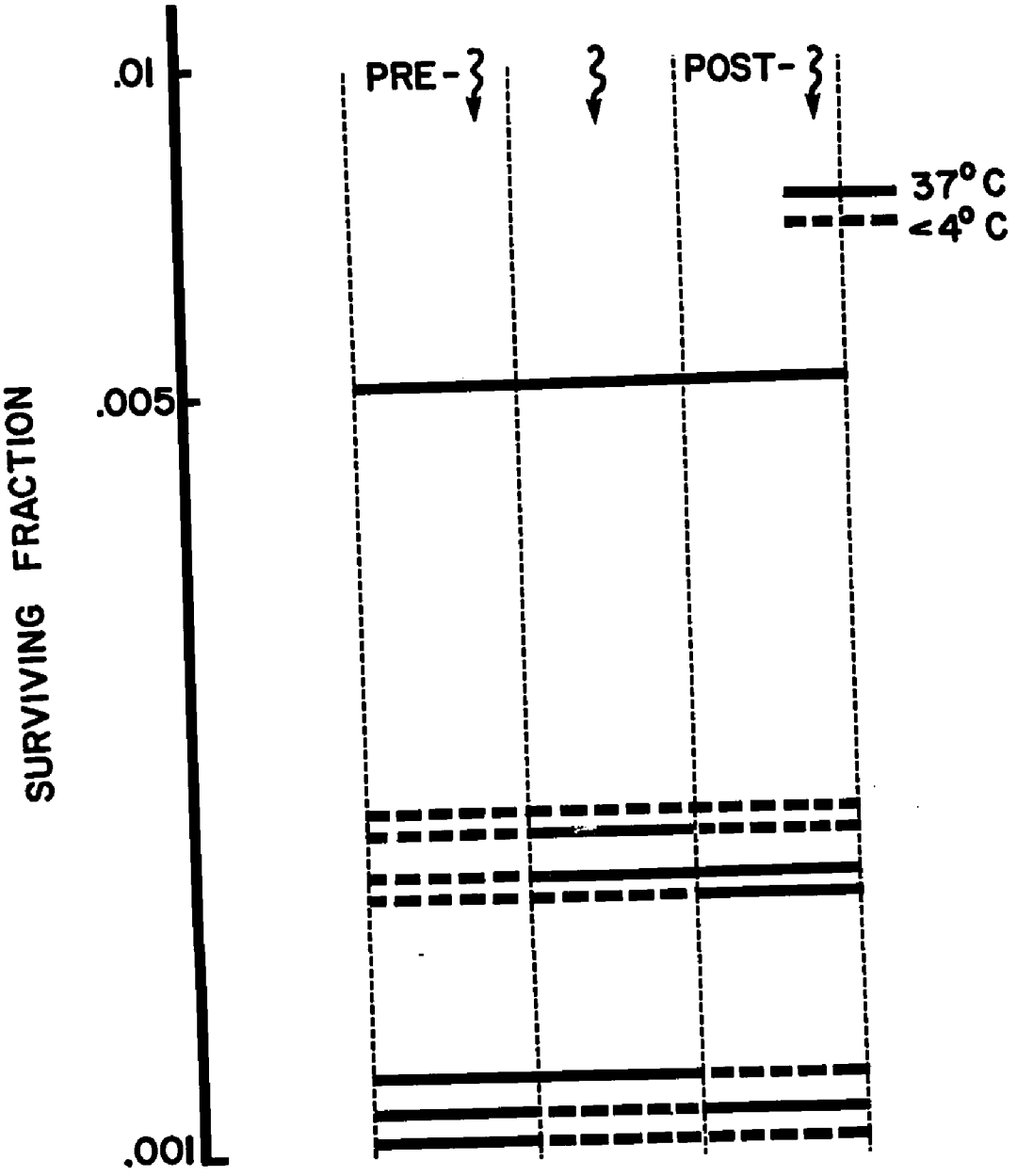
.01
.005
.001
SURVIVING FRACTION
PRE-
POST-
37° C
<4° C

irradiation, survival was reduced by a factor of about 2.5 . Minimum survival (a further decrease by a factor of 2) was seen when the spheroids were warm before being irradiated, but were abruptly cooled at either the beginning or end of the irradiation procedure. The significance of these results is not yet clear, however, they tend to suggest that enhanced accumulation of sublethal radiation damage was negated when metabolic activity was severely inhibited during or immediately after the radiation exposure.

The enhanced survival seen when cells were in contact suggested that cellular cooperation or communication resulted in the enhanced ability to deal with radiation damage. This in turn implies that cells in spheroids may not survive radiation independently, a possibility that can be explored by a conceptually difficult, but technically easy experiment. The electronic cell counter was capable of counting particles of sizes up to .1 mm, which was more than double the average diameter of 1 day old spheroids. Thus, the number of spheroids per ml of culture medium could be counted directly. Spheroids could also be 'plated' intact so that the entire spheroid developed into a colony in a manner similar to single cells. Testing independence of survival of the cells in a spheroid was thus easily performed--appropriate, equal numbers

of spheroids were plated into growth plates and allowed two hours to attach. They were then irradiated, and the medium removed from all plates. Half the plates given one dose were then given 10 ml of complete BME and replaced in the incubator. The other half of the plates were trypsinized by adding 1 ml of trypsin for 8 minutes, then pipetted up and down to produce single cells after addition of 9 ml of complete medium. At this stage, equal numbers of cells should have remained in both sets of plates; in one case, the cells were individuals (final PE = 71%), and in the other case they were spheroids (PE = 56%). Some cell loss might be expected to have occurred in the pipetting procedure, however, this was accounted for by the plating efficiencies.

In the unirradiated plates, N cells were placed in the plates as n spheroids. Then, the single cells from these n spheroids would give rise to n' colonies, where $n' < N$, since not all cells were expected to be viable (i.e., the PE). For radiation doses > 1000 rad, the probability of survival (< .1) was such that less than 1 cell per spheroid was expected to survive. Hence, the number of colonies per plate after irradiation were divided by the total number of spheroids placed on the plate, and by the PE (n'/N) to determine the survival, regardless of whether single cells or spheroids were

plated. A more detailed analysis is required for lower radiation doses where more than one cell survived in each spheroid.

The results of this type of experiment obviously cannot be reproduced exactly in different experiments, due to different average numbers of cells in day 1 spheroids. One experiment representative of the results usually obtained is shown in figure 2.16 . The lower solid curve, which represented the survival of irradiated and trypsinized spheroids, should have been displaced upward from the normal day 1 spheroid survival curve (broken line) by a factor equal to the relative multiplicity. In this particular experiment, the n value of 680 indicated a relative multiplicity of about 4 compared to the normal extrapolation number of roughly 160 . Surprisingly, the curve for intact spheroids was displaced upward by an additional factor of almost 2 (n = 1180). This indicated that the cells had a better chance of survival when they remained in close contact than if they were reduced to single cells. This does not indicate anything about the speed of the repair process which leads to the increased survival, but does at least suggest that it must be rather slow, since the separated cells should have shown higher survival if repair was completed before the cells were trypsinized.

FIGURE 2.16

Survival of day 1 spheroids irradiated and plated intact (▲), or irradiated intact but trypsinized to single cells after irradiation (●). The exposure was at 24°C, with a dose rate of 131 rad/min. The broken curve indicates survival of spheroids irradiated intact, and reduced to single cells and counted before plating (i.e. multiplicity of 1.0).

Symbol	PE	D_o	n
▲	56%	180	1180
●	71%	195	680

Standard errors of as much as ±20% of the plotted value were found, but were not plotted in the interests of clarity.

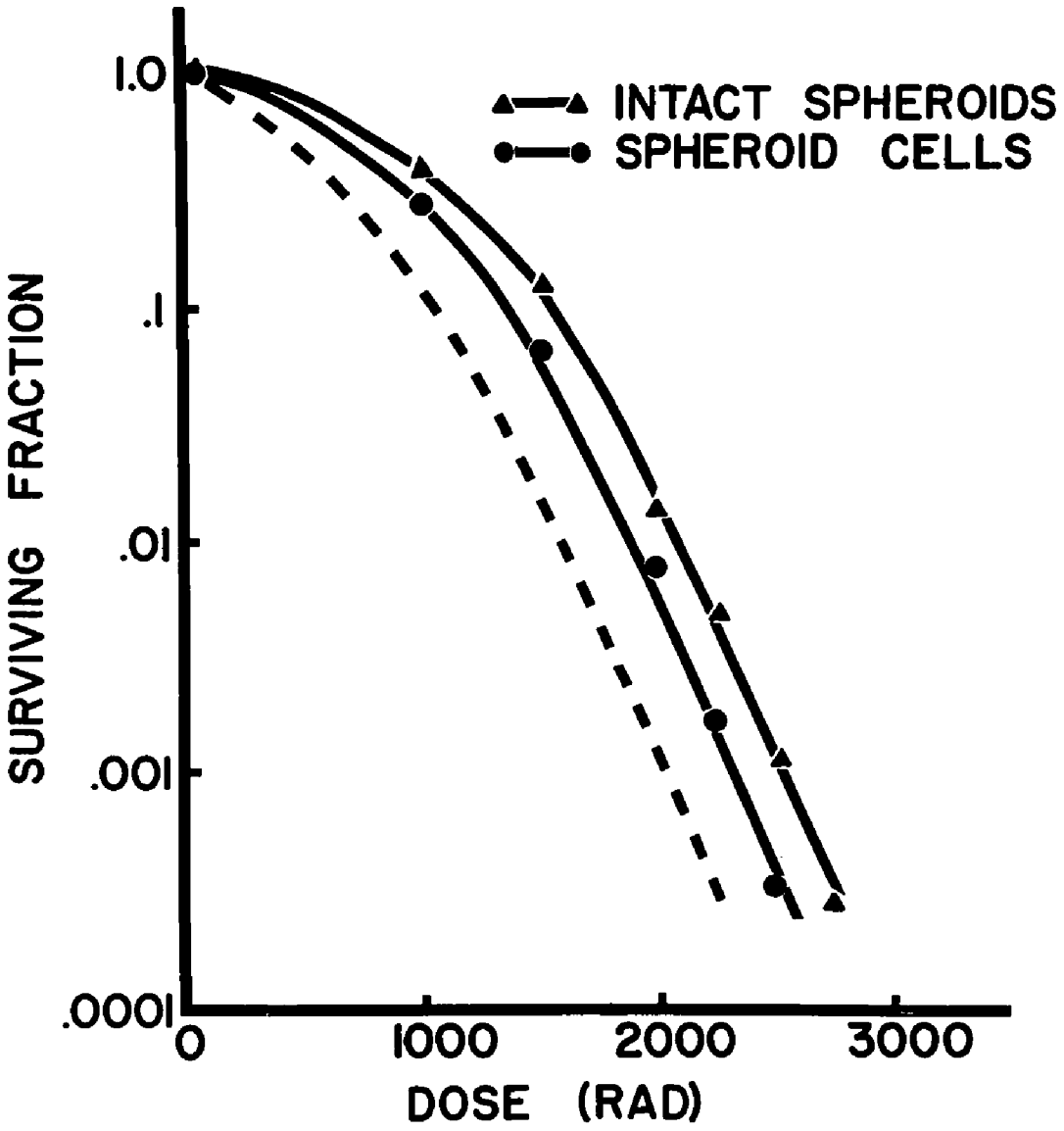
INTACT SPHEROIDS
SPHEROID CELLS
SURVIVING FRACTION
1.0
.1
.01
.001
.0001
0
1000
2000
3000
DOSE (RAD)

2.3.4 Summary

The results presented in this section have indicated that the capacity for accumulation of sublethal radiation damage in the V79-171b cells increases when the cells are grown in contact as spheroids, or in confluent monolayers on plates. Cells from spheroids required about one doubling time to acquire this enhanced repair capacity, and lost the effect as well after about one cell cycle when separated. The enhanced accumulation of sublethal damage was demonstrated to be a metabolically dependent process which was inhibited by low temperatures. Long-term contact after irradiation was found to increase survival even more, suggesting that cells grown in conditions of tight contact might not survive radiation independently.

2.4 Discussion

The results presented in section 2.2 characterized the growth and morphology of Chinese hamster V79-171b cells in suspension culture as multicellular spheroids. It was demonstrated that the degree of cellular organization which occurs in the spheroid leads to a compact structure where intercellular contact is close enough to allow formation of specialized cell junctions. The interpretation of many of the results presented in this

and subsequent chapters is critically dependent on these morphological demonstrations of cellular organization.

The culturing conditions employed provided spheroids of reproducible sizes after one day of growth, but greater difficulty was experienced in maintaining equivalent growth conditions in separate flasks for longer intervals (see figure 2.2). All experiments showing changing radiation survival patterns as a function of time were therefore conducted with the continuous culturing apparatus (see Appendix 1) which ensured that, at any given time, all remaining spheroids had an identical history. Many other single experiments were, however, conducted using spheroids grown in the smaller flasks, so care was taken to standardize growth conditions. It was not, however, deemed possible to completely reproduce survival curves for different batches of spheroids grown for more than one day.

The enhanced capacity for accumulation of sublethal radiation damage seen for cells grown in contact may be limited to the V79-171b cell line, since most (Stewart 1968, Little 1969a and 1969b, Belli et al 1970, Berry et al 1970, Chapman et al 1970b, Little 1971) cell lines have a decreased extrapolation number in plateau phase. However, under appropriate conditions of nutrition, at least two cell lines show no decrease in accumulation of

sublethal damage (Stewart et al 1968, Berry 1970). Much larger increases in the survival curve shoulder were found for spheroids, suggesting that degree of contact may be important. It was also consistently observed that spheroids which, for any reason, formed loose aggregates of cells rather than tight clusters, also had a radiation survival characterized by a lesser capacity for accumulation of damage. Assuming that many cell lines on plates do not have close intercellular contacts may explain, at least in part, the results previously cited for confluent cells.

It has been suggested by Little (1971) that under some growth conditions, cells may produce a radioprotective substance which is liberated into the medium. 'Conditioned' medium from spheroid cultures was not found to influence the response of exponentially growing single cells. The post-irradiation trypsinizing procedure was also judged to be incapable of inducing the increased survival, since control cells trypsinized after irradiation showed no increase in survival, but in fact a slight decrease. At the time of irradiation, both spheroids and control cells were in asynchronous exponential growth as determined by autoradiography (see figures 3.2a and 3.2b), indicating that the effects produced were not due to spheroids containing cells prefer-

entially accumulating in a radiation resistant part of the cell cycle. Although growth conditions in suspension culture have not been completely eliminated as an explanation of the results presented, several considerations tend to refute this possibility. The magnitude of the effects observed, as well as the dependence of survival on cell multiplicity in the spheroids suggested that culturing conditions alone were of secondary importance. Medium which contained only the divalent cations of the serum complement was employed in an attempt to grow single cells in the spinner flasks as controls. Spheroids of essentially normal multiplicity developed, but the degree of intercellular contact was found to be visibly reduced. These spheroids had a slightly reduced capacity for sublethal damage accumulation as reflected by an extrapolation number of about .9 of the normal value. In contrast, cells grown on plates in identical medium increased the extrapolation number by a factor of 4 . These results tend to suggest that intercellular contact was of greater significance than the culturing conditions.

Demonstrations that cells in contact are capable of bioelectrical (Loewenstein 1966, Loewenstein and Kanno 1966a and 1966b) and biochemical (Bendich et al 1967, Burk et al 1968, Subak-Sharpe 1969, Kolodny 1971) com-

munication certainly suggest cell responses to physical stimuli may be influenced by neighboring cells. In addition, more direct influence of healthy cells on the growth properties of irradiated cells of the same type has been demonstrated by Froese (1967). If cells in contact are able to sustain more damage after irradiation, one would speculate that neighboring cells may exchange large molecules (repair enzymes or 'complexes') at the time of irradiation. The recent demonstration by Kolodny (1971) that cells in contact can exchange RNA suggests that cells have this capability.

It is somewhat more difficult to interpret the enhanced capacity for repair of sublethal damage which results from growth as spheroids, and the reversion of the cells to a 'normal' state with time as suggested by figure 2.10 . One can speculate, however, that growth as spheroids, or at least under conditions of intercellular contact, constitutes an environment in which the cellular 'repair mechanism' is capable of operating at increased efficiency. This may be somewhat analogous to the proliferation-inhibiting environment required for repair of potentially lethal radiation damage (Belli and Bonte 1963, Phillips and Tolmach 1966, Hahn et al 1968, Stewart et al 1968, Little 1969a and 1969b, Belli et al 1970, Mauro and Little 1970, Little 1971), although cellular prolifer-

ation does continue normally in the present case. If this hypothesis is correct, one would expect repair capabilities to return to the 'normal' state as the cell readjusted to the 'normal' environment. The converse is of course true as the spheroids develop.

The data presented concerning non-independence of cellular survival contains an apparent contradiction. Evidence presented in the next chapter will indicate that spheroids irradiated at a given time, and allowed to remain as spheroids for intervals as long as one cell cycle period do not show an enhanced survival relative to spheroids trypsinized and assayed immediately. In the present case, the cells remained in contact for 8 days, suggesting one of two possibilities. As one alternative, it may be that the non-independence of survival occurs in a succeeding generation, that is, contact is required to retain viability of daughter cells of those actually irradiated. Conversely, the trypsinization procedure at any time during the first generation cycle after irradiation may be synergistic with that radiation, and thus cause the decreased survival. If the latter interpretation is correct, the survival decrease associated with trypsinized spheroids (figures 2.9 and 2.10) may be an artifact, and growth in contact may be responsible for the entire contact effect. Synergism of trypsin and rad-

iation must be invoked, since the survival of the irradiated spheroids was corrected for the plating efficiency of the unirradiated, trypsinized spheroids. Although extrapolation of results obtained with single cells to the spheroid system may not be justified, preliminary experiments with trypsin and single cells failed to detect any trypsin-radiation synergism, but did confirm that cell growth was inhibited for short times after trypsinization as reported by Berry et al (1966).

III. CELL CYCLE REDISTRIBUTION AND RADIATION SURVIVAL

3.1 Introduction

The individual cells of the multicellular spheroid receive essential nutrients only by diffusion from the periphery. The internal cells are thus handicapped due to the large distances the metabolites must traverse as well as the fact that the more external cells actively consume at least part of all nutrients that reach them (Tannock 1968, Tannock 1970). Cellular waste products may also accumulate internally, due to similar diffusion limitations. One would thus predict that not all cells of large spheroids would enjoy optimal growth conditions, and the observation of central necrosis shows that, in the center of the spheroid, conditions must indeed be far from optimal.

A similar situation has been postulated to occur in tumors *in vivo*, and has been demonstrated histologically for several experimental and human tumors (Thomlinson and Gray 1955, Tannock 1968, Tannock 1970). The exact state of individual cells at the intermediate stages where nutrient supply is impaired by diffusion limitations but not completely eliminated is not yet known. However, it appears that the cells remain viable and undergo redistribution into different phases of the

cell cycle (Mendelsohn 1962a and 1962b), or simply cycle at much slower rates with one or more periods of the cell cycle extended (Tannock 1968 and 1970, Hermens and Barendsen 1969, Denekamp 1970).

Accumulation of cells in a specific part of the cell cycle may prove to be advantageous or disadvantageous to the radiotherapist, due to the radiosensitivity of the cells at that particular position and ability of the cells to accumulate and repair radiation damage (see Appendices 2 and 3). In any event, it is highly likely that a mixed cell population with respect to cell cycle position does occur in most in vivo tumors, thus altering the tumor response to radiotherapy (Oliver and Lajtha 1961, Hermens and Barendsen 1969).

3.2 Cell Cycle Redistribution in the Spheroid

3.2.1 Introduction

Evidence will now be presented to confirm that a redistribution of cells in the cell cycle does occur in the spheroid as it enlarges. Like many solid tumors, the mature spheroid will be shown to contain an external population of cells that are actively proliferating, and another, internal fraction which progresses through the cell cycle slowly if at all.

3.2.2 Methods of assessing cell cycle position in the spheroids

Large spheroids were reduced to single cells by trypsinization in a manner analogous to the trypsinization of small spheroids described in section 2.2.3, with two exceptions. Spheroids were typically collected in a tube, and allowed to sediment to the bottom. The supernatant was then removed by aspiration, and the spheroids resuspended in 3 ml of 37°C trypsin (prepared as previously described). They were then allowed to sediment again, and the process repeated, then transferred in the trypsin to the dishes on the mechanical agitator. The remainder of the process was identical to the procedure previously described in section 2.2.3 .

Information about cell cycle distributions was obtained by allowing the cells to incorporate thymidine having tritium substituted at the 5-methyl position (purchased from New England Nuclear, .05 mM, specific activity 20 Ci/mM). For short or 'pulse' labelling experiments (10-20 minutes), a concentration of .001 mCi/ml was typically used for single cells or spheroids; for continuous exposures this was reduced by ten, and fresh medium and isotope were supplied daily. At the termination of either labelling period, spheroids were washed with BME (containing thymidine) and reduced to single cells by trypsinization. These cells were then swollen in slightly hypo-

tonic medium prepared by adding an equal quantity of distilled water to the medium-trypsin solution containing the single cells. After 15 minutes, Carnoy's fixative (75% ethanol plus 25% glacial acetic acid) was added, the cells were centrifuged to a pellet (400g for 6 minutes) and the supernatant was discarded. This procedure was repeated after resuspension in Carnoy's fixative, and the final pellet was resuspended in a drop of fixative and dispersed on a clean microscopic slide. The cells were then stained with aceto-orcein until nuclear detail was clear and dried. At convenient times, slides were dipped in Kodak NTB-3 nuclear grain emulsion at 40°C (diluted 1:2 with distilled water, v/v), dried at room temperature for about 45 minutes, and placed in light-tight boxes at 4°C to develop for 8 days. The slides were developed for 2 minutes in Kodak D-19 developer at 16°C, washed and fixed 3 minutes in Kodak acid fixer. A region of the slide devoid of cells was examined to determine the background or non-specific exposure of silver grains, and cells with a higher density of exposed silver grains above the nucleii than the background level were scored as having been in S phase and incorporated the labelled thymidine into replicating DNA.

Regrowth experiments were used to determine the

distribution of cells in the cell cycle by observing their positions and growth phase immediately after being introduced into an environment of optimal growth conditions. In the case of the spheroids, a single cell suspension was prepared and inoculated into replicate growth plates containing BME + 15% FCS. Various aspects of growth were studied thereafter at the specific intervals indicated.

The cells analyzed by the Cytograf and Cytofluorograf instruments were prepared from exponentially growing cells on plates and day 11 spheroids. Both samples were reduced to single cells by trypsinization, and held in suspension in BME at room temperature for about an hour before analysis. This delay was unavoidable as the equipment was located in another laboratory. The cells were metachromatically stained by adding .001 ml of acridine orange per ml of cell suspension ten minutes before analysis.

3.2.3 Results

Dramatic evidence that a redistribution of cell cycle times actually occurs in the spheroid is shown in figure 3.1, which is an autoradiograph of three spheroids grown for 48 hours (> 4 normal generation times for exponentially growing single cells, as in figure 2.12) in

FIGURE 3.1

Photomicrograph of autoradiographic sections of spheroids of increasing sizes, labelled with ^{3}H-thymidine for 48 hours. Development of the decreased growth fraction is clearly shown, as all cells were labelled in the small spheroid (a), but only external cells were heavily labelled in the larger spheroids (b) and (c).

Magnification: X 250

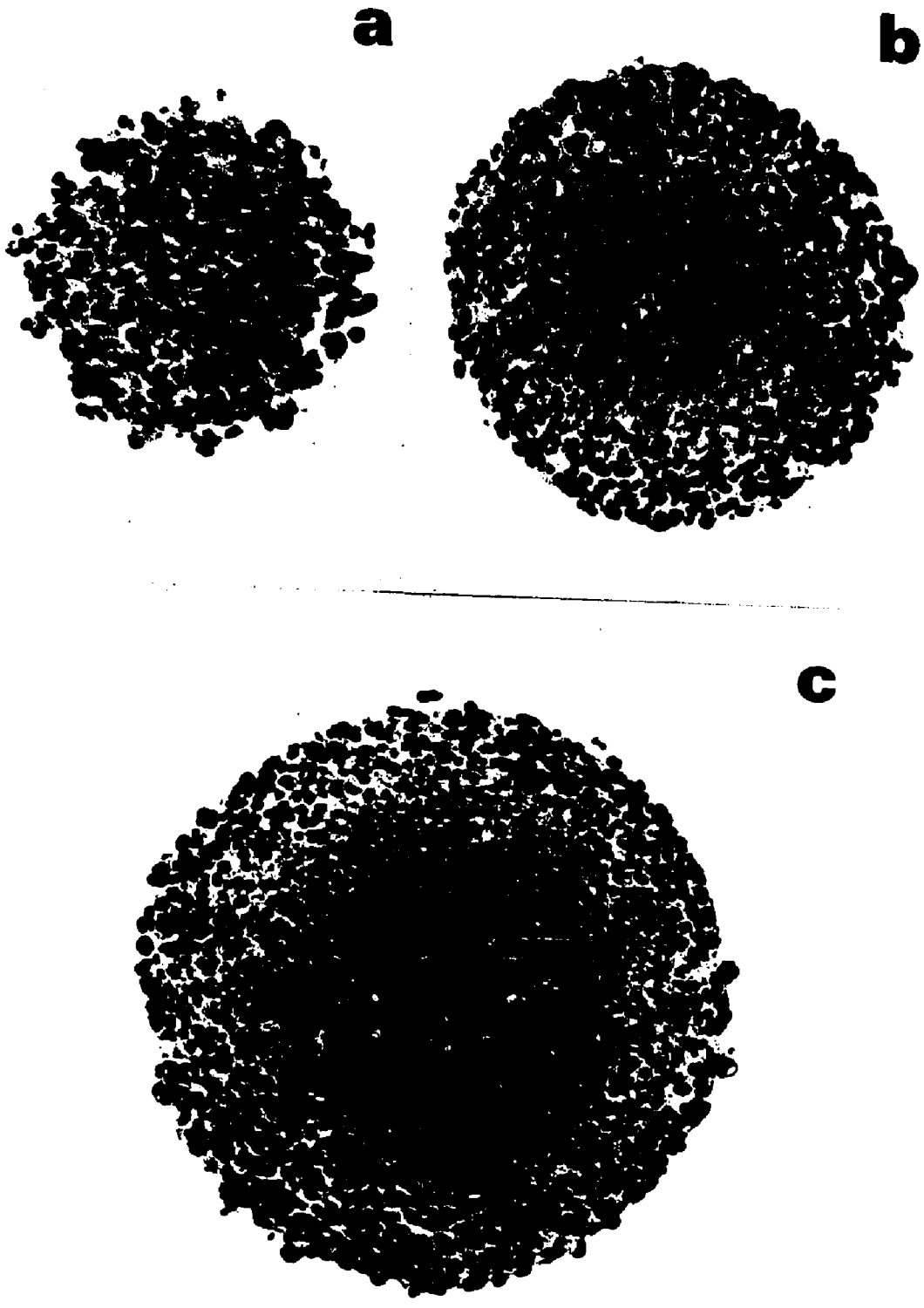
a
b
c

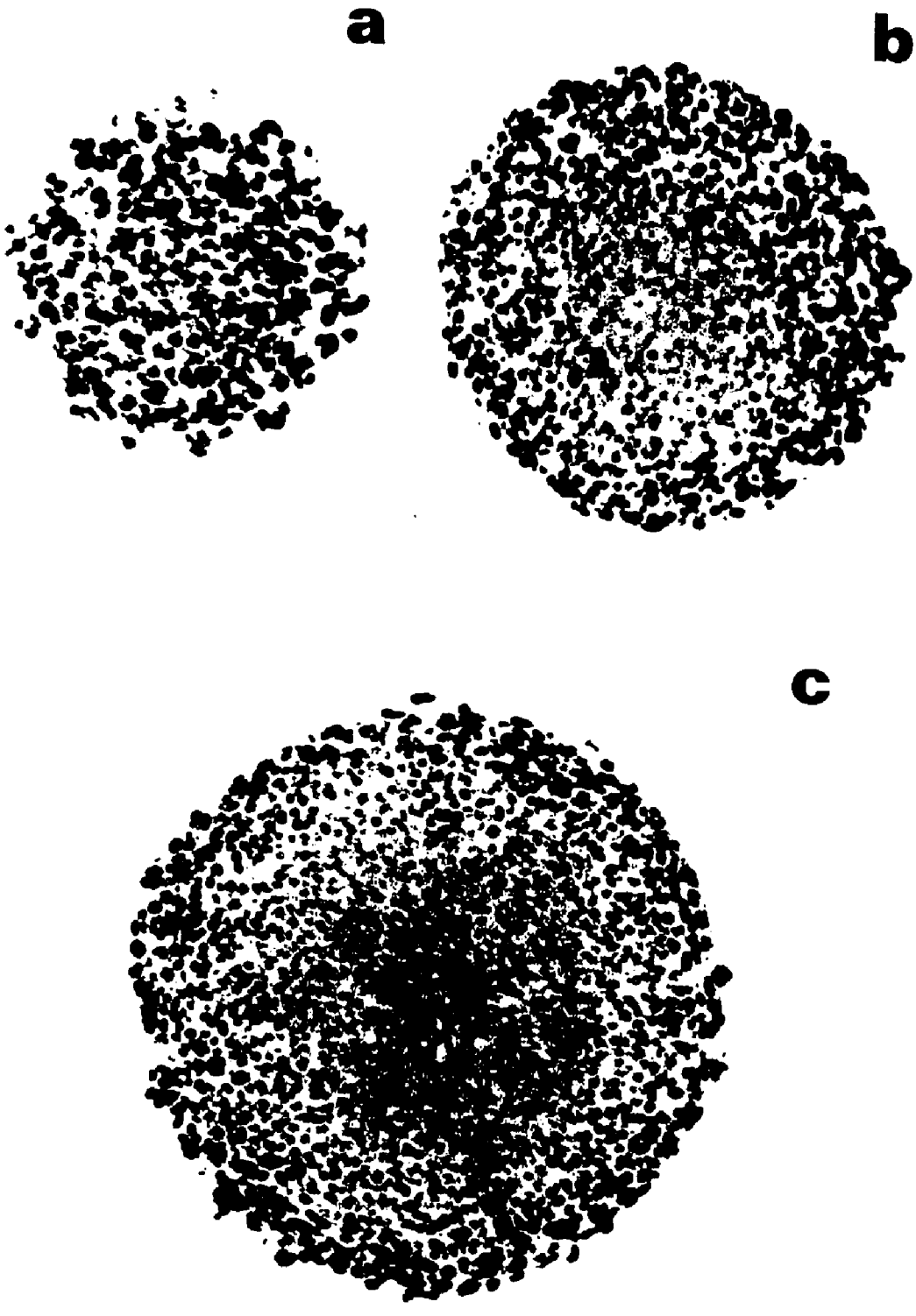
a
b
c

the presence of ^{3}H-thymidine. The small spheroid of figure 3.1a has every nucleus labelled, suggesting that all cells replicated their DNA at least once during the labelling period. Although the magnification of the figure is inadequate for examining the labelling density, examination of the actual slide under high power showed a very uniform labelling density. This suggested that all the cells synthesized roughly the same amount of DNA, which indicates that all of the cells were cycling at approximately the same rate.

The larger spheroid of panel (b) also had the external cells labelled with a density similar to those of (a). However, the internal cells were not as heavily labelled, suggesting either that these cells were synthesizing DNA at a slower rate, or that DNA had not been replicated as often in the internal cells.

More extreme differences in incorporation of ^{3}H-thymidine are shown in the large spheroid of figure 3.1c. The external cells were heavily labelled, but the label density decreased with depth into the spheroid until many of the cells bordering the necrotic zone did not appear to have incorporated any thymidine. This decrease in labelling density was not an artifact of the labelling procedure due to limited diffusion of the labelled thymidine, as other experiments where spheroids were pulse

labelled before or after reduction to single cells showed equal labelling indices and identical labelling patterns.

Quantitative experiments to determine the distribution of cells in the cell cycle were relatively easy to perform. One measure of proliferation is the mitotic index, that is, the fraction of cells which can be recognized morphologically as being in any stage of mitosis. Another useful technique is quantitative pulse labelling, where the fraction of cells that incorporate ^{3}H-thyminine (and thus were in S phase at the time of addition of the label) can be determined. While this technique is somewhat less informative with regard to the reproduction of the cell, it does indicate the relative length of S phase in comparison to the entire cell generation time (e.g. Ham 1970).

Two features were noted when intact spheroids were examined for mitotic cells. Only the external layers of cells included mitotic figures, with none found more than about six layers deep. In addition, the fraction of mitotic cells decreased as the spheroid size increased. Quantitative results were difficult to obtain in the intact spheroid however, as peripheral sections contained many more mitotic or labelled cells than did central sections. Thus, accurate counts could only be conducted by following serial sections of the spheroid and count-

ing every cell of the sections from at least half the spheroid. Additional problems in distinguishing between mitotic and necrotic cells occur for cells bordering the necrotic region.

The mitotic and labelling index data shown in figure 3.2 were obtained by analysis of spheroids reduced to single cells as described in section 3.2.2 . The decrease in mitotic index indicates a decreasing growth fraction (Mendelsohn 1962a and 1962b) as the age of the spheroids increased, while the decreased labelling index indicates that S phase occupied progressively less of the mean cell cycle time. These results, in combination with the observations made with regard to figure 3.1 suggested that there was a development of an internal, slowly cycling population of cells. Since the labelling effectively showed the average response of both the internal and external cells, it is apparent the DNA synthesis period occupied only a very small fraction of the cell cycle time of internal cells, if it occurred at all.

The cell cycle position of a majority of the internal cells was defined by a regrowth experiment. Single cells from day 12 spheroids were placed in petri dishes at time zero, and tritiated thymidine was added to the plates at various times after inoculation to

FIGURE 3.2

Mitotic and labelling indices of spheroids as a function of spheroid age.

(a) Mitotic index, or number of mitotic cells per 2000 cells observed as a function of time in culture.

(b) Labelling index, or number of cells that incorporated ^{3}H-thymidine into replicating DNA (during a 10-minute pulse) per 500 cells observed autoradiographically, as a function of time in culture.

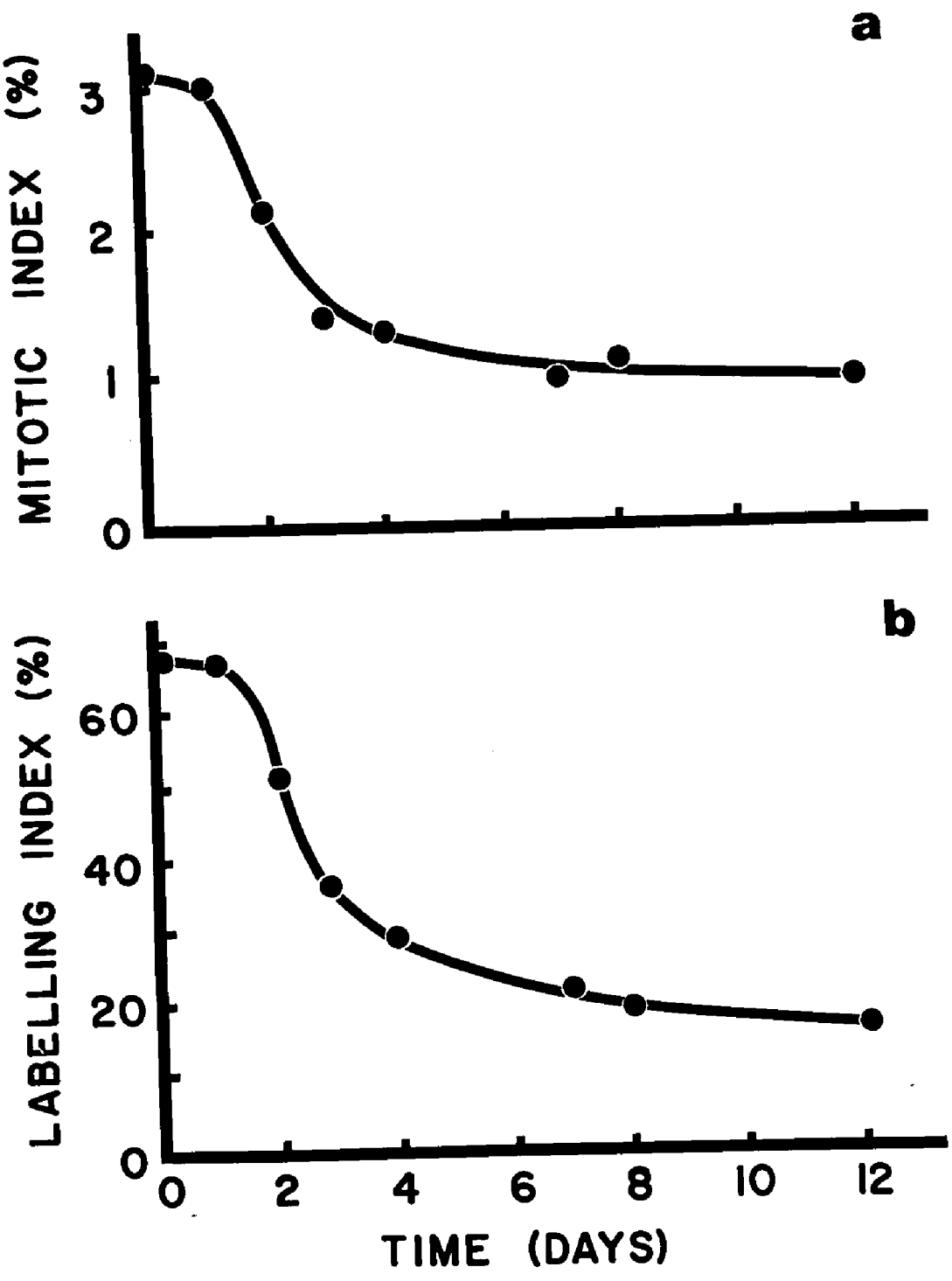
a
MITOTIC INDEX (%)
3
2
1
0
b
LABELLING INDEX (%)
60
40
20
0
0
2
4
6
8
10
12
TIME (DAYS)

determine the number of cells synthesizing DNA. As indicated in figure 3.3b, about 20% of the cells were in S phase anytime during the first six hours, but nearly 80% of the cells were labelled at 15 hours. The rapid increase in labelling index from 9 to 15 hours, and the subsequent mitotic peak at 21 hours (figure 3.3a) showed that the majority of the spheroid cells were synchronized in a pre-DNA synthetic phase of the cell cycle (i.e. G_1 or a G_1-like phase). Unless partial synchrony had developed, one would expect a very gradual rise in the labelling index, starting immediately after incubation of the growth plates. The slight increase in mitotic index at 9 hours, prior to the labelling index peak, suggested that a small fraction of the cells may have accumulated in G_2 phase.

An additional method of characterizing the spheroids was provided by electronic equipment designed by Biophysics Instruments. The Cytograf directs a single-file flow of cells through a micro-laser beam. Disruption of the beam by individual cells varies according to their cross-sectional area, and can be electronically recorded and displayed as in the top panels of figure 3.4 . If the first vertical grid mark is taken as channel 0 on the abscissa, then there are 100 channels of information, 10 channels per grid. As can be seen in the

FIGURE 3.3

Mitotic index and labelling index of cells regrown for various times, and obtained from a day 12 spheroid at time 0.

(a) Mitotic index, or number of mitotic cells per 2000 cells observed as a function of time after initiation of regrowth.

(b) Labelling index, or number of cells that incorporated ^{3}H-thymidine (during a 10-minute pulse) per 1000 cells observed autoradiographically, as a function of time after initiation of regrowth.

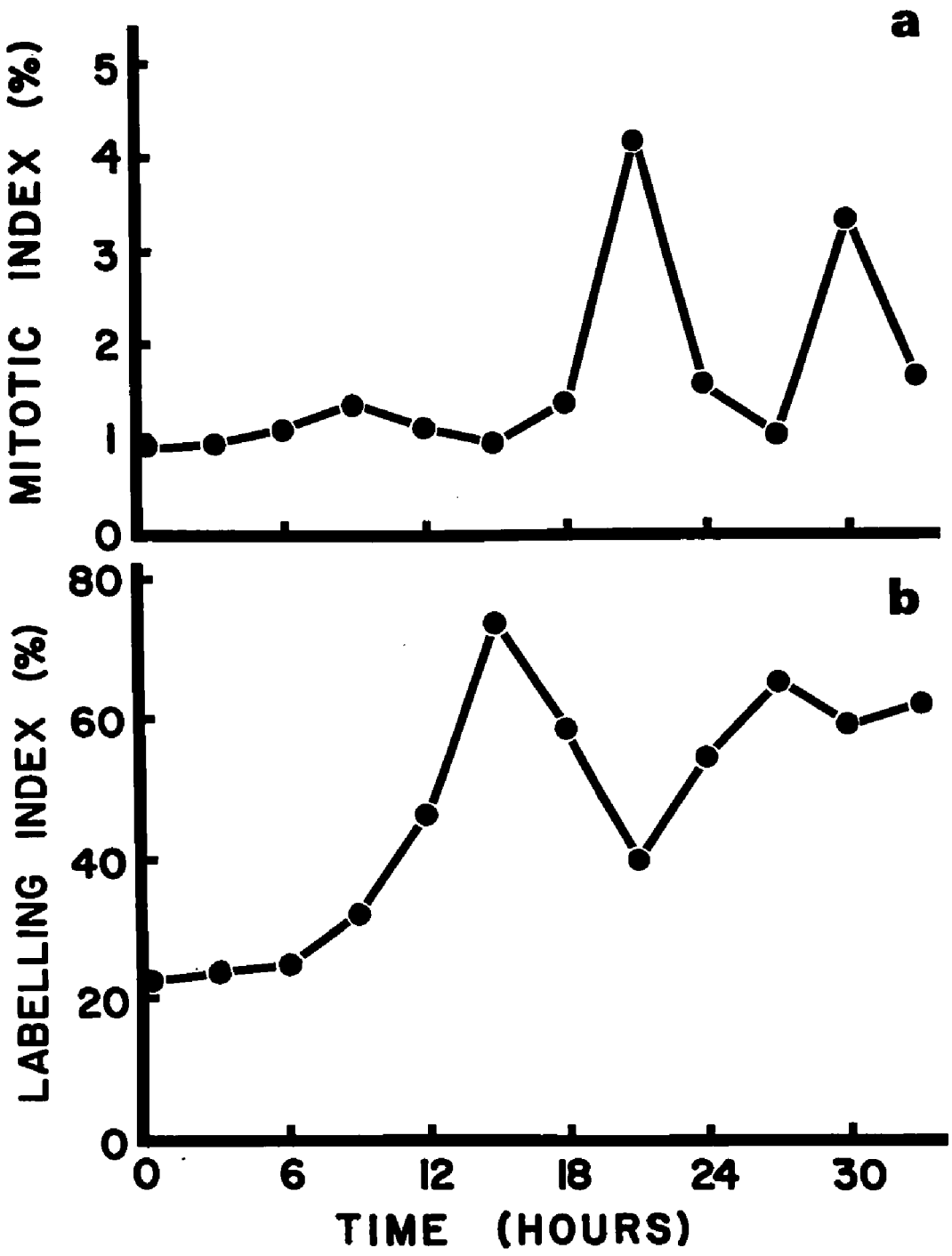
a
MITOTIC INDEX (%)
0
1
2
3
4
5
b
LABELLING INDEX (%)
0
20
40
60
80
0
6
12
18
24
30
TIME (HOURS)

FIGURE 3.4

Characterization of cells grown on petri dishes or from a day 11 population of spheroids. The upper panels show histograms of cell sizes (cross sectional area) for the two growth conditions. Using acridine orange as a metachromatic stain, the relative cellular quantity of RNA (red fluorescence) and DNA (green fluorescence) was observed for the two growth conditions (see text for additional details).

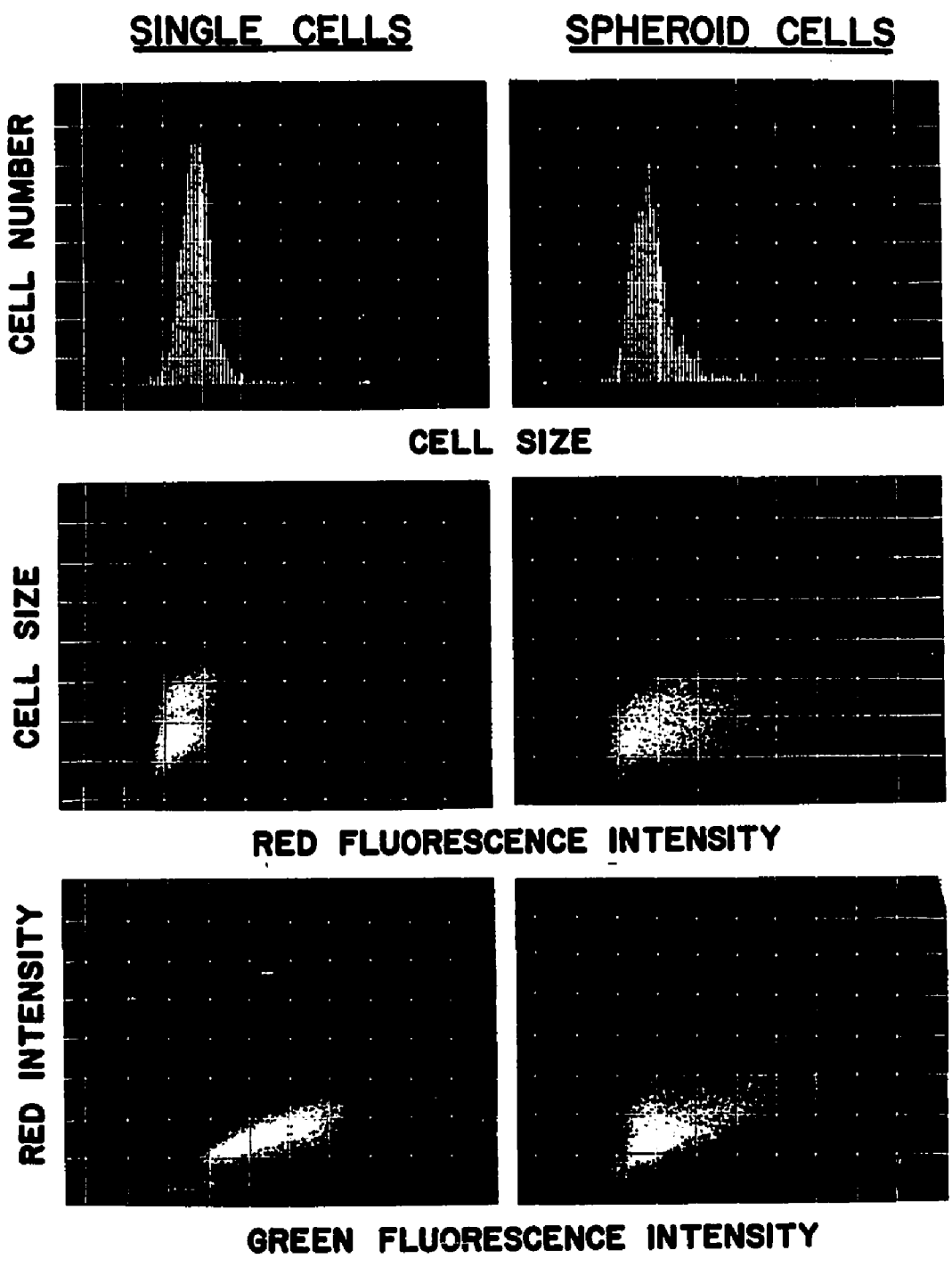
SINGLE CELLS
SPHEROID CELLS
CELL NUMBER
CELL SIZE
CELL SIZE
RED FLUORESCENCE INTENSITY
RED INTENSITY
GREEN FLUORESCENCE INTENSITY

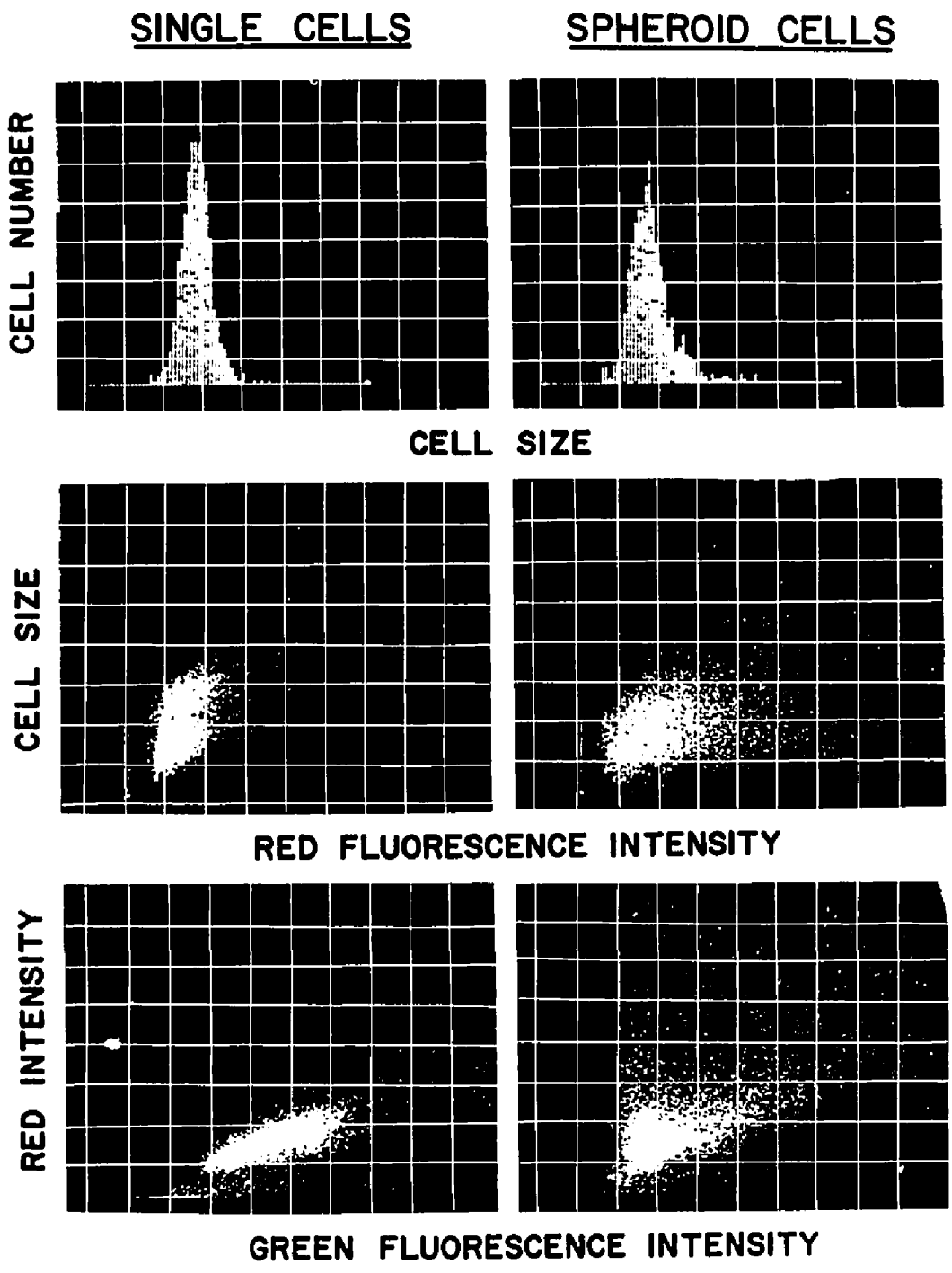
SINGLE CELLS
SPHEROID CELLS
CELL NUMBER
CELL SIZE
CELL SIZE
RED FLUORESCENCE INTENSITY
RED INTENSITY
GREEN FLUORESCENCE INTENSITY

histograms, the modal cross-sectional area of single cells corresponded to channel 28, whereas the spheroids had a modal cell area corresponding to channel 27. More cells were found in channels 29-35 for single cells than for spheroids. In contrast, more spheroid cells were found in channels 24-27, thus indicating that the mean cell size was smaller in the spheroids. Since cell size is known to increase as the cell ages in its generation cycle (e.g. Chapman 1970b), the present results suggest that the cells in the spheroid were accumulating in an early stage of the cell cycle. This, together with the results of the previous figure (3.3), suggests that the cells had accumulated in a G_1-like phase.

Further characterization of the cells was accomplished with the Cytofluorograf, a miniature fluorometer which used a laser beam to activate metachromatic fluorescent dyes (Adams et al 1971, Melamed et al 1972). Acridine orange binds to DNA and RNA, and fluoresces green and red respectively. Since total fluorescence is measured by the instrument, this can be related directly to the total DNA or RNA content per cell. The middle panels of figure 3.4 show red fluorescence as a function of cell size for the two growth conditions. Cells were again slightly smaller in the spheroid, but many cells had an increased red intensity, or greater

RNA content. The significance of these results alone is difficult to interpret, but may suggest either that the increased RNA content per cell represents a type of 'maintenance' operation within the spheroid cells, or perhaps simply represents a greater cytoplasmic volume in the spheroid cells.

The lower panels of figure 3.4 show red fluorescence as a function of green fluorescence, which is essentially the cytoplasmic to nuclear ratio (Melamed et al 1972). Most interesting in these panels was the position of the mean intensity of green fluorescence (about channel 45) in the single cells as compared to spheroid cells (channel 30). This indicated that the mean DNA content per cell was about 50% larger in the single cells, consistent with accumulation of a G_1 population in the spheroids. It was also interesting to note that the cells which had large amounts of red fluorescence (and thus presumably large quantities of cytoplasm) were not necessarily found to always have equally large quantities of green fluorescence. These large cells probably represented 'giant' cells for low levels of green fluorescence, and multinucleated cells for the higher levels. These results were obtained with only one sample during a demonstration of the instruments by the manufacturer, but have been included here

since they provide additional and unique collaborative data.

Figure 3.5 is a high power view of a spheroid grown in the presence of ^{3}H-thymidine for 48 hours. Comparison with figure 3.1 shows that, at the higher magnification, many of the internal cells were clearly labelled. This would indicate that the internal cells were in fact cycling slowly, or at least most had incorporated some of the label during the labelling time. Longer labelling times resulted in a higher proportion of the internal cells being labelled, but complete labelling was never observed indicating that some of the cells had stopped cycling completely, or at least were unable to replicate their DNA. Alternate explanations of the internal labelling include degradation of the labelled thymidine and non-specific uptake, or possible maintenance or repair of DNA in the internal cells. It is also possible that cells may not occupy fixed positions in the spheroid, and may thus become labelled when in the external layers of cells and then migrate into the central regions. In view of the evidence of section 2.2, this suggestion was deemed unlikely.

3.2.4 Summary

The data presented in this section has shown that as the spheroids increase in size, there is a progressive

FIGURE 3.5

High-power photomicrograph of an autoradiography section through a ^{3}H-thymidine-labelled spheroid. The spheroid was grown in the presence of the label for 48 hours. Note that many internal cells are lightly labelled.

Magnification: X 700

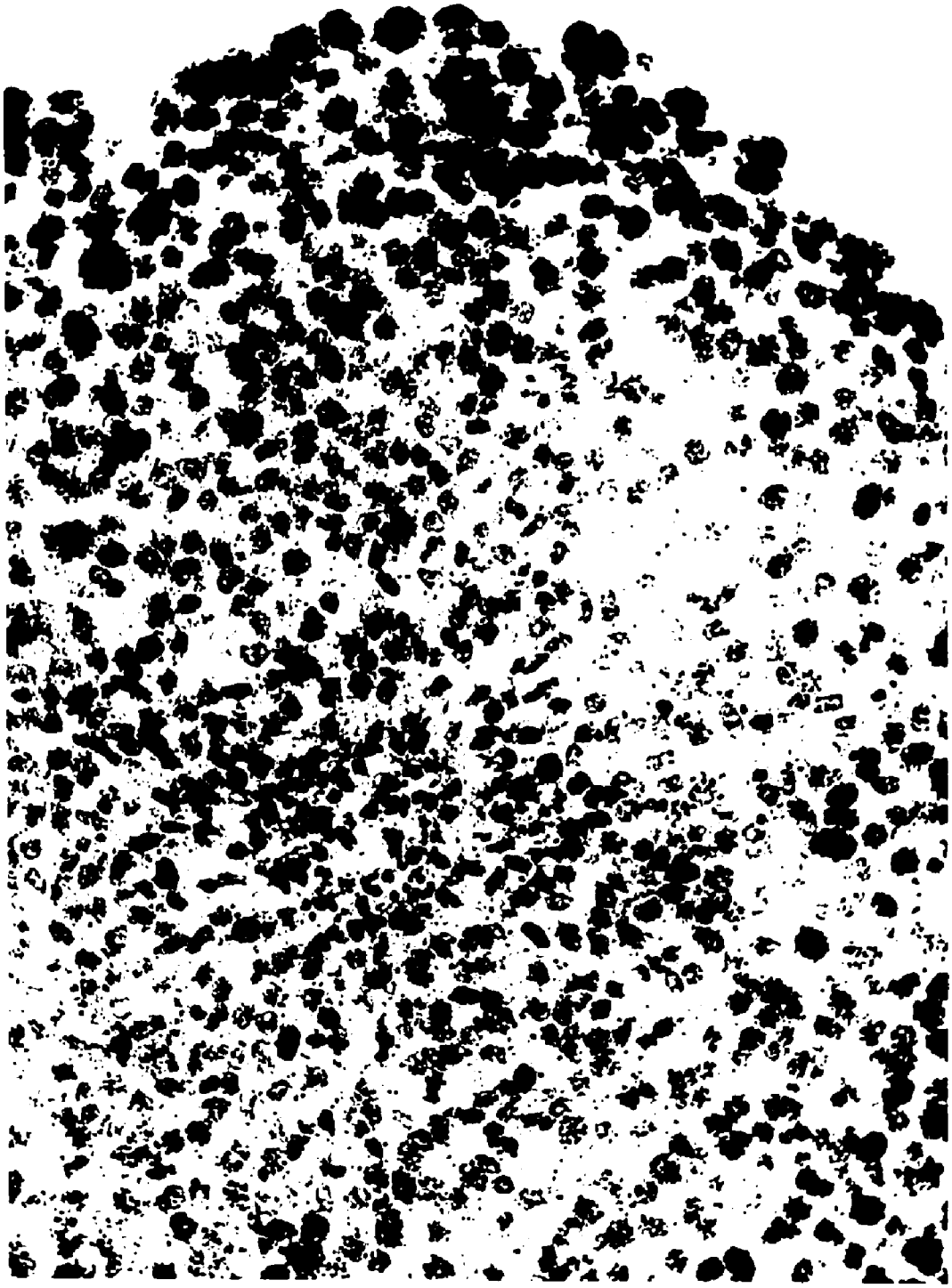

decrease in the growth fraction. The actual status of the internal cells in the division cycle has not yet been unequivocally established, as partial synchrony in a G_1-like position of the cell cycle is suggested by figures 3.3 and 3.4, whereas figure 3.5 suggests that most of the cells eventually incorporate labelled thymidine and thus are cycling slowly.

3.3 Radiation Survival and Intercellular Contact at Different Stages of the Cell Cycle

3.3.1 Introduction

It is well known that the survival of single mammalian cells shows large fluctuations when the cells are irradiated at various stages of the cell cycle (Terasima and Tolmach 1963, Sinclair and Morton 1966, Elkind and Whitmore 1967, Sinclair 1968, Okada 1970). Since the spheroid system develops populations of cells that are redistributed in the cell cycle as the spheroid ages, the survival of large spheroids is obviously dependent on both contact and cell cycle effects.

This section contains data which characterize the effects of intercellular contact as the spheroid cells progress through their cell cycles, by comparing responses of the maturing spheroids with synchronous, small spheroids. Correlation of the enhanced capacity for

accumulation of sublethal radiation damage and the capacity for repair of such damage is made.

3.3.2 Methods of synchronizing small spheroids

Small spheroids were synchronized after 24 hours of growth by adding colcemid at a final concentration of 0.5 microgram/ml to the culture flask. Fourteen hours later, the spheroids were centrifuged and washed twice with BME at 4°C, then resuspended in fresh, warm medium in the culture flask. Single cells from plates were either collected by mitotic selection (Terasima and Tolmach 1963) or similarly exposed to colcemid, removed from the plates in the supernatant and treated identically to spheroids except that the single cells were replaced in plates. Samples of the synchronous spheroid or single cells were then removed and treated as required.

Partial synchronization of Chinese hamster cells by removal of all those in S phase was accomplished by treatment with hydroxyurea (HU). Preliminary experiments established that HU was selectively lethal to only S phase cells, and that all cells would attach to growth plates equally well with the chemical present or absent. No potentiation of radiation damage was ever observed (see Sinclair 1968, Phillips and Tolmach 1966). Selection of non-S

cells was always performed after irradiation and trypsinization by plating the single cell suspension directly into complete medium containing 2 mM hydroxyurea. Two hours later, the medium + HU was aspirated off the plates and discarded, the plates washed with BME, and fresh growth medium (BME + 15% FCS) added to the plates.

3.3.3 Results

The survival of cells from spheroids grown in the continuous culture flask (see Appendix 1) as a function of time in culture are shown in figure 3.6 . The initial inoculum of cells had typical survival characteristics, with D_o = 169 ± 21 rad, and n = 10.2 . After one day in culture, the value of n increased to 210 (the broken curve in figure 3.6b is the curve of figure 3.6a). By day 2, some decrease in survival was apparent, relative to the upper broken curve indicating day 1 survival (n = 104 in panel (c)). Day 4 spheroids showed a definite survival decrease (n = 41), indicating that a population of more sensitive cells was accumulating.

A rigorous analysis of survival curves produced by mixed cell populations is not included here, since it is sufficient for the present data to note that the most resistant population of cells always determines the final

FIGURE 3.6

Survival of cells grown as spheroids and irradiated at 37°C in air (140 rad/min). Broken curve in panel (b) is the curve from panel (a); the broken curves in panels (c) and (d) are the same as the two curves of panel (b).

Panel	PE	D_o	n
(a)	91%	169±21	10.2
(b)	55%	166±20	210
(c)	62%	174±10	104
(d)	65%	171±31	41

Uncertainties in the above parameters represent the 95% confidence intervals.

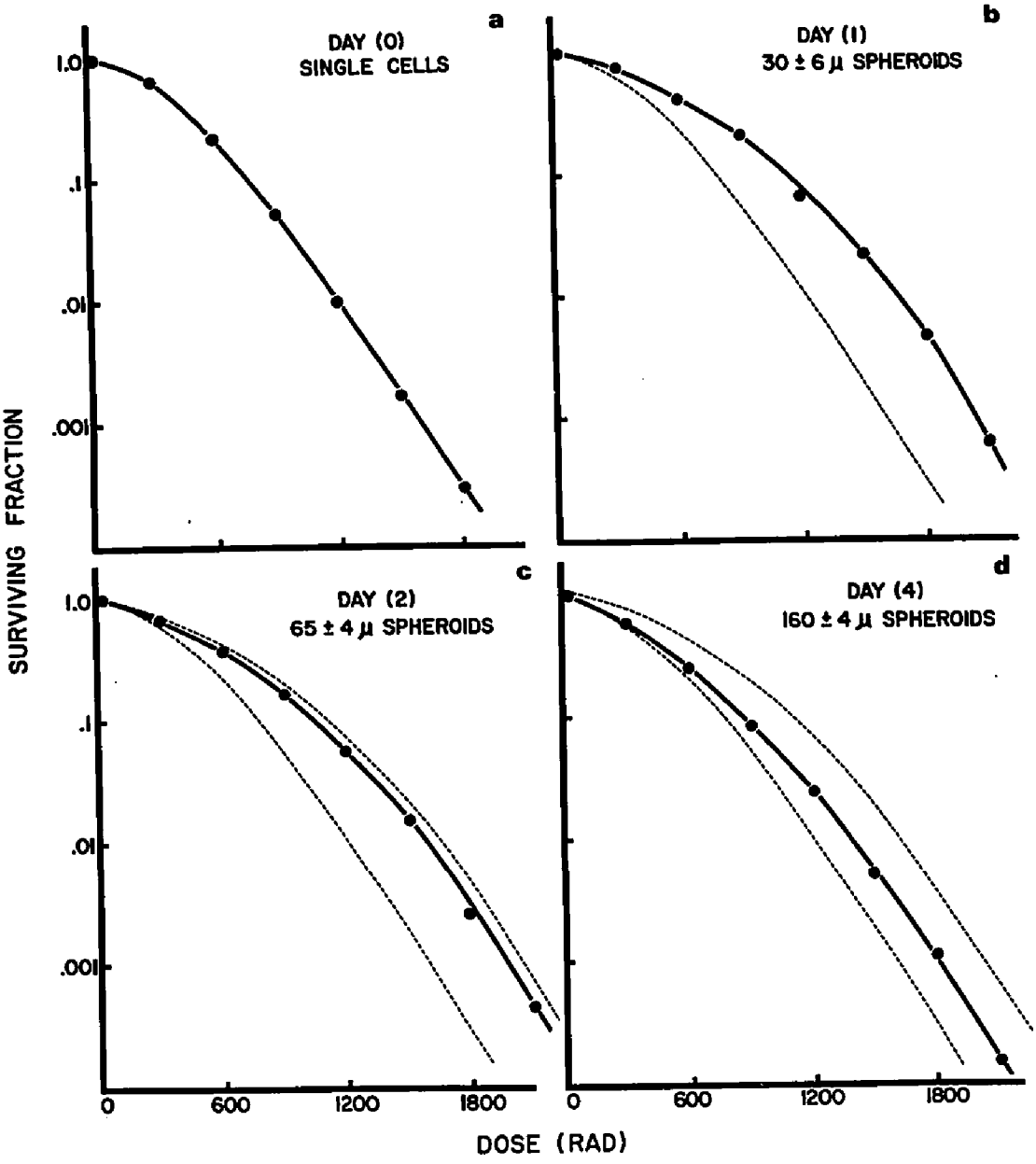
a
DAY (0)
SINGLE CELLS
b
DAY (1)
30 ± 6 μ SPHEROIDS
c
DAY (2)
65 ± 4 μ SPHEROIDS
d
DAY (4)
160 ± 4 μ SPHEROIDS
SURVIVING FRACTION
1.0
.1
.01
.001
0
600
1200
1800
DOSE (RAD)

characteristics of the survival curve, and that a reduction in the extrapolation number of the terminal portion of the survival curve reflects an equal reduction in the relative fraction of such cells (see Appendix 2). Thus, in figure 3.6d, the obvious resemblance of the terminal slope (171 ± 31 rad) with that of asynchronous spheroid cells (166 ± 20 rad) suggested that they were asynchronous, cycling cells and comprised 20% of the population while the remaining 80% had accumulated in a more sensitive region of the cell cycle.

The most resistant stage of the cell cycle in Chinese hamster V79-171 cells is known to be late S phase (Sinclair and Morton 1966), and this was confirmed in preliminary experiments with our subline. Since the chemical hydroxyurea (HU) is known to selectively kill hamster cells in S phase, while blocking non-S cells at the G_1/S interface (Sinclair 1965 and 1967), it was possible to use the chemical to selectively remove the most resistant cells. Control experiments with synchronous single cells confirmed the specificity of HU killing with this cell line.

Figure 3.7 shows the result of treating the same population of cells as shown in figure 3.6 with 2 mM hydroxyurea for two hours after the irradiation. As hydroxyurea was found to be a chemical radiosensitizer

FIGURE 3.7

Survival of cells grown as spheroids and irradiated at 37°C in air (140 rad/min), then treated with hydroxyurea to selectively kill S phase cells. This experiment was performed in parallel with that of figure 3.6, and the broken curves in each panel are the curves for untreated cells as in the same panels of figure 3.6 .

Panel	PE	D_o	n
(a)	38%	163±20	3.4
(b)	21%	174±21	32.6
(c)	31%	158±11	52
(d)	53%	121±15	102

Uncertainties in the above parameters represent the 95% confidence intervals.

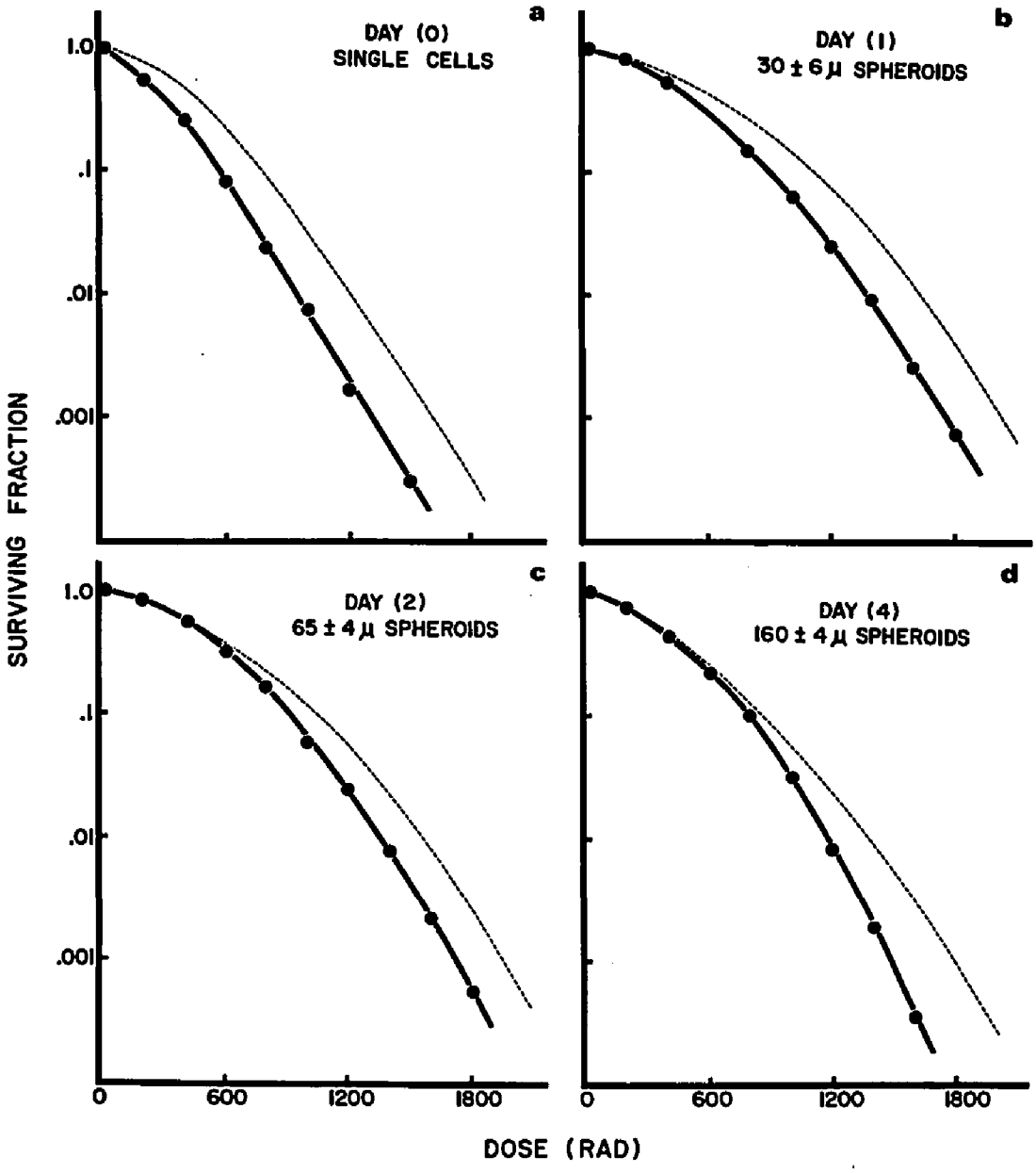
a
DAY (0)
SINGLE CELLS
b
DAY (1)
30 ± 6 μ SPHEROIDS
c
DAY (2)
65 ± 4 μ SPHEROIDS
d
DAY (4)
160 ± 4 μ SPHEROIDS
SURVIVING FRACTION
1.0
.1
.01
.001
0
600
1200
1800
DOSE (RAD)

when present during irradiation in preliminary experiments, post-exposure treatment was always used to ensure that only specific elimination of S phase cells occurred. As can be seen in figures 3.7a and 3.7b, treatment of single cells and day 1 spheroids effectively reduced the extrapolation numbers of the curves compared with the broken curves which duplicate the solid curves of figure 3.6 (n = 3.4 and 32.6 for figures 3.7a and 3.7b respectively). However, by day 2 and definitely by day 4, the non-S phase cells were more radiosensitive. The curve for day 2 has a D_o or mean lethal dose of 158 ± 11 rad, and was significantly different by day 4 with a D_o of 121 ± 15 rad. It is important to note that only a partial selection of the cells can be obtained with the HU treatment, since the viabiliby of G_2, G_1 and M cells was unaffected by the chemical.

Comparison of these results with those presented in section 3.2, which indicated that an internal population of G_1-like cells developed in large spheroids, suggested that these cells were responsible for the decreased survival seen in day 4 spheroids (compare figures 3.6d and 3.6b). The survival pattern of spheroid cells irradiated after various intervals of regrowth on plates confirmed that the partially-synchronized cells were relatively radiosensitive. Figure 3.8 shows that the cells from the spheroids had the usual decrease in

FIGURE 3.8

Multiplicity and radiation survival of cells regrowing from a population of day 9 spheroids.

(a) Number of cells per microcolony on the plate, or multiplicity as a function of time after regrowth was initiated.

(b) Isodose (1450 rad) survival of cells incubated at 37°C and regrowing for various times before irradiation at 24°C (155 rad/min).

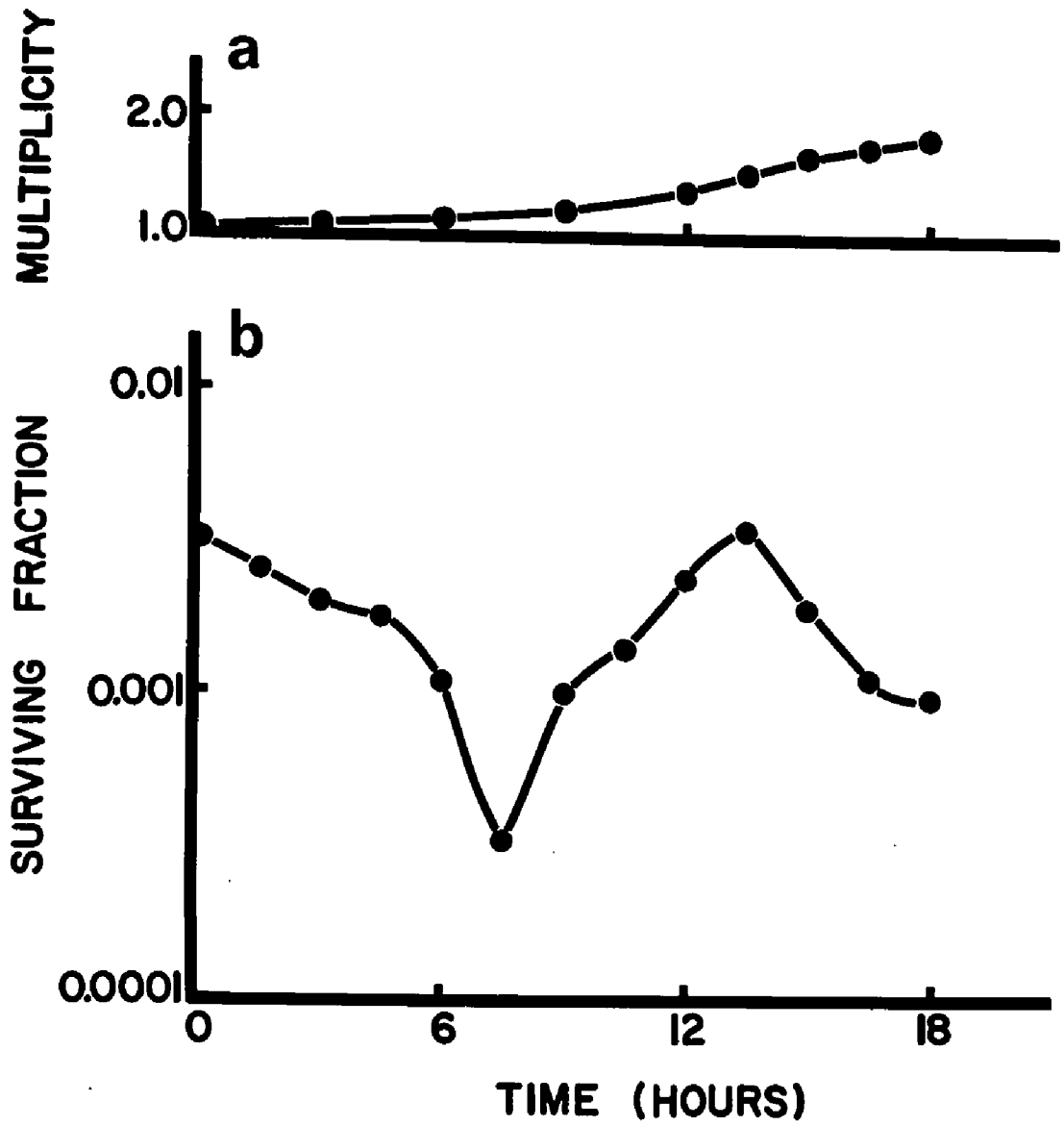
a
b
MULTIPLICITY
2.0
1.0
SURVIVING FRACTION
0.01
0.001
0.0001
0
6
12
18
TIME (HOURS)

survival accompanying separation, then increased survival during S phase with maximum survival preceeding cell doubling (figure 3.8a) by about 3 hours as with synchronous single cells. Comparison of the initial survival level of the spheroids with that of the most resistant regrowing single cells indicates that survival was about equal, which in turn implies that the spheroids were considerably more sensitive to radiation than after one day of growth.

A more detailed characterization of these cells was possible only if the entire spheroids could be synchronized. The synchrony obtained by exposure of small (day 1) spheroids to colcemid is shown for a typical experiment in figure 3.9 . After release of the mitotic block, the mitotic index (figure 3.9a) declined rather slowly, with mitotic cells observed for almost 6 hours. This slow completion of the first mitotic division was a characteristic of the spheroids only. No explanation for the decreased mitotic rate can be offered, as single cells treated on plates completed the first division within 30 minutes and then cycled with the normal generation time of about 11 hours. The 'end' of the first mitotic division, or the M/G_1 interface, was defined to be the point where the mitotic index had decreased to one-half its initial value, that is, at a time of about

FIGURE 3.9

Characterization of synchronous day 1 spheroids released from a mitotic block (colcedid-induced) at time 0. The mitotic index, or number of mitotic cells per 500 cells counted (a); labelling index, or number of cells per 500 that became autoradiographically labelled with a pulse of ^{3}H-thymidine (b); plating efficiency (c); and isodose survival (1380 rad at 155 rad/min, 24°C) are shown as a function of time after release.

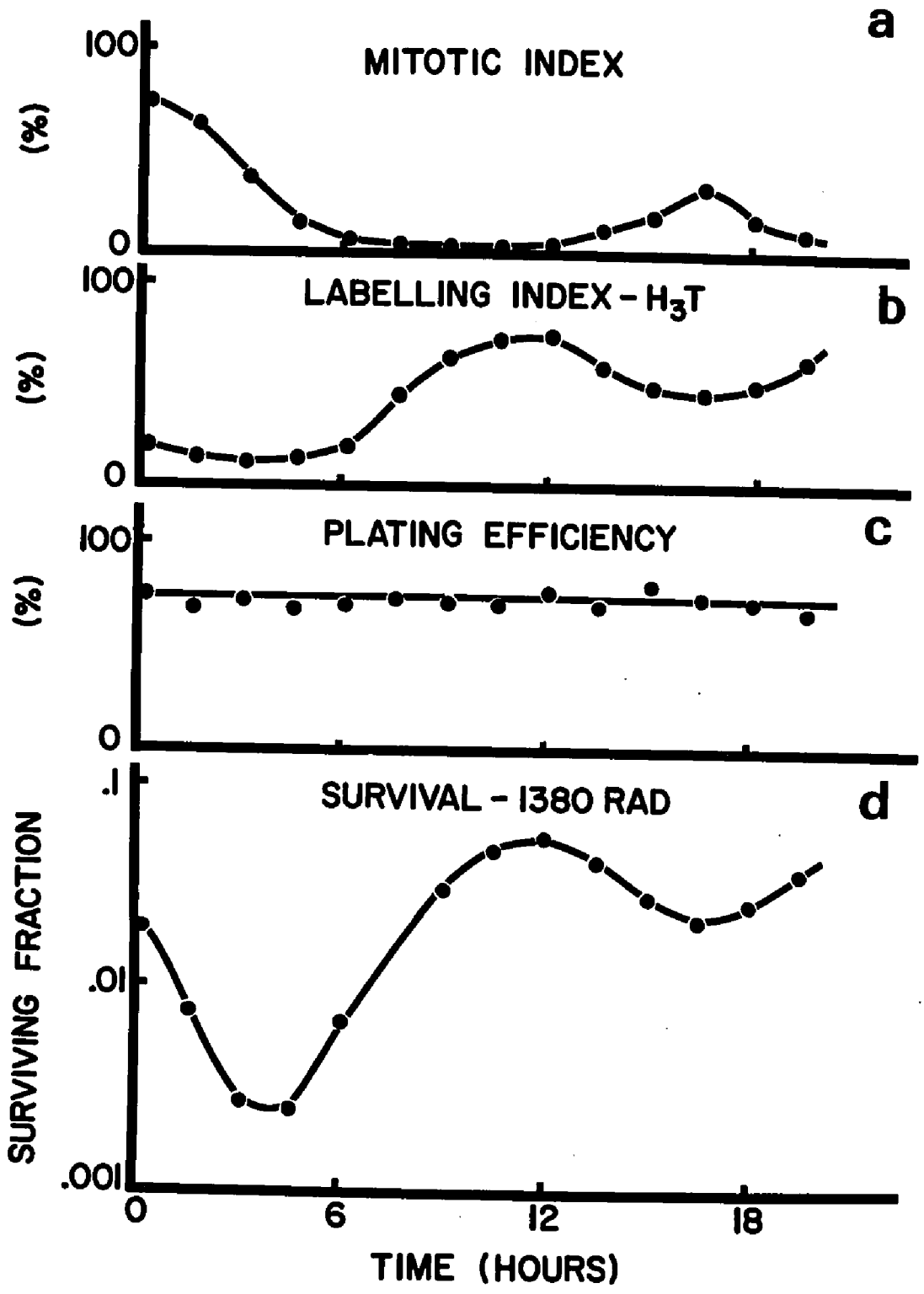
a
MITOTIC INDEX
100
(%)
0
b
LABELLING INDEX - H_3T
100
(%)
0
c
PLATING EFFICIENCY
100
(%)
0
d
SURVIVAL - 1380 RAD
.1
.01
.001
SURVIVING FRACTION
0
6
12
18
TIME (HOURS)

3 hours after release.

The labelling index (figure 3.9b) indicated that the spheroids began synthesizing DNA about 6 hours after release, with the half-maximum time (G_1/S interface) at about 7.5 hours. This suggested that the cells experienced an extended G_1 phase of about 4.5 hours, compared with the usual 2 hours when grown as single cells. The extensions of M and G_1 lengthened the cell cycle to roughly 14.5 hours for the first synchronous generation cycle, in contrast to the usual volume doubling time of about 11 hours for asynchronous spheroids.

Two features of the labelling index data of figure 3.9b suggested that only partial synchrony had been obtained by the colcemid treatment: about 15% of the cells were found to incorporate ^{3}H-thymidine immediately and up to 5 hours after release of the colcemid block, and the maximum labelling index was found to be only about 80%, whereas a figure of 65-70% had been observed for asynchronous spheroid cells (figure 3.2). These results, however, cannot be immediately interpreted as an indication of partial synchrony. The plating efficiency, or number of viable cells in the spheroid cultures with or without colcemid treatment, ranged from 35 to 65% in most experiments, with the data of figure 3.9c showing a PE of 65% at all positions of the cell cycle in that

particular experiment. Since the labelling index data could not be corrected for subsequent cell viability, it is not unreasonable to assume that some of the doomed cells may have non-specifically incorporated the label, and thus appeared as a 'background' count. Similarly, other non-viable cells would not incorporate ^{3}H-thymidine at all and would thus provide an unlabelled fraction of cells.

To test these possibilities, an additional method of assaying the synchrony of the cultures was devised, using hydroxyurea. Exposure of the synchronized spheroids to HU at any time from 0 to 5 hours after release of the colcemid block was not found to reduce the plating efficiency significantly, indicating that the 15% of the cells which had incorporated label were possibly not in S phase, or else may have been in S phase but were also resistant to HU. A third, and much more appealing explanation was that the cells simply were incapable of proliferation, despite uptake of the label. Conversely, treatment of cells with HU at the time of maximum labelling (11-12 hours) typically reduced the PE to less than 5% survival. These results, in contrast to the labelling data, suggested a high degree of synchrony even 11 hours after removal of the synchronizing agent.

Variations in radiosensitivity through the cell

cycle are shown by the cyclic survivals of figure 3.9d. The spheroid cells were most sensitive 3 to 4 hours after release (very early G_1 phase) and most resistant in late S phase as was found in control experiments with single cells. Unlike single cells, spheroid cells were relatively resistant in mitosis, though this was partly due to the fact that no correction for multiplicity was made during the early times shown in figure 3.9d, as survival was calculated by considering a cell in any stage of mitosis to be only one cell.

Complete survival curves were generated for spheroid and single cells at the most sensitive and resistant stages of the cell cycle. Figure 3.10a shows that survival differences as single cells progressed through the cell cycle were due to differences in the ability to accumulate sublethal damage, since the extrapolation number increased from 1.3 for M/G_1 cells to 28 for late S phase. No significant difference in slope was observed, as the D_o's varied from 172 ± 15 to 196 ± 23 respectively. In the spheroids, the most resistant cells had a similar terminal slope of 195 ± 49 rad, with a much higher extrapolation number of 328. The large errors in the 95% confidence interval can be associated with the convexity of the survival curve, indicating that it was doubtful whether the terminal slope had indeed been reached in

FIGURE 3.10

Survival of synchronized cells grown on petri dishes or from day 1 spheroids and irradiated in air at 24°C (162 rad/min).

	Symbol	PE	D_o	n	D_q
(a)	▲	81%	196±23	28	645
	X	92%	184±17	10.8	438
	●	85%	172±15	1.3	45
(b)	▲	63%	195±49	328	1008
	X	65%	182±31	180	940
	●	60%	101	1150	710

Uncertainties shown above represent the 95% confidence intervals.

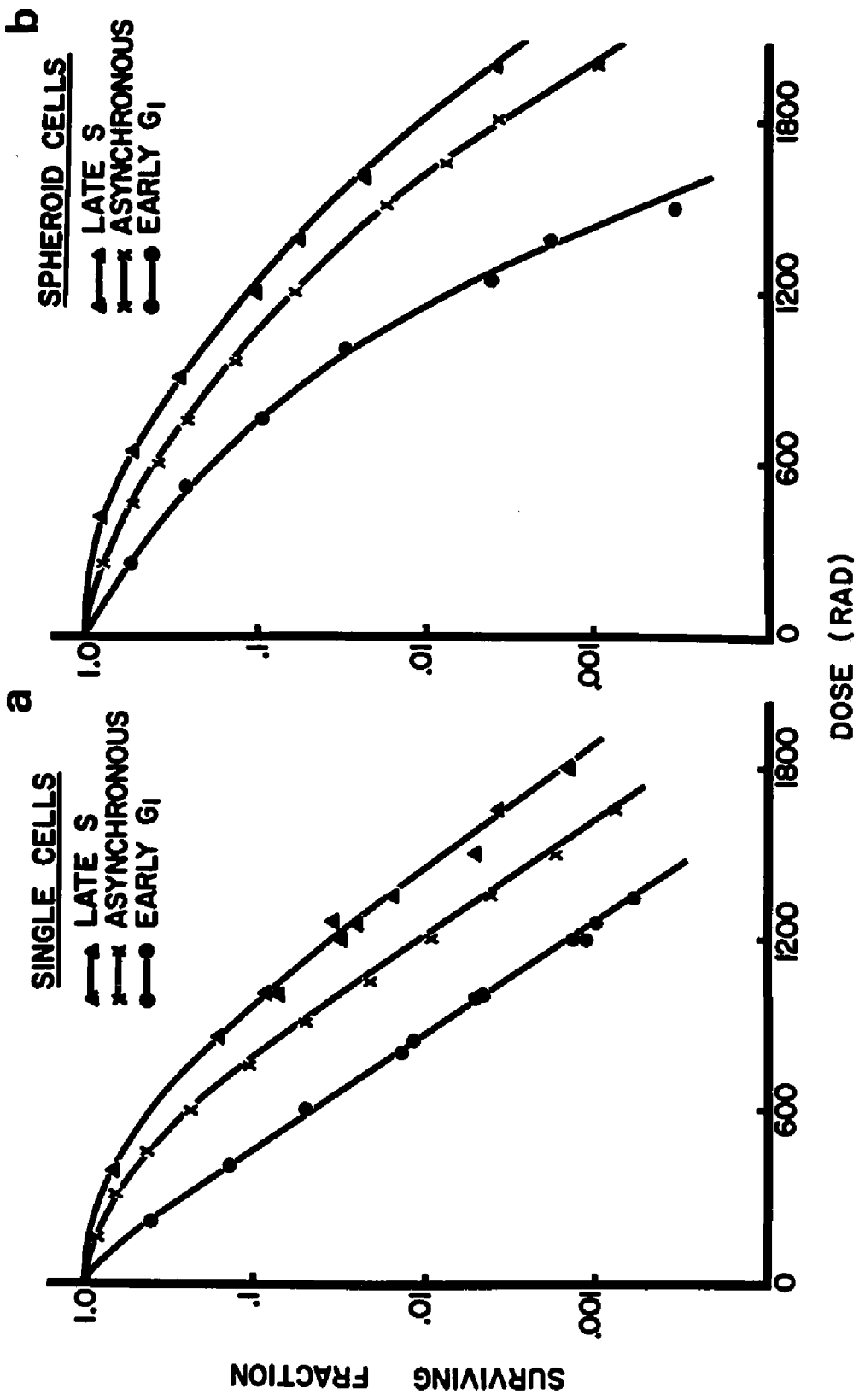
a
SINGLE CELLS
LATE S
ASYNCHRONOUS
EARLY G1
b
SPHEROID CELLS
LATE S
ASYNCHRONOUS
EARLY G1
SURVIVING FRACTION
1.0
.1
.01
.001
0
600
1200
1800
DOSE (RAD)

the survival range shown. A marked effect of intercellular contact can be seen at the M/G_1 stage of growth for cells in contact. Several experiments have shown that the curve was indeed concave downward and that the relatively large shoulder was always observed. Assuming that the last experimental points of figure 3.10b were on the exponential region of the curve, a D_o of 101 rad would result.

These large shoulders on the survival curves make quantitative estimates of the amount of Elkind type repair (see Elkind and Whitmore 1967, also Appendix 3) extremely difficult (see Malone et al 1971). However, a method of analysis was developed with the intention that recovery should be independent of the dose given when synchronous, non-progressing cells were considered. A complete description of the technique is given in Appendix 3. For the present discussion, it is sufficient to define the recovery, or the capacity for repair, to be the ratio of the net survival increase occurring when radiation is given in two doses to that expected if the cells fully regained the ability to accumulate sublethal damage.

The repair capacity of spheroid cells, relative to single cells, is shown in figure 3.11, where progression of cells through the cell cycle was inhibited

FIGURE 3.11

Survival of single cells and spheroid cells following two doses of radiation separated by varying times, and repair capacity or recovery of these cells (see Appendix 3). Synchronized single cells and spheroids were maintained at 24°C during and between exposures (142 rad/min). Survival was constant over the shown time intervals if assay was delayed after only the first dose. Plating efficiencies of 85% (▲); 81% (0); 60% (X); and 63% (●) were found. Standard errors were omitted in the interests of clarity, but were never greater than ±10% of the plotted values.

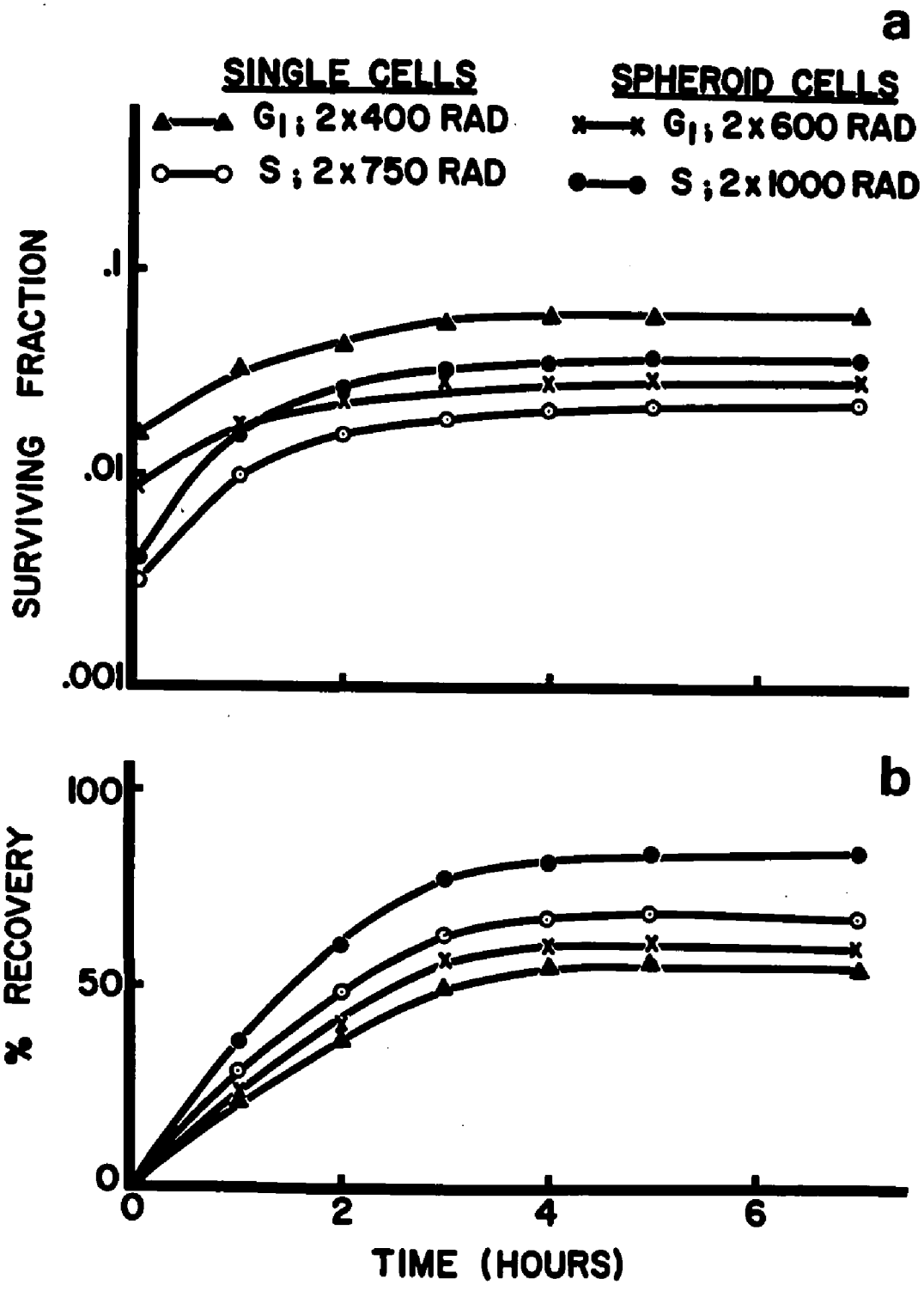
a
SINGLE CELLS
SPHEROID CELLS
G1; 2x400 RAD
G1; 2x600 RAD
S; 2x750 RAD
S; 2x1000 RAD
SURVIVING FRACTION
.1
.01
.001
b
% RECOVERY
100
50
0
0
2
4
6
TIME (HOURS)

by maintaining the cells at room temperature. Panel (a) shows the actual survival curves obtained, where survival following the two doses of radiation was plotted as a function of time between doses. Due to the different survival levels, no direct comparison can be made. However, when the data were normalized as in Appendix 3, two apparent features were observed. Late S phase cells, whether grown as spheroids or as single cells exhibited more recovery than did M/G_1 cells. In addition, the repair capacity of the cells grown as spheroids appeared to be greater at both stages of the cell cycle. Although the increased repair was not statistically significant in any one experiment, and survival levels were not absolutely reproducible between different experiments, qualitatively similar results were observed in all experiments.

Further observations on the repair capacities of partially synchronized cells in contact were obtained by studies with confluent monolayers of cells. Since most cells in the contact-inhibited monolayer were in early G_1 phase (Durand and Sutherland 1973), another experiment was designed to compare the repair capacities of synchronous early G_1, late S and day 8 plateau phase cells. As shown in figure 3.12, late S phase single cells again exhibited a higher repair capacity than

FIGURE 3.12

Recovery of synchronized and day 8 plateau phase cells grown on petri dishes as a function of time between two 600 rad doses of radiation (146 rad/min). The cells were maintained at 24°C during and between doses, and survival was constant after the first dose over the time interval shown. Plating efficiencies of 81% (■); 64% (X); and 78% (●) were observed. Standard errors were omitted for clarity, but were never greater than ± 8% of the plotted values.

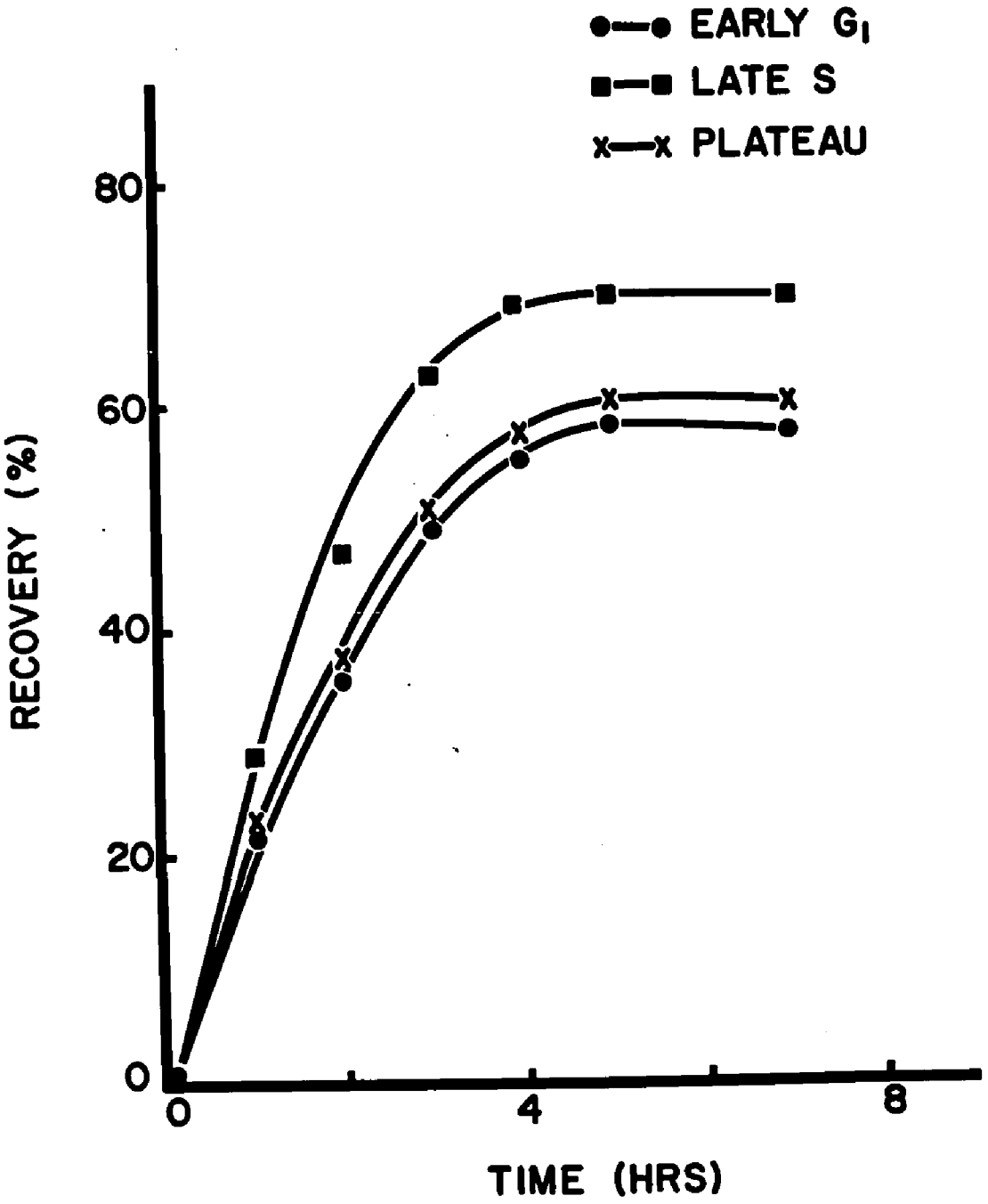
EARLY G1
LATE S
PLATEAU
RECOVERY (%)
80
60
40
20
0
0
4
8
TIME (HRS)

either plateau phase or early G_1 phase cells. Although the plateau phase cells did show a slightly higher recovery than did G_1 single cells (by about 5%), the effect was only about half that seen for G_1 phase cells in the spheroids, and may again have been related to the smaller degree of intercellular contact found in the plateau phase cells.

It is technically quite difficult to obtain well-chraacterized mixed populations of cells experimentally, but mixed populations can easily be considered theoretically. Theoretical curves were thus generated for populations of cells having sub-populations with the survival characteristics documented in this chapter, and the resulting theoretical curves were compared with the experimentally-obtained curves. Figure 3.13 shows broken curves representing the survival of 80% of the population being the non-S population of the day 4 spheroids shown in figure 3.7d, and the remaining 20% being cycling cells as in figure 3.6b. The solid curve represents the theoretical curve predicted for survival of a mixed population of cells with these components, and the data points of figure 3.6d are included for comparison. More detail concerning theoretical synthesis of mixed population survival curves can be found in Appendix 2.

FIGURE 3.13

Theoretical survival (solid line) of a population of cells comprised of the two sub-populations represented by the broken survival curves. The broken curve intersecting the ordinate at .8 represents the survival if 80% of the population were non-S phase with survival as in figure 3.7d; the broken curve intersecting the ordinate at .2 represents the survival of 20% of the population being asynchronous cells in contact as in figure 3.6b. The data points represent the observed survival of a day 4 spheroid, previously shown in figure 3.6d.

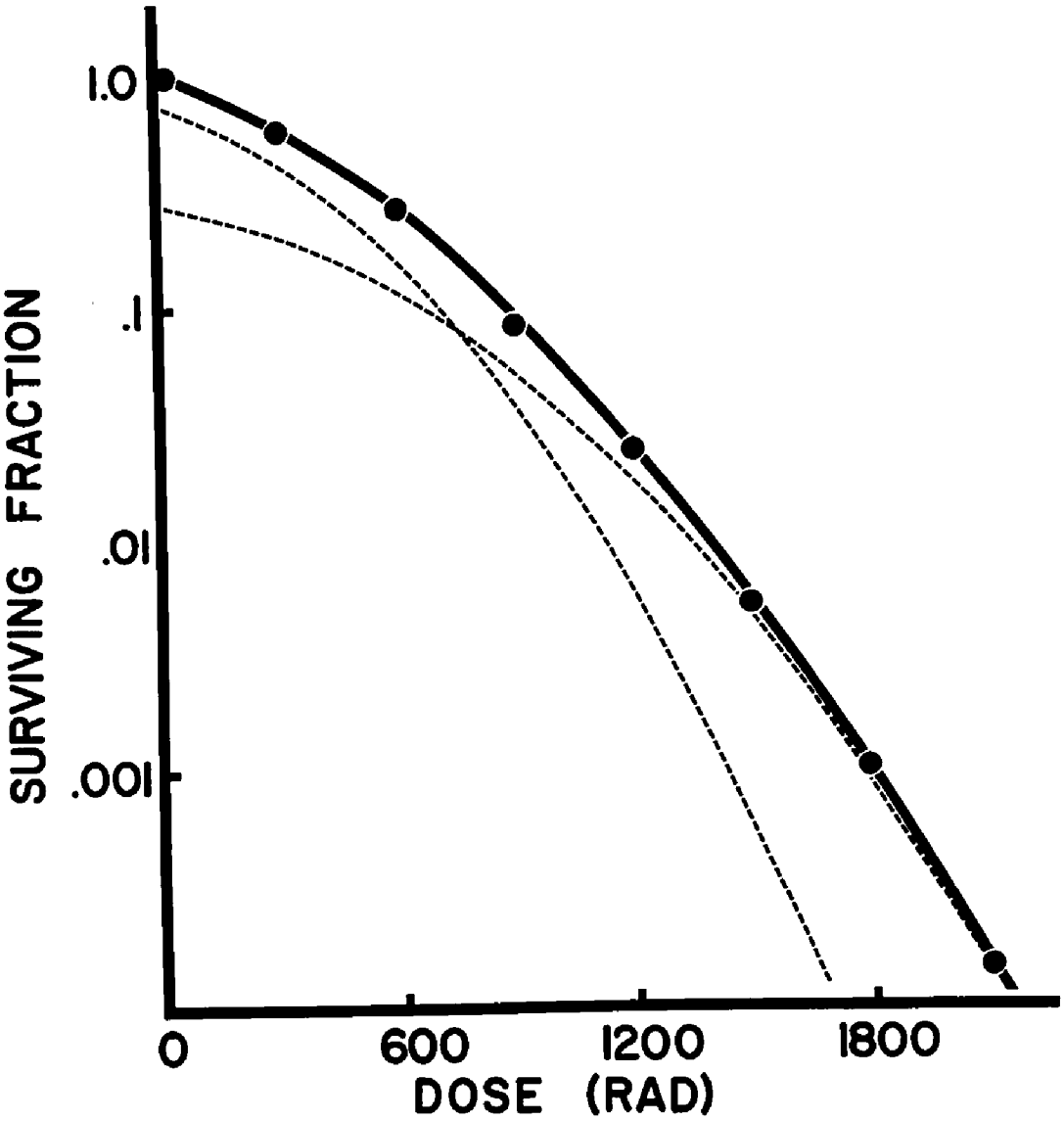
1.0
.1
.01
.001
SURVIVING FRACTION
0
600
1200
1800
DOSE (RAD)

3.3.4 Summary

The data presented in this section have shown that the radiation survival of cells grown in contact varies according to the position of the cells in their generation cycle. Cells in contact had the ability to accumulate large amounts of sublethal damage at all stages of the cell cycle, but contact also increased radiosensitivity at very early stages of the division cycle. Recovery between two doses of irradiation was enhanced by intercellular contact, and the amount of recovery was observed to be dependent on cell cycle position with a maximum at late S phase.

3.4 Discussion

The cell cycle kinetics studies detailed in section 3.2 and the variations in radiation response of the growing spheroids (section 3.3) both show that a redistribution of cells with respect to cell cycle position occurs in the maturing spheroid. As the distribution of cells in the cell cycle when grown as spheroids has not been unequivocally established (see section 3.2.4), the internal cells have been referred to as G_1 or G_1-like cells, particularly at the early stages of growth already discussed. However, since the concept of an infinitely long G_1 phase (that is, some

cells are definitely not cycling) may not be attractive, the internal cells of large spheroids will hereafter be referred to as 'G_0' cells, with the proviso that this is strictly a working definition. The special characteristics necessary in this G_0 stage, and its relation to the normal cell cycle are discussed at length in Chapter V.

Intercellular organization and contact has been demonstrated to enhance the capacity of these cells to accumulate and repair sublethal radiation damage. It was thus reasonable to assume that close association with dead, as opposed to normal neighboring cells would also influence cellular processes other than accumulation of sublethal damage. Therefore, in obtaining these synchronized populations of spheroids, an attempt was made to ensure that none of the spheroid cells were lethally damaged by the synchronizing procedure alone. Colcemid-treated cells should be acceptable under these criteria (see Ross and Sinclair 1972), since all cells were expected to be viable at the time of release from the mitotic block. In fact, no decrease in plating efficiency was ever found to be attributable to the synchronizing procedure. The prolongation of mitosis after removal of the chemical was unexpected on the basis of single cell results, and suggested that membrane interaction may influence cellular

responses to agents other than ionizing radiation.

The degree of asynchrony introduced by the prolonged initial mitosis was difficult to assess. In any event, the results presented in this chapter were not critically dependent upon absolute synchrony, and in fact, would only be more pronounced if increased synchrony were attained. Increasing the degree of synchrony would accentuate the survival fluctuations through the cell cycle. As an example, increased synchrony at the position of maximum resistance in figure 3.9d could only increase survival, since asynchrony at that point would reduce the fraction of cells that were most resistant. The situation was exactly opposite at the position of maximum sensitivity, in that increased synchrony would result in even lower survival. Thus, the results obtained cannot be explained merely on the basis of partially synchronized spheroids, and must be a result of variations in response at the different stages of the cell cycle.

The increased survival associated with the spheroid cells immediately after removal of the mitotic block cannot be entirely explained by the undetermined cell multiplicity (a factor of 2 at most). Since the mitotic rate was retarded, the cells may have been arrested in a state where repair of potentially lethal radiation

damage could occur (Belli and Bonte 1963, Phillips and Tolmach 1966, Hahn et al 1968, Stewart et al 1968, Little 1969a and 1969b, Belli et al 1970, Mauro and Little 1970, Little 1971). Due to the difficulty in clearly demarcating M and G_1 phases, it is also possible that the cells had an extended G_1 phase having sensitive and resistant parts (Chapman et al 1970b). In any case, it is clear that the intercellular contact modified the cellular survival differently as the cells progressed through their division cycles.

The high radiosensitivity of early G_1 phase spheroid cells was unexpected. When the curve for these cells in figure 3.10b was extrapolated and compared with the equivalent curve of figure 3.10a, the curves intersected. This would suggest that, at high doses and at this particular stage of the cell cycle, the intercellular contact might actually contribute to increased cell killing. Unfortunately, the assay technique used does not give reliable data at such low survival levels, nor would synchrony likely be adequate to test this suggestion. The great radiosensitivity of the early G_1 phase spheroid cells might be simply an artifact of the colcemid treatment, since no other agent has been used to study spheroids as early in the generation cycle. However, the cells of larger spheroids had a survival curve with D_o of

121 rad when S phase cells were selectively killed (figure 3.7d). Assuming, as before, that cycling cells comprised 20% of the population (figure 3.7d), and with the further assumption that G_2 and M cells represented about 15% of that population (i.e. only G_1 phase was elongated), then only about 3% of the surviving cells might be expected to be non-G_1 cells, indicating that a reasonable degree of synchrony (with respect to the phase of the cell cycle, but not the position in that phase) had developed in these larger spheroids. There is, of course, no reason to expect the G_1 cells of the spheroids to accumulate in the most radiation sensitive part of G_1 (i.e. very early G_1 with D_o = 101 rad as in figure 3.10b). Perhaps interaction of the cell membranes in the synchronous spheroids in early G_1 leads to conformational changes in the cellular DNA leading to increased radiosensitivity, as has been proposed for Chinese hamster ovary cells treated with hypertonic solutions (Dewey et al 1972).

The effects of intercellular contact were not constant through the cell cycle. This was first noted in figure 3.9d, where the ratio of maximum to minimum survival at the one dose used was a factor of about 30. With single cells, an equivalent ratio of 12 was typically observed, and was independent of dose for doses on the

exponential regions of the survival curves. The normalization technique designed for comparison of repair capacities of the cells at room temperature also suggested that the influence of intercellular contact was variable through the cell cycle. Late S phase cells repaired more damage at room temperature for both single and spheroid cells, and the additional repair capacity of the spheroid cells was most pronounced at late S phase. This dependence of the enhanced repair capacity on cell cycle position suggested that different types of damage may have been caused (see Elkind and Kano 1971), or else that a unique 'repair mechanism' or increased 'efficiency' of existing mechanisms may have been responsible for the differential response.

IV. HYPOXIC CELLS AND RADIATION SURVIVAL

4.1 Introduction

It is now well known that mammalian cells irradiated in the absence of oxygen are killed less readily (Elkind and Whitmore 1967, Okada 1970, Fabrikant 1972), and that this radioresistance (see Appendix 2) requires that the radiation dose be increased by about a factor of 3 to achieve killing comparable to the well-oxygenated case (Gray 1957, Revesz and Littbrand 1964, Bedford and Hall 1966, Kruuv and Sinclair 1968, Legrys and Hall 1969, Van den Brenk 1969). This is thought to be one of the major problems in tumor radiotherapy (Gray 1957, Inch and McCredie 1968, Cheshire and Lindop 1969, Urtasun and Merz 1969, Du Sault 1971, Wideroe 1971), as cells outgrowing their vascular supply may be deprived of oxygen as well as other metabolites (Tannock 1970 and 1972, Folkman 1971 and 1972).

The object of radiotherapy is to selectively kill the malignant cells, so the problems created by any radioresistant, hypoxic cells in tumors can be emphasized by considering the survival curves shown in Appendix 2. When two populations of cells are characterized by different radiosensitivities, the survival curves diverge. Thus, for large doses of radiation, the probability of

survival is many orders of magnitude higher for hypoxic cells. Stated inversely, this implies that, to destroy a hypoxic tumor cell population, millions or even billions more healthy, oxygenated cells may also have to be lethally damaged. To circumvent the problems introduced by a hypoxic fraction of cells, different radiotherapy schemes have evolved (Lajtha and Oliver 1961, Kallman 1968, Van Putten and Kallman 1968, Badib and Webster 1969, Howes 1969, Thomlinson 1968), and have proved successful enough that some controversy exists as to whether the oxygen effect is pertinent or irrelevant to clinical radiotherapy (Hall 1967, Alper 1968, Bewley 1968).

Another consideration which may be dependent upon the oxygenation status of individual tumor cells is the capacity of the cell to recover the ability to accumulate sublethal damage between radiation doses of a multi-dose treatment program. Recovery has been shown in both in vivo (Kallman 1968, Van Putten and Kallman 1968, Suit and Urano 1969) and in vitro systems (Hall et al 1966, Elkind and Whitmore 1967, Elkind et al 1968, Belli et al 1970, Foster et al 1971) under certain conditions, but absence of recovery has also been found in the animal (Urtasun and Merz 1972) as well as in tissue culture systems under more stringent conditions of hypoxia (Littbrand and Revesz 1964, Phillips and Hanks 1968,

Elkind and Whitmore 1967, Littbrand and Revesz 1969, Koch and Kruuv 1971, Hall 1972, Koch 1972).

Despite the various responses of hypoxic tumor cells to radiotherapy indicated above, there is at least some convincing evidence that hypoxia does in fact occur in many *in vivo* tumors. Clinical studies by Thomlinson and Gray (1955) suggested that poor oxygenation correlated with presence of necrosis. Other work, using oxygen electrodes and other techniques, has shown that many experimental nodular tumors do develop hypoxic regions (Powers and Tolmach 1963 and 1964, Kruuv et al 1967a and 1967b, Bergsjo and Evans 1968, Van Putten and Kallman 1968). In addition, it has been shown that hypoxic regions can occur without central necrosis (Van Putten and Kallman 1968), in very small tumors (Reinhold and Debree 1968), and even in ascites tumors (Del Monte 1969).

The potential of the spheroid as an *in vitro* tumor model would obviously increase tremendously if hypoxic cells could be demonstrated. In addition, the spheroid system would be unique in that it is the only *in vitro* culturing system in which the hypoxic cells would develop spontaneously and gradually, and would be maintained for long periods in intimate contact with normal, aerobic cells.

4.2 Hypoxic Cells in the Spheroid

4.2.1 Introduction

This section presents evidence that the multicellular spheroid is histologically similar to human and experimental nodular tumors, and thus provides the best *in vitro* simulation of the conditions which develop in the *in vivo* tumor. Central necrosis will be shown to correlate with oxygenation in the spheroid, thus suggesting that a hypoxic fraction of cells does develop. In addition, the presence and location of the hypoxic cells will be demonstrated visually by the technique of autoradiography, using a labelled compound that preferentially binds to hypoxic cells during irradiation.

4.2.2 Methods of spheroid growth under low oxygen tensions and hypoxic cell visualization

The effects of reduced concentrations of oxygen and other metabolites in the medium on the growth of large spheroids was investigated by growing the spheroids under normal conditions for either 5 or 14 days. These times were chosen to allow growth to a diameter of approximately .2 mm (5 days) where few hypoxic cells would be expected or to a diameter of more than .3 mm (14 days) where significant numbers of hypoxic cells would be

found. On these days, the spheroids were divided equally into 3 flasks containing 75 ml of medium. Two flasks were gassed continuously with 97% air plus 3% CO_2. Two-thirds of the medium in one of these was replaced with fresh medium daily thereafter (fed), while the medium in the other flask was not changed (starved). The third flask was gassed continuously with 5% O_2 plus 3% CO_2 in nitrogen, and fed daily with pre-equilibrated medium with the gassing continued during the feeding procedure. Spheroids were grown as long as 7 days under these controlled conditions.

Samples of spheroids were withdrawn from the flasks and sized or processed for histological studies at various times as described for the particular experiments. Serial sections 5 microns thick were prepared on each day of growth, and spheroids were considered only if enough sections could be followed microscopically to ensure that the center of the spheroid had been bypassed. When the central section had been determined, a range of adjacent sections (never exceeding 6 on either side) was observed and the thickness of the viable rim on each side of the central necrotic region was measured in perpendicular directions. Each section thus yielded 4 values of rim thickness, so as many as 48 separate measurements of rim thickness per spheroid were made. These were then

averaged for several spheroids from each growth condition.

Nitrofurazone labelled with ^{14}C was added to spheroids for 20 minutes before, and during an irradiation period long enough to deliver 40 krad to the spheroids (about 4 hours). The nitrofurazone was dissolved directly in complete BME with a final concentration of .5 mM, and control spheroids were sham-irradiated at 37°C or irradiated at 24°C. Standard autoradiographic procedures were then used (see section 3.2.2).

4.2.3 Results

Visual evidence of the different cellular states which develop in one type of nodular tumor is readily evident in the photomicrograph of figure 4.1, which shows the type of growth often seen in the C3HBA mouse mammary carcinoma. Panel (a) shows a nodule of the tumor in which the blood supply was confined to the periphery. The central cells became necrotic, and some of the cells near the necrotic region stained more darkly. Tannock (1968) has shown that cell cycle kinetics are markedly different in similar regions of other tumors.

Different regions of the tumor may develop in the exactly opposite manner, where the malignant cells form

FIGURE 4.1

Photomicrograph of two regions from a C3HBA nodular mouse mammary carcinoma. Panel (a) shows the appearance of a nodule where the blood supply was confined to the periphery; panel (b) shows the cellular organization around a capillary. Necrosis is evident at large distances from the blood supply in each case.

Magnification: X 230

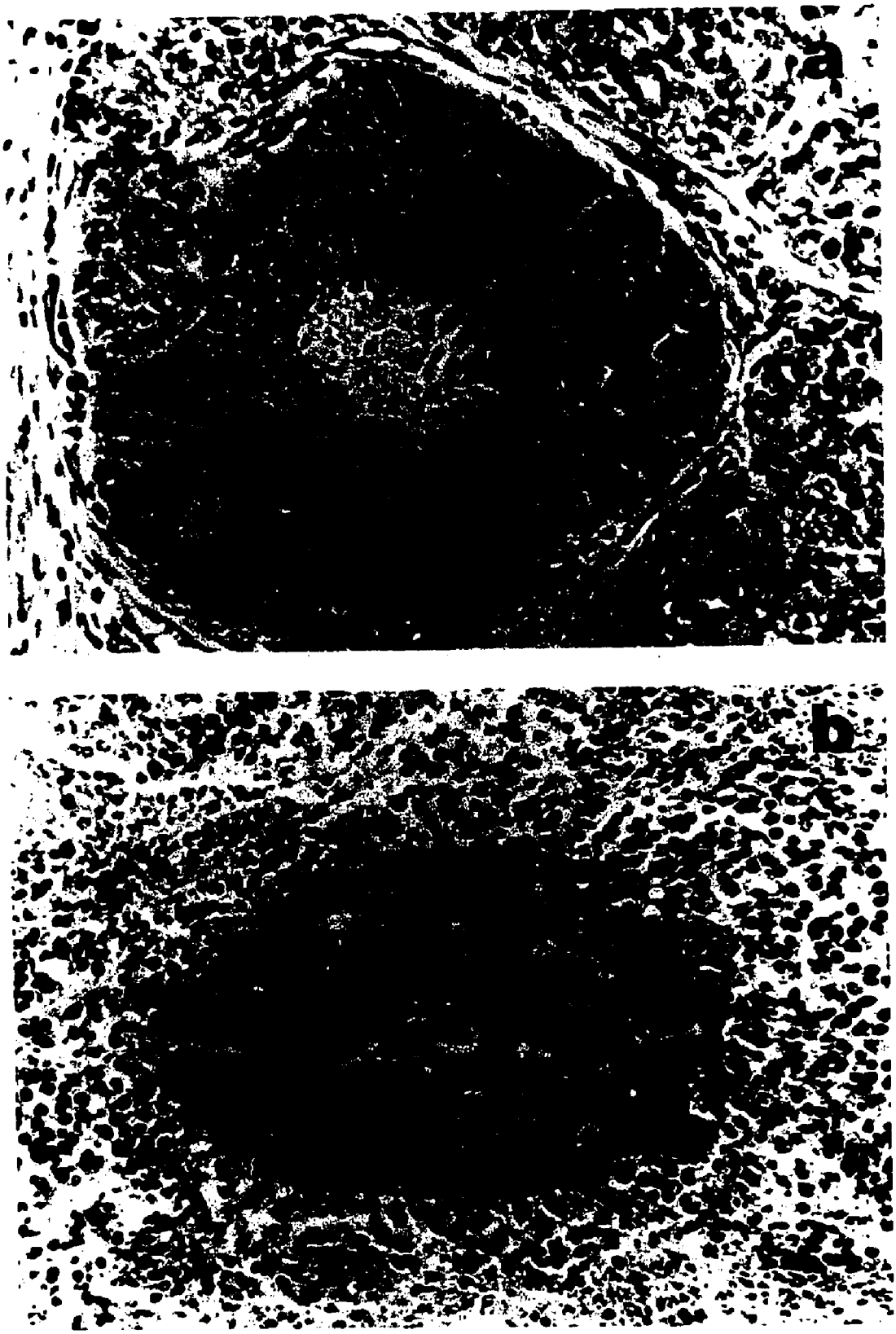
a
b

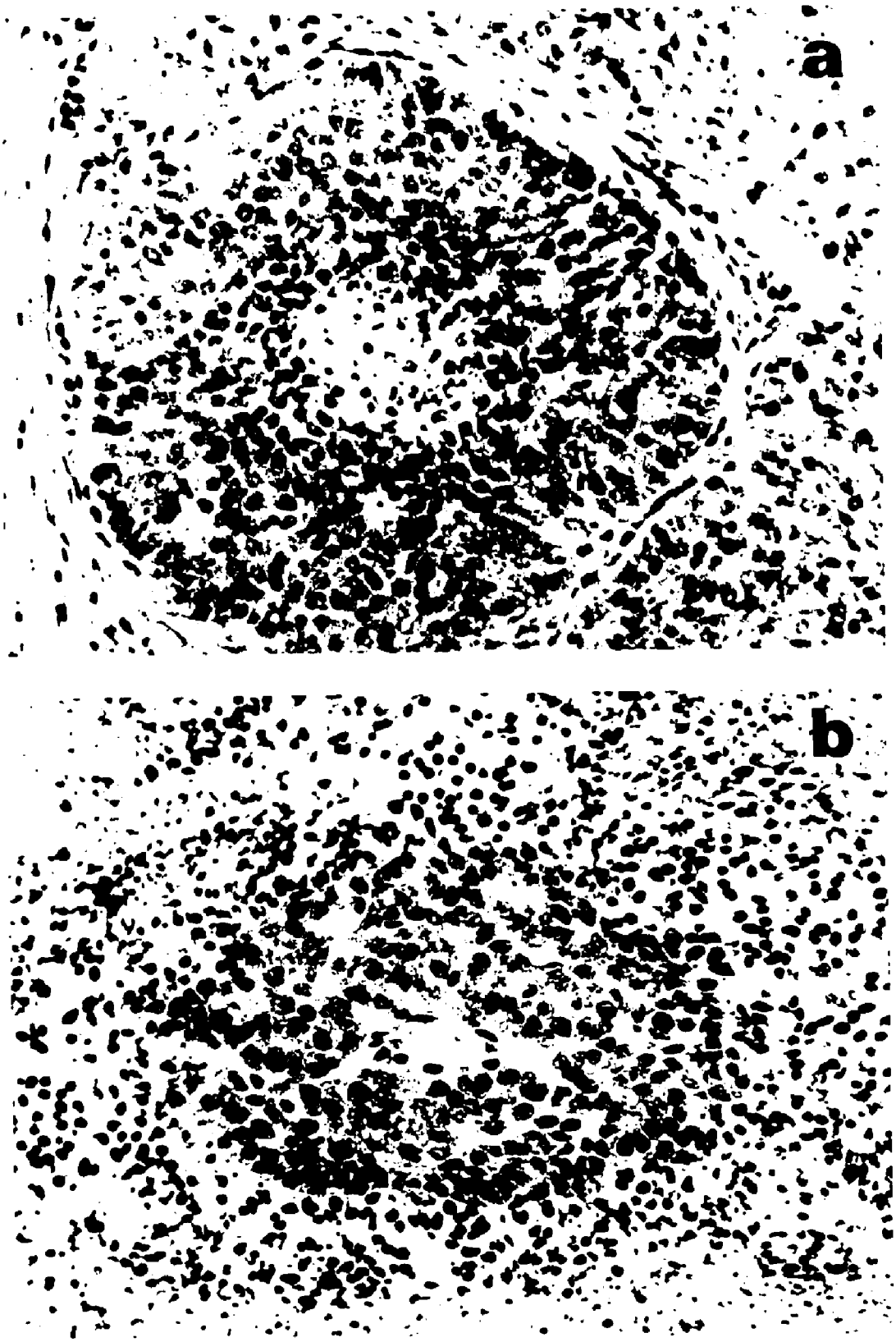
a
b

a cord-like or cylindrical structure around blood vessels as in figure 4.1b. The cells nearest the blood supply again were much more metabolically active, and tended to proliferate faster than the more distant cells. Qualitatively, there is little difference between the structures shown in figure 4.1, and the resemblance of figure 4.1a to the largest spheroid of figure 2.4 is very striking. In the spheroid, as in the tumor, cells grow in a situation dependent upon the diffusion properties of the necessary metabolites.

One particular human tumor which undoubtedly contained hypoxic cells is shown in figure 4.2 . This figure shows a lung metastases from a primary adenocarcinoma of the colon. The viable rim of cells varied in thickness between 150 and 180 microns, somewhat larger than the 80 micron figure reported for mouse mammary carcinomas (Tannock 1968), but comparable with the viable rim of bronchogenic carcinomas (Thomlinson and Gray 1955), and almost exactly identical to spheroids. This particular tumor is rather unique, in that the single malignant nodule can be represented in almost every detail by a spheroid. The radiotherapeutic problem of hypoxic cells is also particularly well illustrated by this type of tumor, since normal lung tissue is well oxygenated and quite radiosensitive.

FIGURE 4.2

Photomicrograph of a human lung metastases of a primary adenocarcinoma of the colon. The nodular structure of this type of tumor is particularly well simulated by a spheroid.

Magnification: X 190

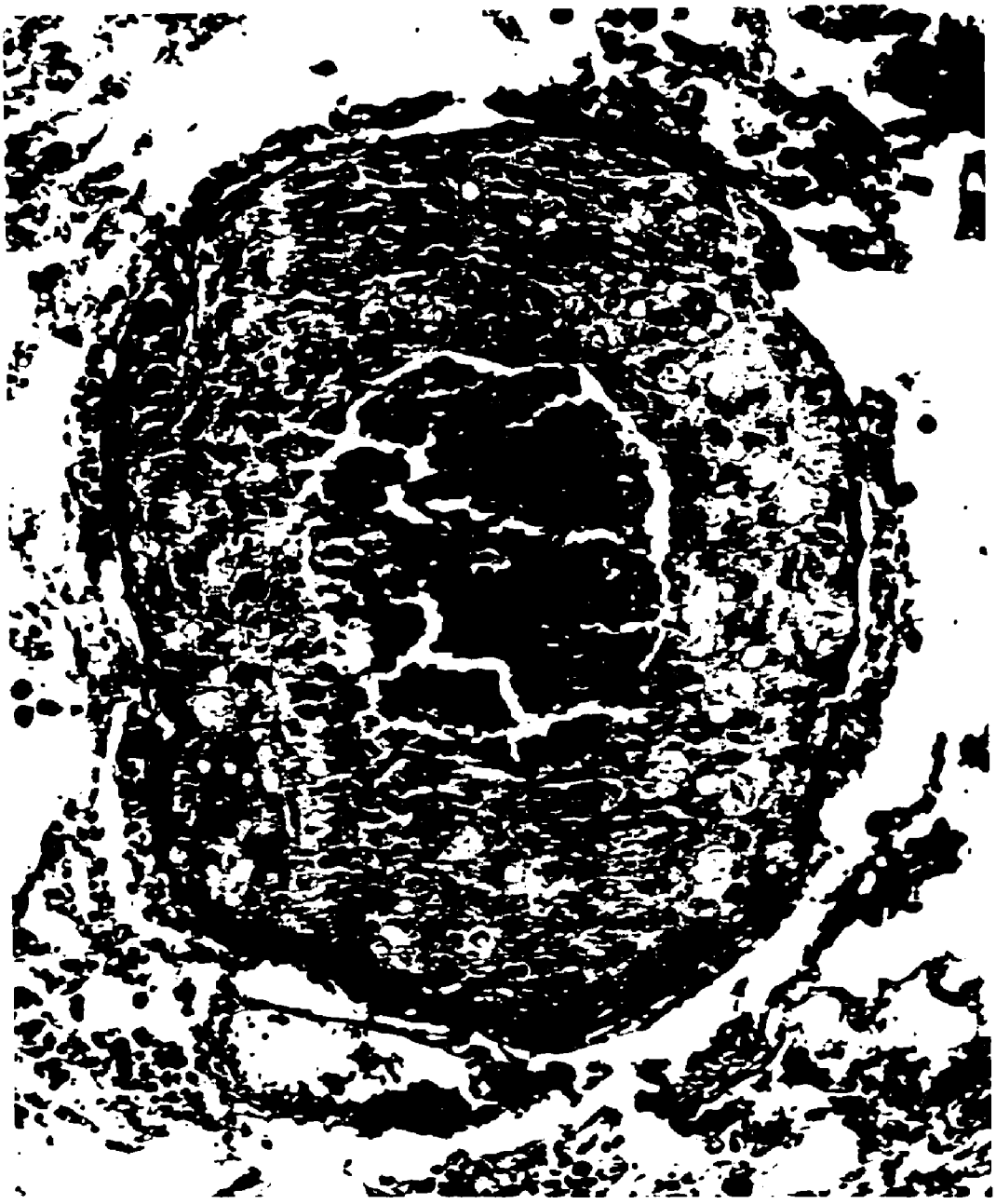

Although no direct measurements of oxygen tension were carried out in the spheroid, hypoxia was inferred from several indirect experiments (see also Appendix 4). The role of hypoxia compared with deficiencies of other metabolites in controlling cell proliferation during the retarded growth phase indicated in figure 2.2 was investigated by comparing growth of large spheroids under optimal conditions of oxygenation and nutrition, hypoxia (5% oxygen in N_2) but good nutrition, and good oxygenation but poor nutrition (starved). When spheroids grown to the beginning of the retarded growth phase (day 5) were subjected to the new conditions, the mean size of starved spheroids was essentially unchanged (figure 4.3), although some larger spheroids were observed in the histological sections (Table 1). The reduced oxygen concentration decreased the growth rate from a doubling time of 36 hours in the control to 60 hours. However, there was little development of central necrosis in the starved spheroids, in marked contrast to growth in low oxygen where necrosis was evident even after 1 day. The average radius of the viable rim under hypoxic conditions was 96 microns (Table 1). This compared with 187 microns for spheroids grown under optimal conditions. The thickness of these viable rims was constant under low oxygen for the week of growth observed.

FIGURE 4.3

Effects of deprivation of oxygen or nutrient factors on the growth of spheroids (previously grown 5 days under optimal conditions). See text for detailed experimental conditions.

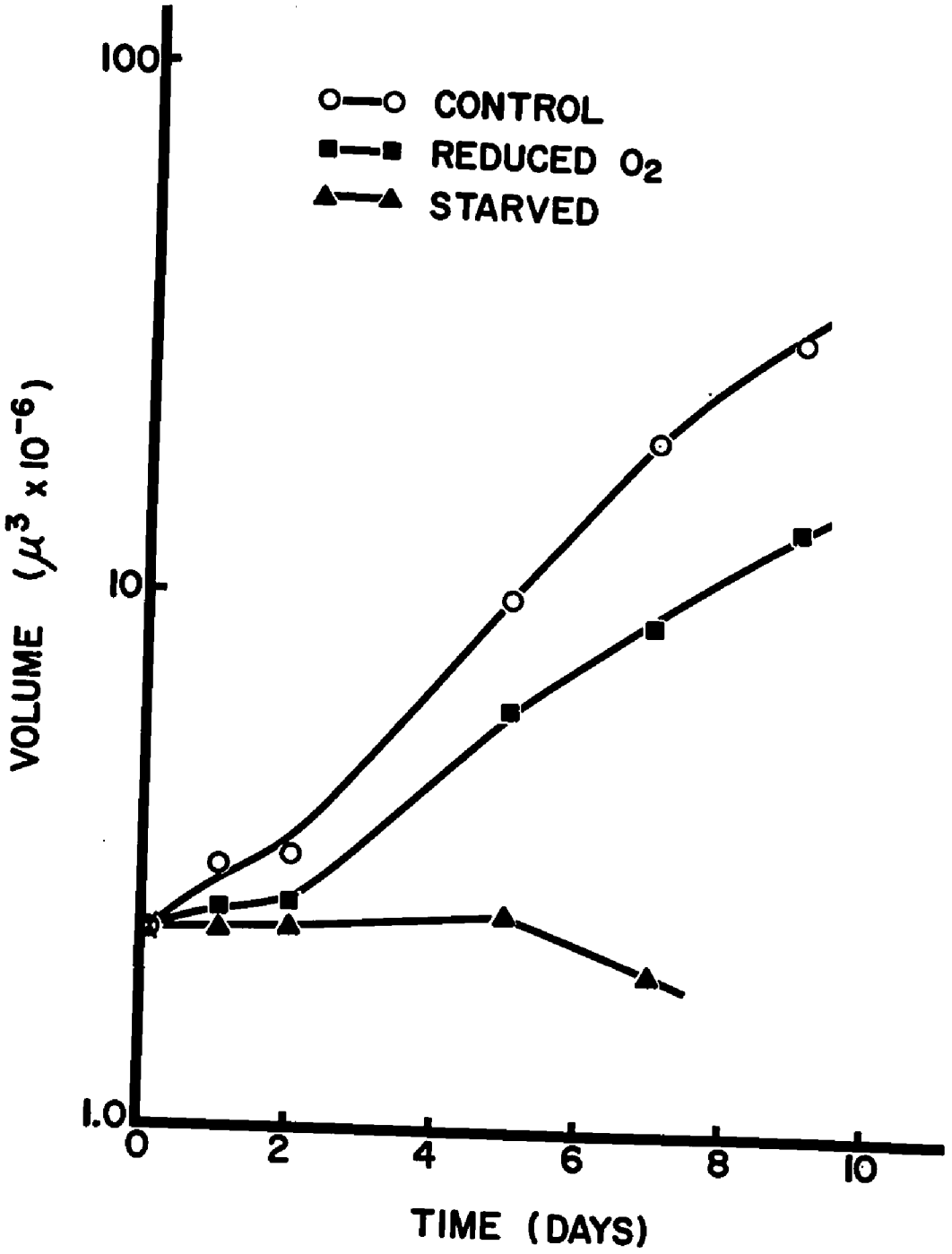
100
10
1.0
VOLUME ($\mu^3 \times 10^{-6}$)
CONTROL
REDUCED O_2
STARVED
0
2
4
6
8
10
TIME (DAYS)

TABLE 1.

Thickness of viable rim of cells in spheroids under different growth conditions.

Growth Conditions	No. of Spheroids	Range of Mean Diameters (microns)	No. of Central Sections	Mean Rim Thickness (microns)
		PREHYPOXIC SPHEROIDS (Day 5)		
Fed	20	270 - 418	19	187 ± 5*
Starved	20	224 - 256	--	---
Hypoxic	9	228 - 344	65	96 ± 2
		HYPOXIC SPHEROIDS (Day 14)		
Fed	17	421 - 503	92	182 ± 3
Starved	11	391 - 438	76	158 ± 3
Hypoxic	17	328 - 445	118	99 ± 2

*Central necrosis was observed only in spheroids >360 microns in diameter. Mean rim thickness of such spheroids is indicated with the standard error of the mean. A detailed description of the experiment is given in section 4.2.2 .

In another experiment spheroids were grown for 14 days to diameters >300 microns, where many had developed central necrotic as well as hypoxic cells. The flasks were then gassed with 5% O_2 and within one day a ring of necrotic cells was observed, again at a distance not significantly different than 96 microns from the outside (Table 1). Spheroids which had already developed necrotic centers under the standard growth conditions also developed the new necrotic regions. Starved spheroids of increased size were observed, but did not develop as large an area of central necrosis as did the spheroids grown in hypoxic conditions. These results suggest that the main cause of the central necrosis was the limitation in the oxygen supply. In addition they suggest that the cells could gradually adapt to low oxygen tensions, but were not able to survive abrupt shifts in oxygen concentration in this tumor-like environment.

The hypoxic cells of the spheroid were demonstrated autoradiographically using ^{14}C-nitrofurazone. This agent has been previously shown to bind preferentially to DNA, protein and whole cells when irradiated under hypoxic conditions (Chapman et al 1972). As demonstrated in figure 4.4, there was little or no binding in the outer, well-oxygenated layers of the spheroid, but there was a graded increase in binding to a maximum

FIGURE 4.4

Photomicrograph of an autoradiographic section of a spheroid labelled with ^{14}C-nitrofurazone, a compound which preferentially binds to hypoxic cells during irradiation, thus indicating which cells were hypoxic. Total radiation dose was 40 krad (160 rad/min at 37°C). Magnification: X 600

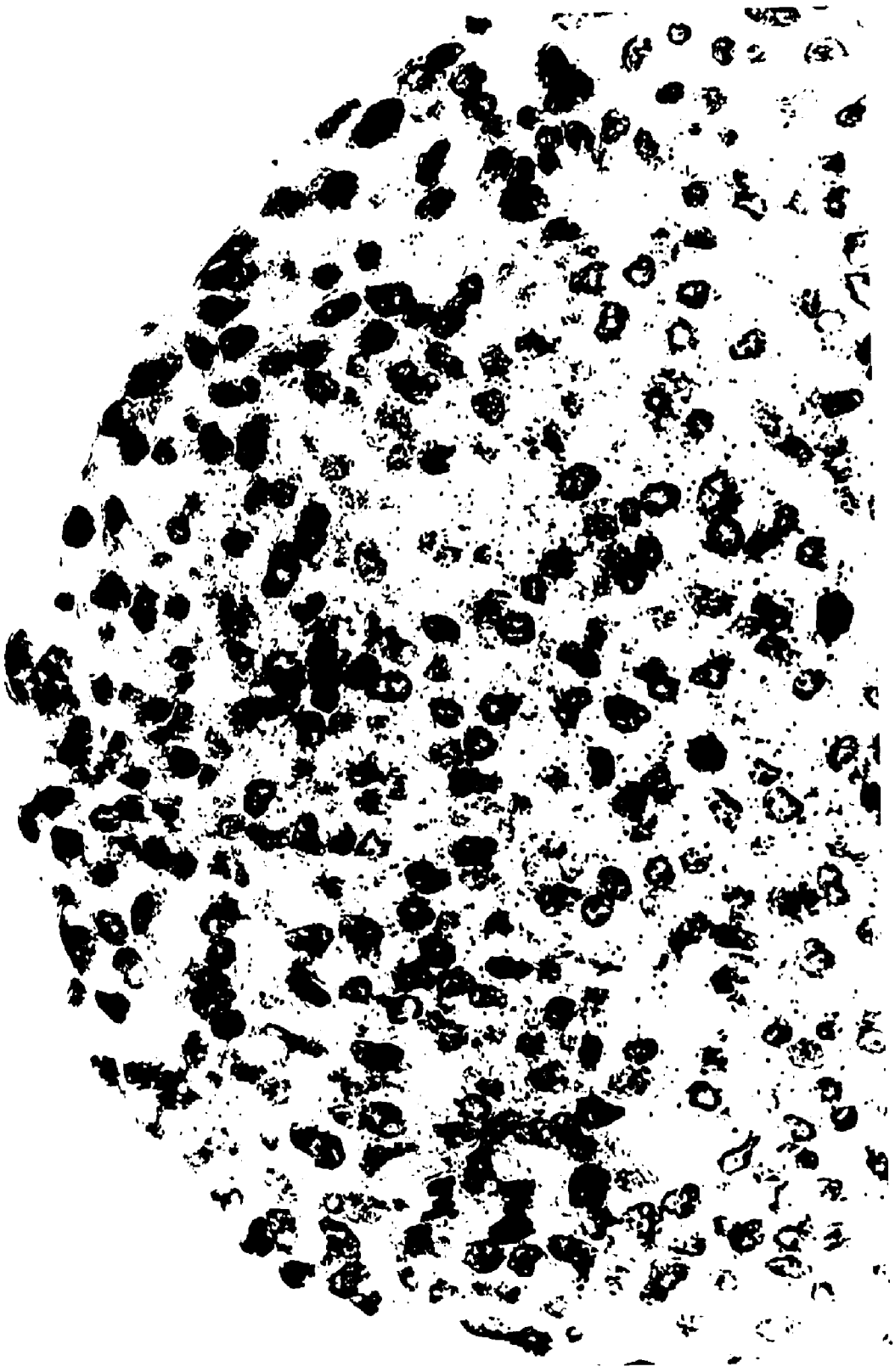

in the central area. No localization of the label was found in unirradiated controls, or in spheroids irradiated at 24°C (see section 4.3.3).

The remarkable morphological resemblance of the spheroid to the tumor nodules of figure 4.1a and especially 4.2 can be seen in the high-power photomicrograph of figure 4.5 . In very large spheroids such as the one in this figure, four distinct regions were generally visible. The external cells were rather fibroblastic, whereas cells more than about three cell diameters from the surface were somewhat more compressed, smaller and more spherical. These outer regions contained the actively proliferating cells, and a mitotic cell can be seen near the right side of the figure. Vacuoles were very numerous near the necrotic region, and the cells typically stained in an eosinophillic manner, despite the darker nucleii. Central necrosis and occasional scattered necrotic cells were found near the middle of the section. In conjunction with the results presented in sections 2.2 and 3.2, these morphological features demonstrate that the spheroid simulates the cellular organization, decreasing growth fraction, and development of hypoxic regions seen in vivo during tumor growth. Development of multinucleated and tetraploid cells in the spheroid, albeit in small num-

FIGURE 4.5

High-power photomicrograph of a central section of a very large spheroid. Four areas can be seen, including external, fibroblast-like cells; an intermediate area of more spherical and compact cells with well-defined nuclear detail; cells bordering the necrotic zone that are highly vacuolated and have darkly-staining nucleii; and internal necrotic cells.

Magnification: X 500

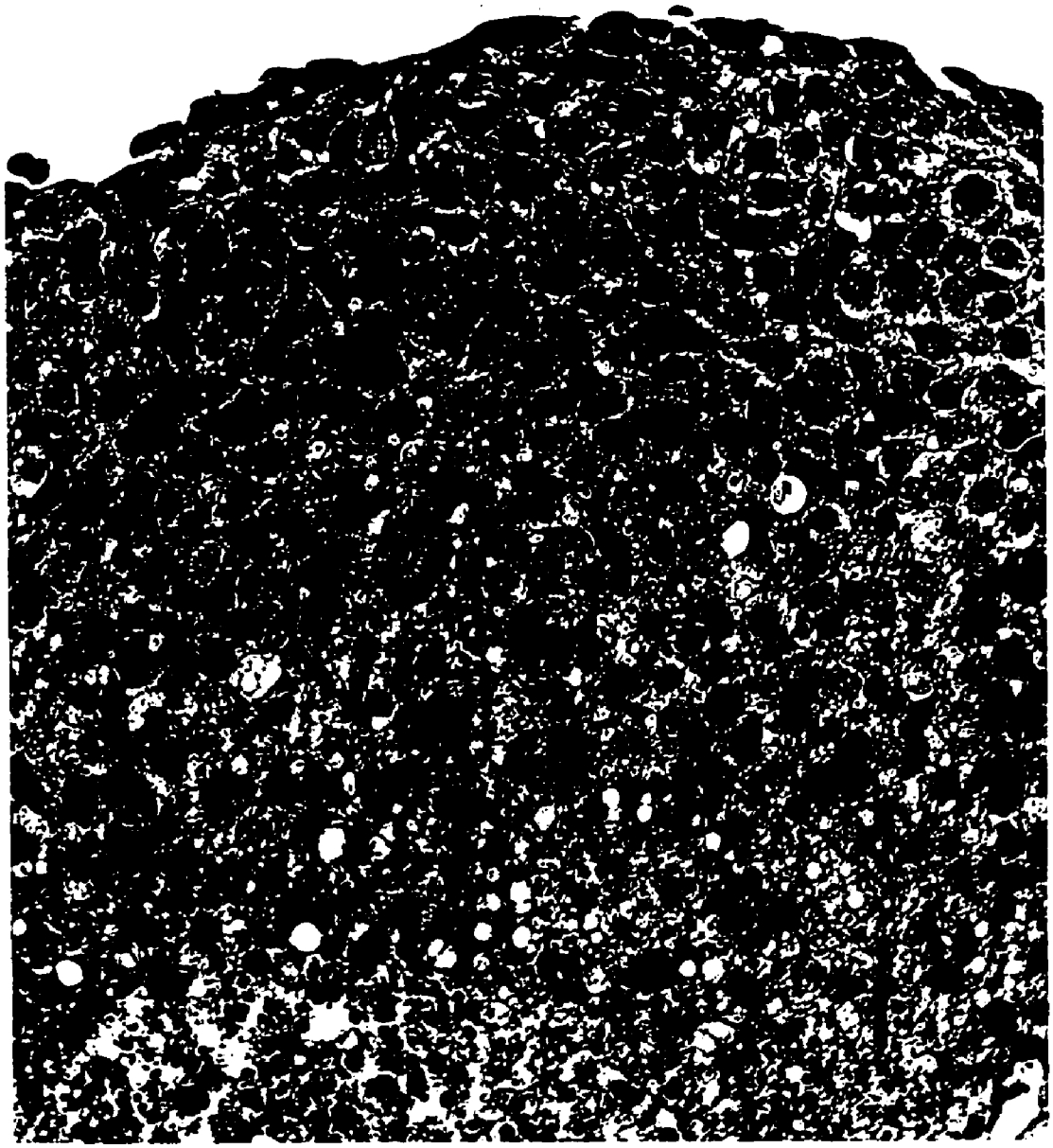

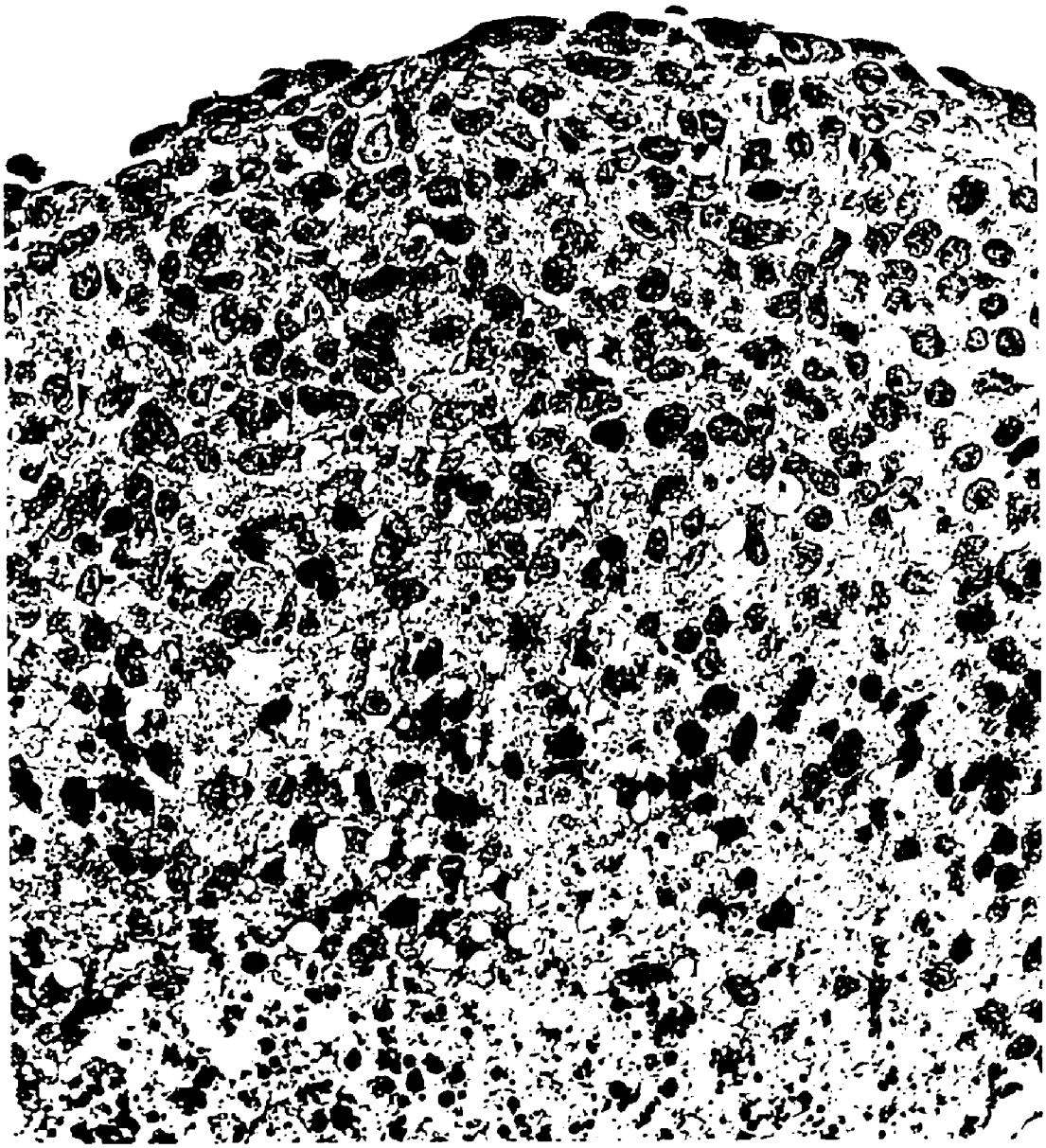

bers, may at least partially lead to cells of somewhat different radiosensitivities such as those that result from differentiation in a tumor.

4.2.4 Summary

The evidence presented in this section has shown that spheroids provide an exceptionally accurate model of both human and experimental nodular carcinomas. Development of central necrosis was shown to correlate with oxygen tension in the medium, and the viable rim was found to decrease by a factor of two when oxygen was reduced to one-quarter its original value, as predicted theoretically (see Boag 1969, and Appendix 4). The hypoxic cells were also demonstrated by an autoradiography technique, using ^{14}C-nitrofurazone.

4.3 Radiation Survival and Hypoxic Cells

4.3.1 Introduction

A large spheroid has a cell density which approaches that of organized tissue in vivo, and thus introduces the problem of oxygen depletion in the medium due to cell respiration. Even at moderate spheroid densities, the large number of cells in each spheroid required that diffusion of oxygen be adequate to maintain this respiration. Radiation adds an additional problem, that of radiation induced binding or removal of molecular oxygen from the

system, so a careful analysis of the radiation conditions used has been presented in Appendix 4. It is sufficient to indicate, in introduction to this section, that the hypoxic cells found in the spheroid resulted during spheroid growth, and significant levels of induced hypoxia were not produced under the radiation conditions described.

The results presented in this section will show that a fraction of highly radioresistant cells develops as the spheroid increases in size, and that this component of the survival curve disappears under conditions designed to produce equal oxygenation of all cells in the spheroid. Electron affinic chemicals known to selectively sensitize hypoxic cells to radiation will also be shown to reduce the survival of cells from large spheroids.

4.3.2 Methods of irradiation of large spheroids

Unless otherwise specified, all irradiations of large spheroids were performed in the glass radiation vessels at 37°C as previously described (section 2.3.2), with the exception that the flow rate of the humidified air or nitrogen was increased by a factor of ten to ensure about 20 volume changes per minute in each vessel. This flow rate was found to produce agitation in the

medium without significant evaporation, and thus maintained the best possible oxygenation of the medium. Standard techniques for survival determination following the irradiation procedure were employed.

4.3.3 Results

The same population of spheroids previously shown in figure 3.6 was maintained for a total of 12 days, and survival curves were obtained on these later days. A separate experiment has been included in figure 4.6 to show the typical survival of very large spheroids. Progressive development of a third, highly radioresistant population can be seen in figure 4.6 . This fraction usually comprised less than 20% of the population (about 9% in figure 4.6c and 16% in 4.6d), and the cells were typically less radioresistant in smaller spheroids (D_o = 232 rad in figure 4.6b, 271 rad in 4.6c and 302 rad in figure 4.6d).

Evidence that the most resistant fraction of cells was indeed hypoxic is presented in figure 4.7 . If hypoxia was in fact the reason for the great resistance of the final component of the curve obtained under normal conditions (control curve), it would be expected that irradiation of the spheroid under anoxic conditions would increase the size, but not the resistance of this

FIGURE 4.6

Survival of cells grown as spheroids and irradiated at 37°C in air (130 rad/min). Spheroids were from the same experiment shown in figures 3.6 and 3.7 .

Panel	PE	D_o
(a)	62%	-
(b)	65%	232
(c)	62%	271
(d)	54%	302

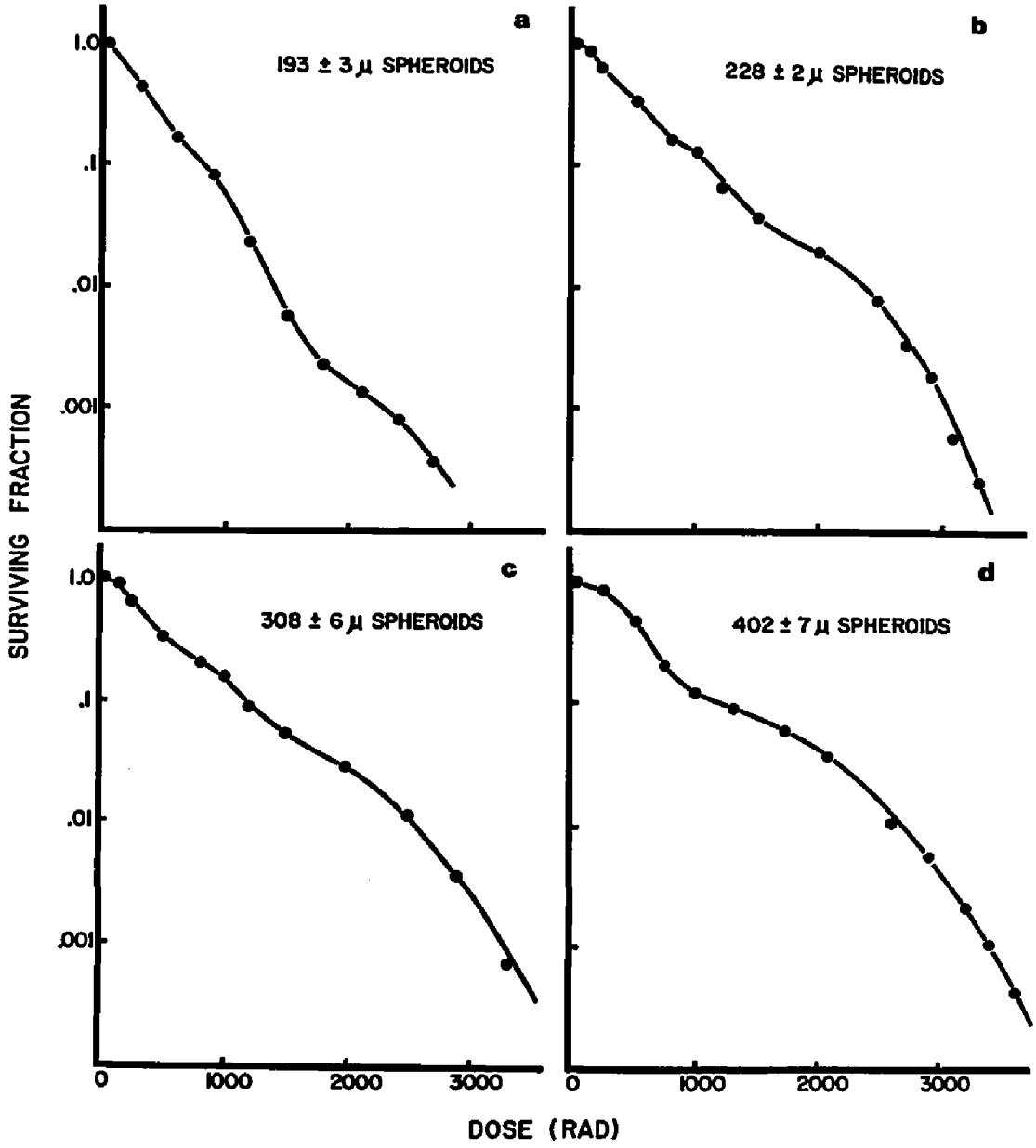
a
193 ± 3 μ SPHEROIDS
b
228 ± 2 μ SPHEROIDS
c
308 ± 6 μ SPHEROIDS
d
402 ± 7 μ SPHEROIDS
SURVIVING FRACTION
1.0
.1
.01
.001
0
1000
2000
3000
DOSE (RAD)

FIGURE 4.7

Survival of cells grown as spheroids and irradiated in air at 37°C (X); in air at 24°C (●); in air at 37°C after reduction to single cells by trypsinization (▲); or in nitrogen at 37°C (0), at 141 rad/min.

Symbol	PE	D_o	n
X	55%	210	-
●	56%	160	42
▲	62%	159	29
0	62%	430	-

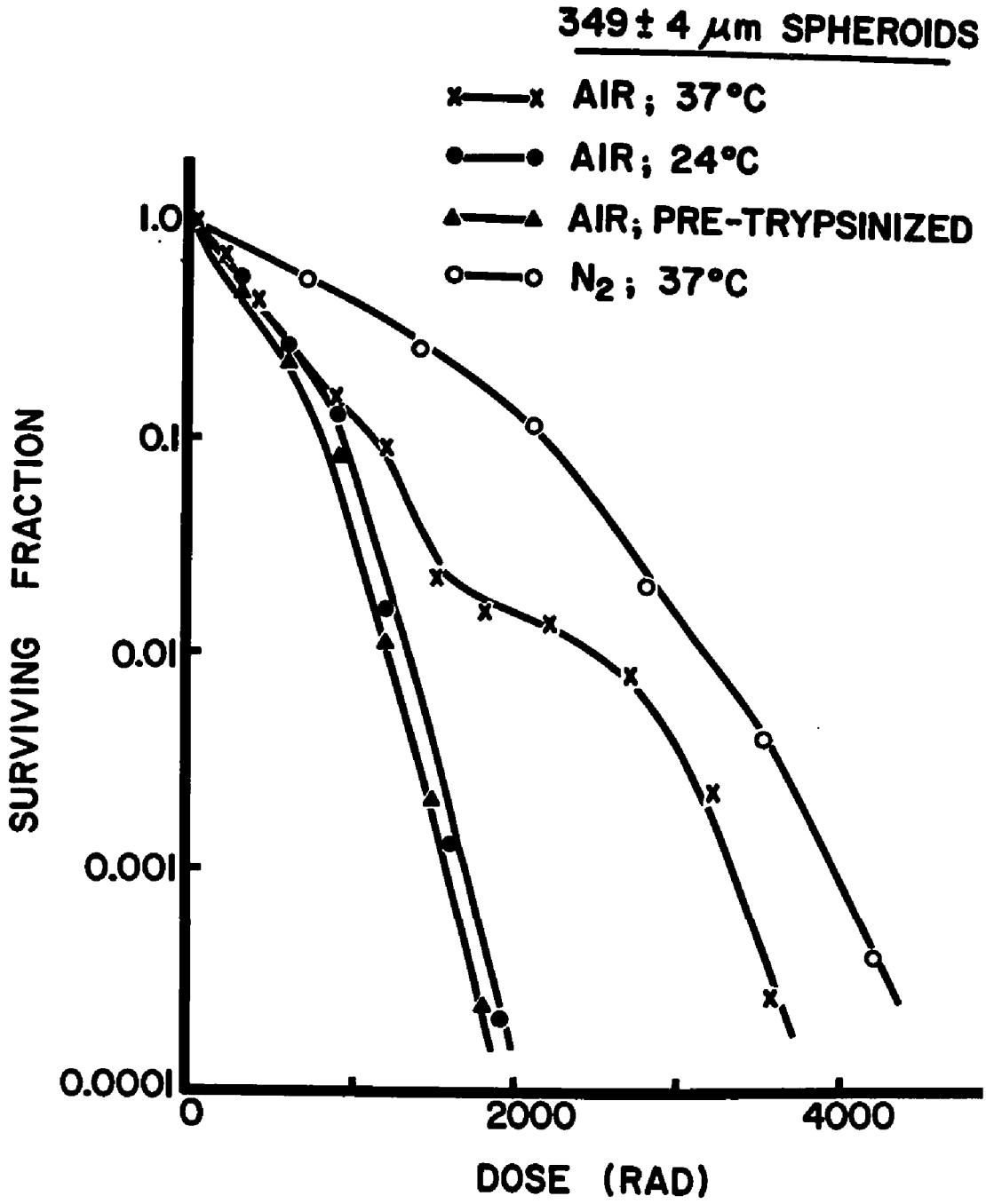
349 ± 4 μm SPHEROIDS
AIR; 37°C
AIR; 24°C
AIR; PRE-TRYPSINIZED
N2; 37°C
SURVIVING FRACTION
1.0
0.1
0.01
0.001
0.0001
0
2000
4000
DOSE (RAD)

population of cells. This appeared to have occurred in the upper curve of figure 4.7, resulting in a biphasic survival curve. Smaller spheroids with more cycling cells showed the two components more clearly (see figure 4.9). The increase in radioresistance found (D_o = 430 rad versus 210 rad for the control curve) was entirely attributable to cell cycle effects (see figures 3.6d, 3.7d and 3.10b), since, under anoxic conditions, the cycling S phase cells would be most resistant. The elimination of the third component of the curve under anoxic conditions thus suggested that the most resistant cells under normal conditions were likely hypoxic.

Under steady-state conditions, concentration of oxygen within a sphere of metabolizing tissue is determined by the ambient oxygen concentration and by the rate of consumption (Appendix 4, equation 16). Complete reoxygenation of the cells from hypoxic regions of the spheroids occurred if the spheroids were reduced to single cells immediately prior to irradiation. Minimal progression through the cell cycle was expected in the short treatment time, and, as shown by figure 4.7, elimination of the resistant fraction of cells did occur. Another means of allowing oxygen to reach the internal cells was to reduce metabolic activity in the spheroid by lowering the temperature to 24°C for 20 minutes before and during

the irradiation. This allowed more oxygen to diffuse in and reoxygenate the hypoxic cells, and the final resistant component of the curve was completely eliminated (figure 4.7). Intercellular contact at the time of irradiation has been shown to enhance survival in this system (figures 2.9 and 2.10), and the slight survival increase seen with the latter method of reoxygenation reflected this contact.

Very large spheroids have previously been shown to contain only a small fraction of cycling cells (figures 3.1 and 3.2), so it was expected that irradiation of such large spheroids would show a very small, and possible unresolved component due to the cycling cells. The detailed survival curve analysis suggested in Appendix 2 indicates that cycling cells would not contribute noticeably to the survival curve whenever a larger fraction of cells was more resistant. This was observed experimentally in figure 4.8, where the initial survival curve shoulder is somewhat wider than normal, but cannot be resolved into more than one component. It was interesting to note that even with such large spheroids, only about 20% of the cells were found to be hypoxic, as in many animal tumors (Van Putten and Kallman 1968).

The hypoxic cells have been shown to be the cells

FIGURE 4.8

Survival of cells grown as single cells on petri dishes or as spheroids, and irradiated at 37°C in air (143 rad/min).

Symbol	PE	D_o	n
X	58%	395	-
O	86%	177	9.9

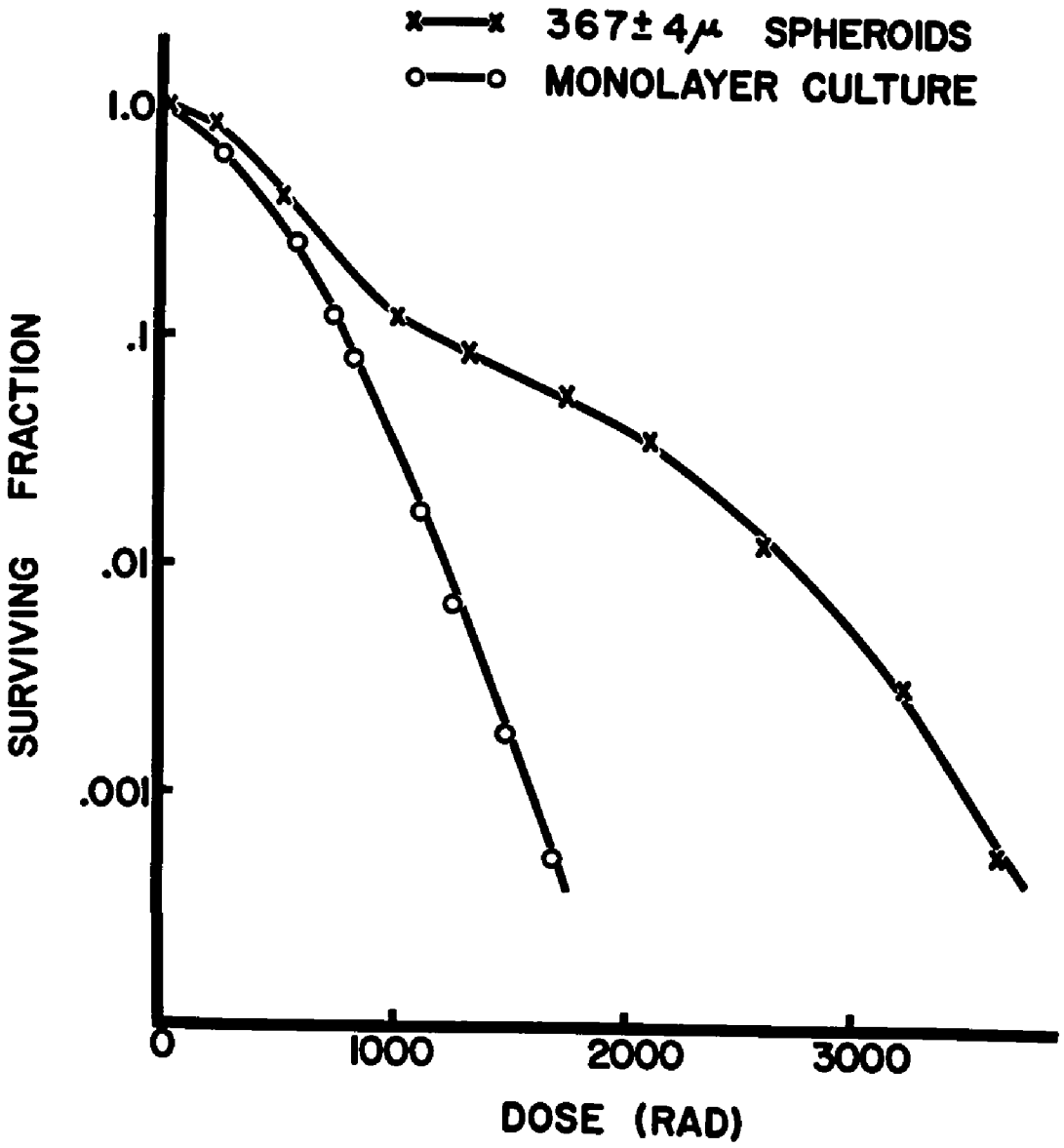
367± 4μ SPHEROIDS
MONOLAYER CULTURE
SURVIVING FRACTION
1.0
.1
.01
.001
0
1000
2000
3000
DOSE (RAD)

nearest the necrotic core of the spheroid. Some problems might be anticipated in the viability of these cells, particularly after the trypsinization procedure. It should be emphasized at this point that experiments conducted to determine plating efficiencies of cells from various regions of the spheroid following partial trypsinization showed no significant differences in plating efficiency. While these experiments were admittedly rather imprecise, the importance of at least trying to determine the PE of each population is clearly demonstrated in Appendix 2.

The results obtained in section 3.2 indicated that the internal cells of large spheroids accumulated in a G_1-like phase of the cell cycle that was designated G_0 (see section 3.2.4). The properties of these cells were demonstrated in figure 4.9, where anoxic spheroids were irradiated and the single cells were then treated with hydroxyurea to kill those cells in S phase. The two-component survival curve usually found under anoxic conditions was reduced to a single component curve by this treatment. Comparison with synchronous day 1 spheroid cells irradiated in an anoxic environment at the cell cycle position of maximum radiosensitivity (M/G_1) showed that cells in the HU-treated anoxic spheroids were slightly more resistant (D_o = 310 rad versus 240 rad for

FIGURE 4.9

Survival of cells grown as spheroids and irradiated in nitrogen at 37°C as intact, untreated spheroids (X); spheroids with S phase cells selectively removed by treatment with hydroxyurea (▲); and synchronized day 1 spheroids in the most sensitive part of the cell cycle (●). Dose rate was 148 rad/min.

Symbol	PE	D_o	n
X	56%	442	38
▲	43%	310	490
●	46%	240	1180

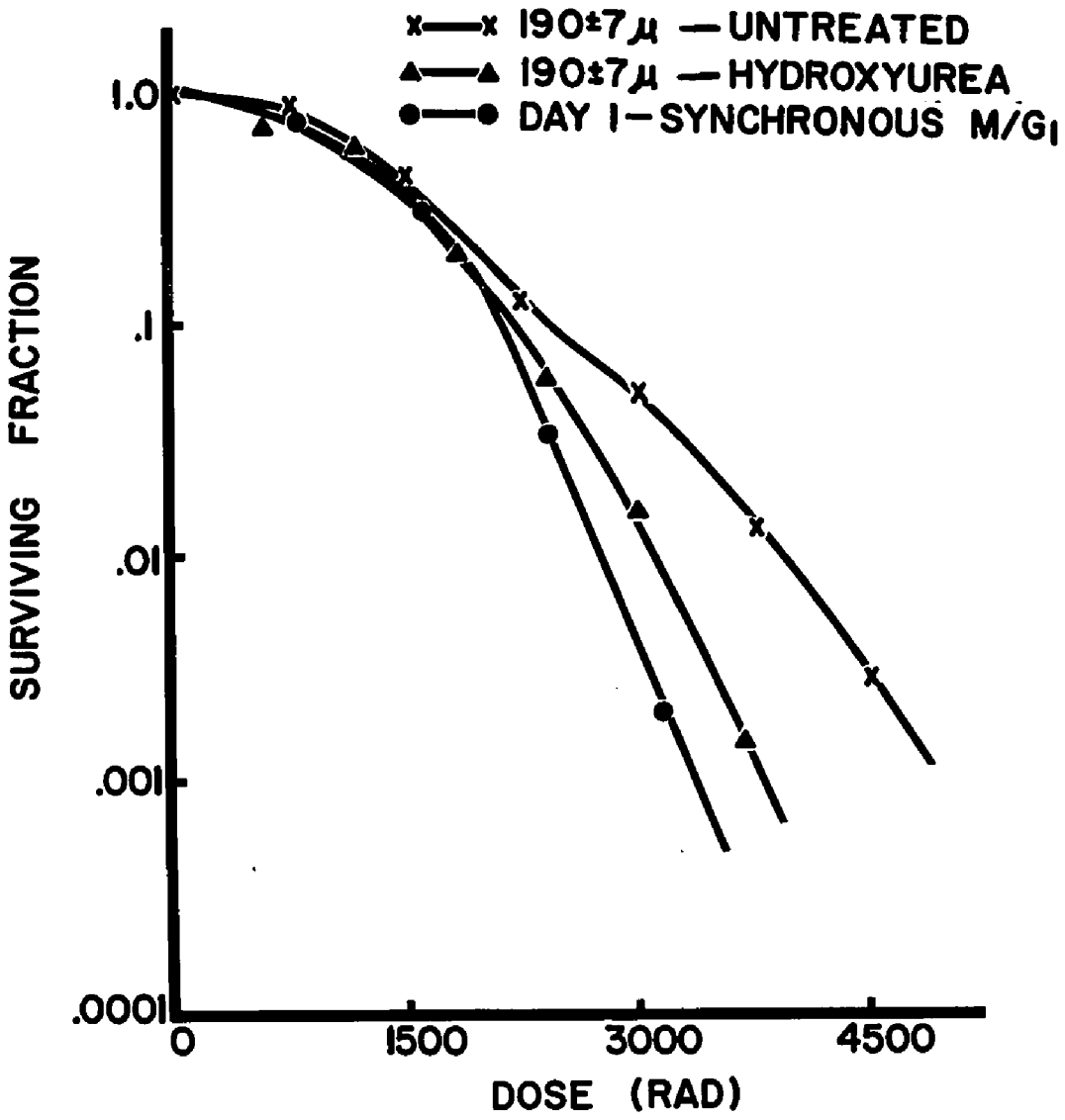
x—x 190±7μ — UNTREATED
▲—▲ 190±7μ — HYDROXYUREA
●—● DAY 1 — SYNCHRONOUS M/G1
SURVIVING FRACTION
1.0
.1
.01
.001
.0001
0
1500
3000
4500
DOSE (RAD)

the synchronous day 1 spheroid cells). This was not unexpected, as some of the cycling cells in G_1, G_2 and M would add to the resistance of the drug-treated spheroids (as found in air when figure 3.7d was compared with figure 3.10b). The similarities of radiosensitivity of the non-S cells (primarily G_0) of the totally anoxic spheroids to the most resistant population of cells found when spheroids were irradiated in air suggests that the latter population was indeed hypoxic G_0 cells.

Additional evidence of the effects of treating the irradiated cells with HU to remove all S phase cells of twelve day old spheroids irradiated under normal (37°C) or lowered (24°C) temperatures is shown in figure 4.10 . At 37°C, the normal three-component survival curve was reduced to only two components by the hydroxyurea, as the component of intermediate resistance (see also figures 3.6 and 3.7) was completely removed. Survival of the most resistant cells remained qualitatively similar. The reoxygenated (24°C) spheroids that were treated with HU also showed a single component survival curve with D_o = 100 rad, similar to previous results for other younger spheroids (figure 3.7) or for synchronous early G_1 phase day 1 spheroids (figure 3.10b).

Interpretation of figure 4.10 is complicated by the presence of the three cell populations. Since the

FIGURE 4.10

Survival of cells from day 12 spheroids irradiated in air at 37°C (X) or at 24°C (▲) at a dose rate of 130 rad/min. Cells from both 37°C (●) and 24°C (■) were then treated with hydroxyurea to selectively remove S phase cells.

Symbol	PE	D_o	n
X	54%	-	-
●	41%	-	-
▲	58%	160	32
■	42%	100	470

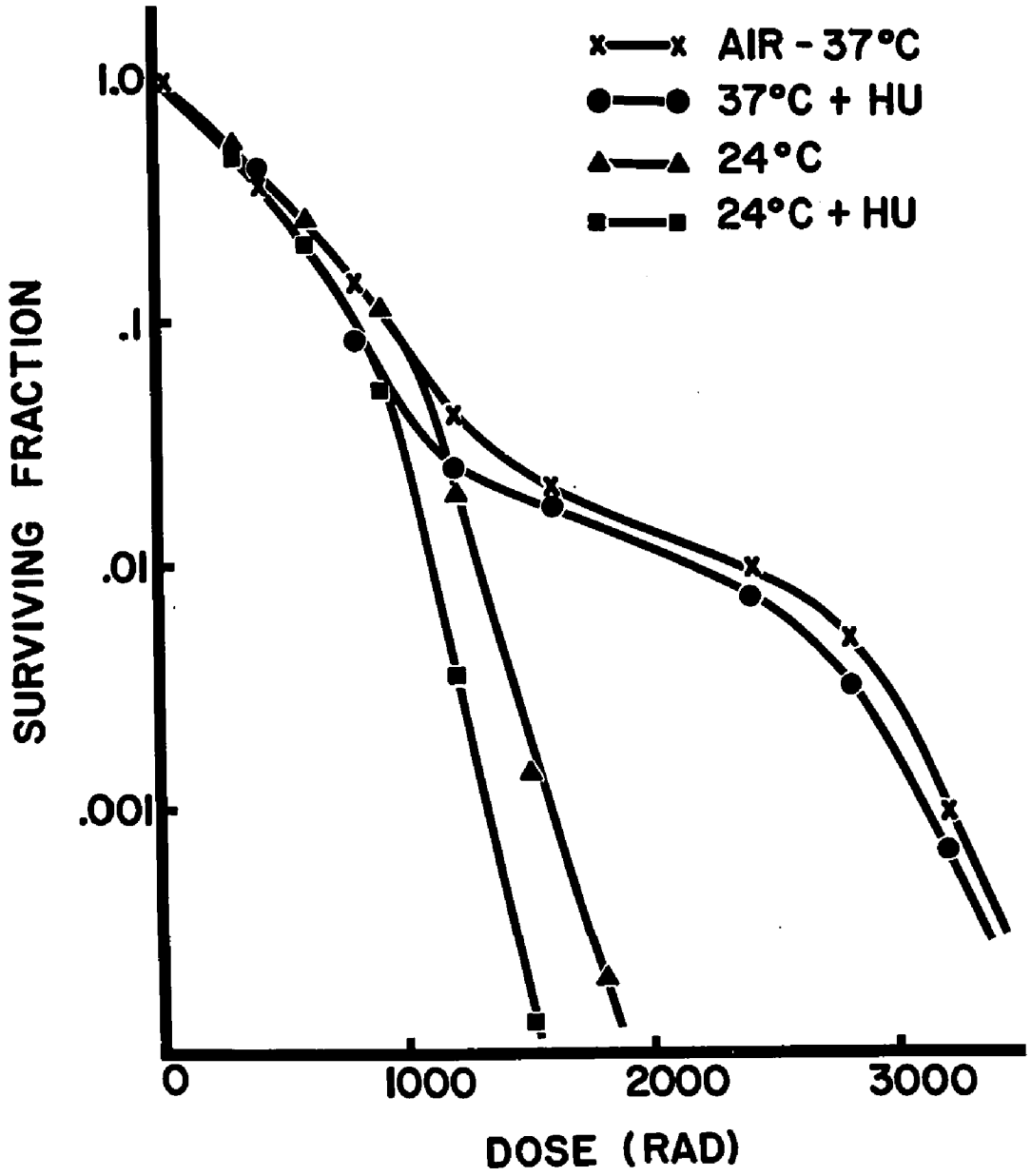
AIR - 37°C
37°C + HU
24°C
24°C + HU
SURVIVING FRACTION
1.0
.1
.01
.001
0
1000
2000
3000
DOSE (RAD)

treatment with hydroxyurea should have eliminated the cycling S phase cells at 37°C (about 20% of the total population), the 8% of the cells that were hypoxic should have formed a larger percentage of the drug-treated cells, and should have been displaced upward in the normalized survival curve where only the viable cells were assayed for radiation damage. As the curve was lower, it must be concluded that the HU treatment also was lethal to some of the hypoxic cells (probably due to the tumor-like environment).

Electron-affinic chemicals selectively sensitize hypoxic cells to radiation (Adams 1970, Chapman et al 1971 and 1972), so they provide another experimental approach to confirm the presence of hypoxic cells in the spheroid. Para-nitroacetophenone (PNAP) at a concentration of 1 mM was added to spheroids which were then maintained at 37°C for one hour prior to exposure to radiation. The effects of this treatment, relative to spheroids irradiated in the absence of the chemical are shown in figure 4.11 . The resistant, hypoxic cells were sensitized by the chemical, but the survival decrease observed was not as large as that found with reoxygenation (figure 4.7). Since PNAP is well-known to sensitize only hypoxic cells (Adams 1970, Chapman et al 1971), the data provide additional evidence for hypoxia

FIGURE 4.11

Survival of cells grown as spheroids and irradiated in air at 37°C (159 rad/min) before (X) or 1 hour after the addition of 1 mM PNAP (O). Sensitization of the hypoxic cells is shown by decreased survival at high doses. Comparison of terminal slopes may not be valid (see text) as a measure of sensitization.

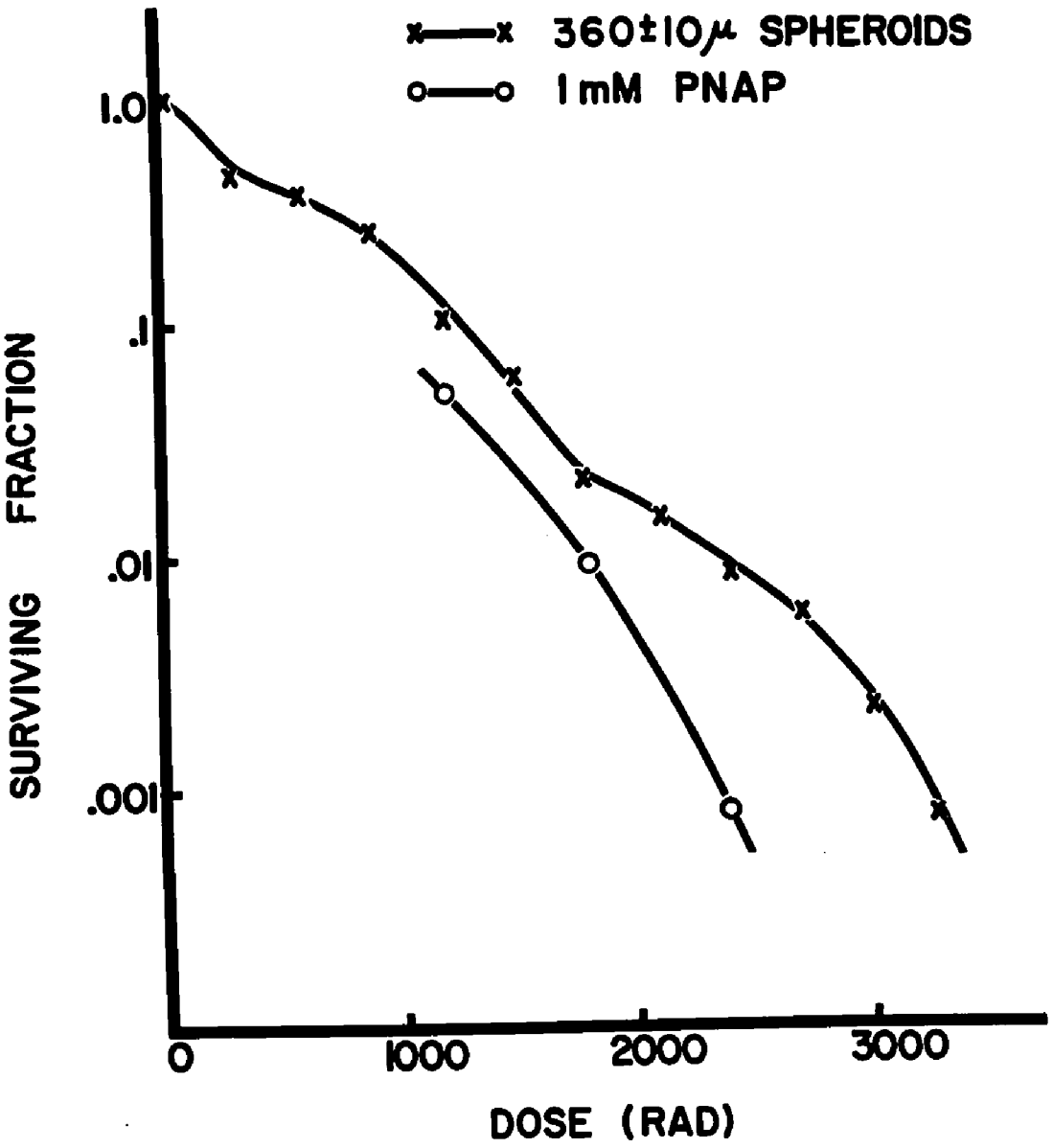
x—x 360±10μ SPHEROIDS
o—o 1mM PNAP
SURVIVING FRACTION
1.0
.1
.01
.001
0
1000
2000
3000
DOSE (RAD)

being the major factor responsible for this most resistant portion of the survival curve.

The complex curve which characterized survival of cells from spheroids irradiated in air has been attributed to three cell states, including hypoxic G_0, aerobic G_0 and aerobic, cycling cells. One should thus be able to predict theoretically the type of survival curve expected for such a population of cells. Figure 4.12 shows broken survival curves for the three cell states outlined above. The aerobic G_0 cell survival was identical to that found in figure 4.10, and the survival of cycling cells in contact was previously shown in figure 2.8 . The curve of figure 4.9 was used to represent the G_0 hypoxic cells. As shown in figure 4.12, a population of cells composed of 73% G_0 aerobic, 18% cycling aerobic and 9% hypoxic G_0 cells would have a survival curve similar to the solid line. Data from a day 9 spheroid were included to show that experimental results can be predicted theoretically.

4.3.4 Summary

Radiation resistant, hypoxic cells have been demonstrated in the spheroid using several different experimental approaches. The fact that irradiation in complete anoxia did not increase the survival of the most

FIGURE 4.12

Theoretical survival (solid line) of a population of cells comprised of the three sub-populations represented by the broken survival curves. The curve intersecting the ordinate at .73 represents the survival if 73% of the population were aerobic G_0 phase with survival as in figure 4.10; the broken curve intersecting at .18 represents the survival of aerobic, cycling cells as in figure 2.8; and the broken curve intersecting the ordinate at .09 represents the survival of 9% of the cells being G_0 hypoxic as in figure 4.9 . The data points show the actual survival of cells from day 9 spheroids. The solid line is not a 'best fit', but does show the multicomponent nature of survival curves from such a mixed population of cells.

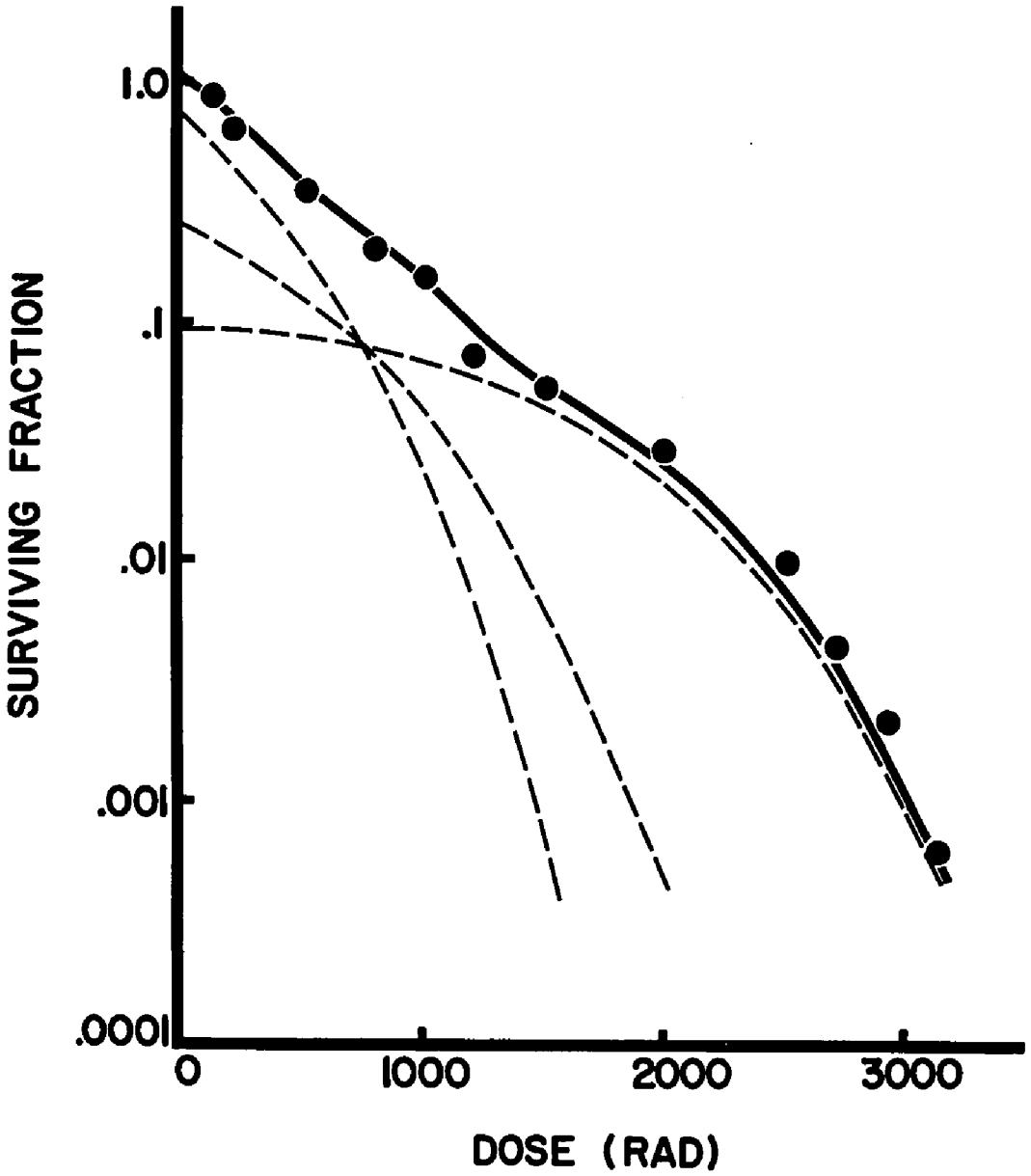
SURVIVING FRACTION
1.0
.1
.01
.001
.0001
0
1000
2000
3000
DOSE (RAD)

resistant cells suggested that hypoxia was responsible for the resistance. Reoxygenation of the hypoxic internal cells occurred when the lower temperature was used to decrease metabolic rate, or when the spheroids were reduced to single cells using trypsin, resulting in the loss of radioresistance shown in figure 4.7 . PNAP, an electron affinic chemical which specifically sensitizes hypoxic cells to radiation reduced the survival of the most resistant cells. Comparison of the survival curve obtained for completely anoxic cells with S phase cells removed by HU treatment after reducing the spheroid to single cells again showed that the most resistant population was the internal, G_0 population of cells.

4.4 Discussion

In addition to the morphological similarities of spheroids and nodular tumors, the results presented in this chapter have demonstrated that hypoxic cells gradually develop in the spheroid and that the net response of the spheroid to radiation is dependent upon both hypoxia and cell cycle position effects as is the response of the <u>in vivo</u> tumor. Table 2 summarizes typical survival curve parameters obtained at various stages of growth with single cells and spheroids. One interesting feature shown is that the non-S, or G_0 cells of larger spheroids were more sensitive in air as the spheroid aged; in

TABLE 2.

Summary of survival curve parameters.

	Irradiation Atmosphere[1]	D_o (rad)	n	D_q (rad)	Figure Reference[2]
		SINGLE CELLS			
Asynchronous	A	168	10.2	388	2.7
Asynchronous	N	456	9.3	1002	2.12
Plateau	A	195	30.5	666	2.7
		SPHEROID CELLS			
Immature					
Asynchronous	A	186	182	965	2.8
Non-S phase	A	121	102	560	3.7
Non-S phase	N	310	490	1920	4.9
Mature					
Non-S phase	A	100	470	615	4.10
Non-S phase	N	395	-	-	4.8

[1] 'A' denotes aerobic irradiation conditions, 'N' denotes hypoxic conditions

[2] Number of the figure in this thesis from which parameters were obtained

normal irradiation conditions of 37°C, these cells were hypoxic and became more radioresistant as the spheroids aged. Thus, prolonged hypoxia, alone or in combination with other factors in the tumor-like environment of the spheroid produced increased resistance to radiation.

Multi-component radiation survival curves have been demonstrated for a variety of in vivo tumor systems (Powers and Tolmach 1963 and 1964, Barendsen and Broerse 1969, Lindop 1970). However, these usually consisted of only two components, similar to the results reported here for large spheroids having a small growth fraction. Results obtained with an in vitro model in stationary phase (Shinohara and Okada 1972) showed only an increased resistance, characterized by a maximum DMF of 2.95 . This probably reflected a high proportion of hypoxic cells in that system during the irradiation procedure, as compared to the relatively small fraction of hypoxic cells (5-20%) in the spheroid system. The large differences in radiosensitivity of spheroid cells in different phases of the growth cycle, as well as the sensitivity of the assay technique also aided demonstration of multicomponent curves with this system.

Alterations in the multicomponent nature of the spheroid survival curve require a more critical analysis than with single cells due to the additional complexities

of the experiments. It was not considered meaningful to calculate dose modifying factors for these experiments since the cells surviving after reoxygenation or other sensitizing procedures were not necessarily the same population whose resistance was greatest under normal conditions. For example, after reoxygenation, the most resistant cells in the mature spheroids were the cycling S phase cells, whereas at 37°C in the intact spheroid, the most resistant cells were the hypoxic G_0 cells. The variation between survival curves for different batches of spheroids of the same size can be explained on the basis of the nutritional state and history of that particular population of spheroids. Absolute reproducibility was neither expected or obtained, despite the care taken to ensure that consistent growth conditions were provided. Similar survival patterns were, however, always observed. Post-exposure handling procedures involving trypsinization and plating were never varied. Multiple determinations of single survival points within an experiment were often done, and demonstrated that excellent reproducibility could be obtained within any experiment.

The sensitization of the hypoxic cells of the spheroid with PNAP was of special interest. In addition to showing that the internal cells were indeed hypoxic, fig-

ure 4.11 demonstrates that at least PNAP is one member of the family of electron affinic compounds that can diffuse into the spheroid and sensitize hypoxic cells in a tumor-like environment. Sensitization was not expected to be as great as in the case of reoxygenation, as the maximum DMF observed with single cell cultures is about 1.6 (Chapman et al 1971), whereas the DMF for oxygen is generally about 3 . However, more electron affinic chemicals have been shown to be even more effective sensitizers of the resistant cells (Hetzel et al 1972, Sutherland and Durand 1972a).

V. GENERAL DISCUSSION

A system of increased complexity inherently requires a more complex analysis, which thus increases the probability of incorrect explanations of phenomena observed. Previous discussions have indicated many such possibilities with the spheroids, and the conclusions presented have been obtained with these limitations in mind. While specific questions can often be easily answered on the basis of a given series of experiments, more general techniques used in most or all experiments may influence the experimental results obtained, and thus merit additional discussion.

5.1 Survival analysis

All survival curves for spheroid cells (with the exception of the experiment shown in figure 2.16) involved trypsinization at some stage of the experiment. It is not known whether trypsin and radiation interact synergistically and thus decrease survival in the spheroid system, particularly since preliminary experiments not reported here showed that survival could be manipulated by changing the trypsinization procedure. This apparent synergism between trypsin and high doses of radiation was eliminated as completely as possible by choosing a trypsinizing technique which resulted in max-

imal survival. Using this procedure, no difference in survival was noted when trypsinization and survival assay were performed immediately, or delayed for times as long as 15 hours post-irradiation (where changes in multiplicity due to division of surviving cells were accounted for).

The data of figure 2.16 may however suggest that trypsinization did in fact affect post-irradiation survival. When the whole spheroids were plated and allowed to develop into colonies, increased survival was noted. This suggested either that cells did not survive independently, or that the trypsinization procedure acted synergistically with the radiation to produce less survival when the spheroid was trypsinized. Although the possibility of such synergism could not be excluded in the results presented, it was possible to determine that trypsin alone or in combination with radiation had essentially no effect on survival of single or crowded cell cultures on petri dishes. If it is valid to extrapolate from the single cell case to the spheroid system, it follows that no anomalous effects should have been introduced by the trypsinizing procedure.

5.2 Survival curve concavity

Some of the survival curves presented appear concave,

that is, they bend downward continuously over the dose range used. According to classical multi-target survival curve theory (see Elkind and Whitmore 1967, Fabrikant 1972) this would be unexpected, although it has been observed experimentally before (Barendsen et al 1960). It is, however, interesting to note that in many reviews and books (Elkind and Whitmore 1967, Okada 1970, Fabrikant 1972) that the data of many survival curves at high doses, while often not significantly different from a straight line, could equally well be represented by curves with considerably larger shoulders (thus increasing the extrapolation number n and decreasing D_o).

If high enough survival could be attained in the present system to accurately trace survival after larger doses of radiation, the curves thus obtained would be more valuable for studying survival and recovery phenomena. Of particular interest was the concavity of curves for early G_1 phase cells in contact, whether synchronized and irradiated in air (figure 3.10b) or under anoxic conditions (figure 4.9). The most resistant cells of the mature spheroids, the G_0 hypoxic cells, also typically displayed a concave-downward curve. A demonstration that concavity really does continue at higher doses and the implications of such a result have yet to be established.

5.3 Cell cycle kinetics

Detailed cell cycle kinetic studies of the growing and mature spheroids have yet to be conducted. Of the results presented in this thesis, the most interesting feature of the spheroid model is the accumulation of the pre-DNA synthesis population of cells, despite the fact that almost all cells incorporated labelled thymidine when exposed to the label for sufficiently long periods of time. The discussion of Chapter II considered the possibility that these data were in conflict with the synchrony indicated in the regrowth experiments as well as in the radiation experiments.

Explanation of the results of Chapter II does require one assumption concerning the regrowth data--it is necessary to postulate that the cells can exist in the spheroid as a non-cycling, viable population of G_0 cells, and in addition, that on the initiation of regrowth, all cells in the G_0 phase simultaneously re-enter the normal division cycle at a particular point in the normal G_1 phase. Since all cells (at least all cells that likely are viable) eventually become labelled, it follows that any cycling cell that reaches this point in G_1 may or may not enter G_0. If the cell does enter G_0, there is a high probability that a current G_0 cell will re-enter the normal cycle at the same position of

G_1 and to then continue through the cycle in the normal manner. Obviously, the external cells of the spheroid have a different mean cell cycle length probably characterized by a shorter G_1 phase, and these cells would not enter G_0.

Under these hypotheses, all data of Chapter II can be explained. The initial rapid decreases in labelling and mitotic indices (figure 3.2) can be explained by the elongation of G_1 phase in the internal cells. As the spheroids increase further in size, the G_0 population gradually develops, and for large spheroids a more or less steady-state develops due to random entry and departure of internal cells in G_0 phase. However, at the time of initiation of regrowth under optimal conditions, the cells which had accumulated in G_0 would re-appear as a synchronous, early G_1 phase population.

It has not yet been established whether the above argument represents the correct interpretation of the cell cycle kinetics in the spheroid. There are still two questionable features, and the conclusions reached depend upon the validity of the labelling of internal cells (i.e. does labelling indicate DNA replication?), or the validity of the regrowth data (to what extent does regrowth represent the <u>in situ</u> circumstances?).

5.4 The 'contact effect'

This line of Chinese hamster cells grown and irradiated in conditions of close intercellular contact displays an enhanced survival after irradiation that has been termed the 'contact effect'. Although growth in contact appears to be responsible for the largest part of the effect, contact during the actual irradiation additionally enhances survival. As previously suggested, the latter effect may have been only an artifact due to the trypsinization. Despite the evidence that the enhanced survival can be reduced at metabolically unfavorable temperatures, a detailed explanation of the phenomena has not yet been found.

It may, however, by useful to speculate on the general problem. The discussions accompanying previous chapters have been made with reference to specific repair mechanisms, and the conditions under which optimal efficiency of these mechanisms may be expected. The more general problem of the cellular state as a whole will now be considered.

A particularly appealing, yet not well-known concept, that of an intracellular 'pool' was made by Powers (1962). Based on this suggestion which was used in the work of Lajtha and Oliver (1961), Laurie et al (1972) have recently suggested a model for explicitly incorporating

a repair process into the explanation of survival curve shape and parameters. This repair process (corresponding to the shoulder of the survival curve) differs from the normal repair of sublethal damage (Elkind and Sutton 1960).

While the present work does not completely support these hypotheses, they provide the basis of a possible interpretation of the contact effect. One can invoke the concept of an intracellular pool in a somewhat more specific sense, in that the pool represents the total functional capacity, or preferably, the 'energy store' of the cell. Under typical in vitro growth conditions, the single cell is in an equilibrium state, in which normal maintenance of and input into this energy pool is balanced by the expenditure of this energy to progress through the cell cycle. If the cell is subjected to stress of any type, it is reasonable to suppose that the cell must draw on this pool to resist the external stress, thus reducing its capacity for growth until the cell has 'adapted' to the stress, or the stress has been removed.

This concept may explain experimental observations made in this laboratory (unpublished), in which changes in growth conditions for single cells (e.g., trypsinization, lowering the serum complement of the growth medium, or replacing the H_2O of the growth medium with D_2O) lead

to a lag phase (or period of adaptation and replenishment of the pool) followed by growth at a normal rate. The concept of the intracellular pool may also explain the well known division delay following irradiation (Elkind and Whitmore 1967, Okada 1970) during which the pool must be replenished. Conversely, potentially lethal radiation damage may be repaired only when the cell is forcibly maintained in a non-proliferating state so that the entire contents of the pool are available for the repair process. Minimal metabolic requirements for all growth and repair processes must of course by maintained (Okada 1970, Ashby et al 1969).

The energy pool of the cell may also be expended differently at different parts of the generation cycle. For example, it seems reasonable to postulate that the most visibly chaotic event in the generation cycle, mitosis, might well be associated with a tremendous expenditure of this intracellular energy. An external stress during the preparation for mitosis (late G_2) or mitosis itself would then be predicted to be more disrupting, as the decreased cellular energy pool would leave the cell more susceptible to the stress. This is seen with at least one external stress, ionizing radiation. Again, after mitosis and in preparation for initiation of DNA synthesis, the pool could still be expected to be somewhat

depleted. These arguments may thus partially explain the differential responses of single or spheroid cells to ionizing radiation as the cells progress through the division cycle.

Extrapolation of these predictions to the case of altered growth conditions is not particularly difficult, especially if growth in contact represents a situation in which growth requires less 'energy' (particularly if sharing of energy pools, or even critical growth enzymes were occurring). Thus, since the cell depletes the pool to a lesser extent by its normal proliferation, more 'energy' remains to resist external stress. The kinetic development and loss of the ability for enhanced accumulation and repair of sublethal radiation damage (figures 2.10 and 2.11) also suggest that the concept of adaptation to the new environment, with differing demands on the cellular pool, is not at all unreasonable. Higher survival would thus also be predicted when minimal demands on the pool (i.e. maintained contact) were made at the time of irradiation. Introduction of another stress, that of sub-optimal temperatures, is inferred to reduce the portion of the energy pool available for repair of radiation damage in the spheroid case, resulting in the decreased accumulation of sublethal damage.

These suggestions are, of course, entirely spec-

speculative, and no attempt has been made to prove or disprove the postulated conditions. However, the concept of the intercellular energy pool does allow a general interpretation of most of the observed events.

5.5 Future applications

Each demonstrable similarity between the *in vitro* tumor model and the *in vivo* tumor leads to new ideas for future applications. Obviously, the ideal system would be a transplantable nodular tumor of some type which would also grow in culture, so that one could investigate the effects of treatments on the single cells in culture, the spheroid model, and finally the *in vivo* tumor. Present priorities include multiple-dose radiotherapy programs to determine optimal fraction sizes and treatment times for sterilization of the spheroid cells, as well as other treatment methods including continuous, low dose-rate irradiation and high-LET radiations. Studies with chemical radiosensitizers specific to hypoxic cells have already generated useful results (Sutherland and Durand 1972a). Similar studies are possible with chemotherapeutic agents, and possibly even studies of immunotherapeutic techniques may become practical. In any of these applications, the tumor-like environment of the spheroid, free from the complexities of tumor-host interactions, provides a model of incomparable potential.

VI. SUMMARY

The present work has made several unique contributions to the general field of radiobiology. Preliminary work from this laboratory had shown that the spheroids were histologically similar to the in vivo tumor (Sutherland et al 1971), grew with comparable kinetics (Inch et al 1970), and had a multicomponent radiation survival curve (Sutherland et al 1970). The present thesis has expanded these results in at least the following significant areas:

(1) Multicellular spheroids have been shown to contain cells in subpopulations that differ with respect to cell cycle position and oxygenation status, as in many tumors.

(2) Cells grown under conditions of extensive intercellular contact in the spheroids were found to have an increased radiation survival due to an enhanced ability to accumulate and repair sublethal radiation damage.

(3) The enhanced ability of these cells in contact to accumulate and repair sublethal radiation damage was shown to be dependent upon the position of the cell in its generation cycle, that is, contact effects were not constant at all stages of the cell cycle.

(4) The internal hypoxic cells of large spheroids were demonstrated to be radioresistant, and became even more resistant in large spheroids where prolonged hypoxia had occurred.

(5) The particular subline of cells used in all these experiments may not survive radiation independently, as cells kept in contact for long periods after irradiation had a higher probability of survival.

BIBLIOGRAPHY

ADAMS, G. E., 1970. Molecular mechanisms of cellular radiosensitization and protection. In: Radiation protection and sensitization, edited by H. L. Moroson and M. Quintiliani. London: Taylor and Francis

ADAMS, L. R. and KAMENTSKY, L. A., 1971. Machine characterization of human leukocytes by acridine orange fluorescence. Acta Cytologica 15:289-291

ALPER, T., 1968. The oxygen effect; pertinent or irrelevant to clinical radiotherapy. Br. J. Radiol. 41:73

ALPER, T., 1972. Aspects of neutron therapy based on an analysis of relationships between RBE and dose. Br. J. Radiol. 45:39-47

AOYAMA, T. and RIXON, R. H., 1967. The modification effect of cellular interaction on the radiation sensitivity of rat thymocytes. Radiat. Soc. Japan 4:135-139

ARLETT, C. F., 1970. The influence of post-irradiation conditions on the survival of Chinese hamster cells after gamma-irradiation. Int. J. Radiat. Biol. 17:515-526

ASHBY, R. R., BONTE, F. J. and BELLI, J. A., 1969. A study of some metabolic requirements for repair of sublethal irradiation damage. Radiology 93:895-899

BADIB, A. O. and WEBSTER, J. H., 1969. Changes in tumor oxygen tension during radiation therapy. Acta Radiologica 8:247-257

BARENDSEN, G. W., BEUSKER, L. T. J., VERGROESEN, A. J. and BUDKE, L., 1960. Effects of different ionizing radiations on human cells in tissue culture. II. Biological experiments. Radiat. Res. 13:841-849

BARENDSEN, G. W. and BROERSE, J. J., 1969. Experimental radiotherapy of a rat rhabdomyosarcoma with 15 MeV neutrons and 300 kV X-rays. I. Effects of single exposures. Eur. J. Cancer 5:373-391

BEDFORD, J. S. and HALL, E. J., 1966. Threshold hypoxia: its effect on the survival of mammalian cells irradiated at high and low dose-rates. Br. J. Radiol. 39:896-900

BELLI, J. A. and BONTE, F. J., 1963. Influence of temperature on the radiation response of mammalian cells in tissue culture. Radiat. Res. 18:272-276

BELLI, J. A., DICUS, G. J. and NAGLE, W., 1970. Repair of radiation damage as a factor in pre-operative radiation therapy. Front. Radiat. Ther. Onc. 5:40-57

BENDICH, A., VIZOSO, A. B. and HARRIS, R. G., 1967. Intercellular bridges between mammalian cells in culture. Proc. Natl. Acad. Sci. U.S. 57:1029-1035

BERGSJO, P. and EVANS, J. C., 1968. Tissue oxygen tension of cervix cancer. Acta Radiologica 7:1-11

BERRY, R. J. and OLIVER, R., 1964. Effect of post-irradiation incubation conditions on recovery between fractionated doses of X-rays. Nature 201:94-96

BERRY, R. J., EVANS, H. J. and ROBINSON, D. M., 1966. Perturbations in X-ray dose response in vitro with time after plating: a pitfall in the comparison of results obtained by different laboratories using asynchronous cell systems. Exptl. Cell Res. 42:512-522

BERRY, R. J., HALL, E. J. and CAVANAGH, J., 1970. Radiosensitivity and the oxygen effect for mammalian cells cultured in vitro in stationary phase. Br. J. Radiol. 43:81-90

BEWLEY, D. K., 1968. The oxygen effect; pertinent or irrelevant to clinical radiotherapy. Br. J. Radiol. 41:73

BOAG, J. W., 1969. Oxygen diffusion and oxygen depletion problems in radiobiology. Curr. Top. Radiat. Res. 5:141-195

BURK, R. R., PITTS, J. D. and SUBAK-SHARPE, J. H., 1968. Exchange between hamster cells in culture. Exptl. Cell Res. 53:297-301

BURTON, A. C., 1966. Rate of growth of solid tumours as a problem of diffusion. Growth 30:157-176

BUSH, R. S. and BRUCE, W. R., 1965. The radiation sensitivity of a transplanted murine lymphoma as determined by two different assay methods. Radiat. Res. 25:503-513

CALKINS, J., 1971. A method of analysis of radiation response based on enzyme kinetics. Radiat. Res. 45:50-62

CHAPMAN, J. D., STURROCK, J., BOAG, J. W. and CROOKALL, J. O., 1970a. Factors affecting the oxygen tension around cells growing in plastic petri dishes. Int. J. Radiat. Biol. 17:305-328

CHAPMAN, J. D., TODD, P. and STURROCK, J., 1970b. X-ray survival of cultured Chinese hamster cells resuming growth after plateau phase. Radiat. Res. 42:590-600

CHAPMAN, J. D., WEBB, R. G., and BORSA, J., 1971. Radiosensitization of mammalian cells by p-nitro-acetophenone. I. Characterization in asynchronous and synchronous populations. Int. J. Radiat. Biol. 19:561-573

CHAPMAN, J. D., REUVERS, A. P., BORSA, M. PETKAU, A., and McCALLA, D. R., 1972. Nitrofurans--radiosensitizers of hypoxic mammalian cells. Cancer Res. (in press)

CHESHIRE, P. J. and LINDOP, P. F., 1969. The influence of intracellular recovery and hypoxic cells on the radiation response of mammary tumours and skin in mice. Br. J. Radiol. 42:215-223

DALEN, H. and BURKI, H. J., 1971. Some observations on the three-dimensional growth for L5178Y cell colonies in soft agar culture. Exptl. Cell Res. 65:433-438

DEL MONTE, U., 1969. Consideration of factors influencing the oxygenations of ascites tumors. Eur. J. Cancer 5:639-640

DENDY, P. P., 1968. The effects of X-rays on a human tumour growing in organo-typic culture. Eur. J. Cancer 4:163-172

DENEKAMP, J., 1970. The cellular proliferation kinetics of animal tumours. Cancer Res. 30:393-400

DEWEY, W. C., DETTOR, C. M., WINANS, L. F., WESTRA, A., and NOEL, J. S., 1972. A model relating changes in X-ray sensitivity during the mammalian cell cycle to changes in configuration of chromatin. Radiat. Res. 51:531

DODSON, E. O., 1966. Aggregation of tumor cells. Nature 209:40-44

DURAND, R. E. and SUTHERLAND, R. M., 1972. Unexpected radiation survival characteristics of V79-171b Chinese hamster cells ageing in monolayer cultures. Radiat. Res. (in press)

DU SAULT, L., 1971. Application of the oxygen factor to clinical radiology. Radiology 100:675-678

ELKIND, M. M. and SUTTON, H., 1960. Radiation response of mammalian cells grown in culture. I. Repair of X-ray damage in surviving Chinese hamster cells. Radiat. Res. 13:556-593

ELKIND, M. M., SUTTON, H. and MOSES, W. B., 1961. Postirradiation survival kinetics of mammalian cells grown in culture. J. Cell. Comp. Physiol. Supp. 58:113-134

ELKIND, M. M., SUTTON-GILBERT, H., MOSES, W. B. and KAMPER, C., 1976. Sub-lethal and lethal radiation damage. Nature 214:1088-1092

ELKIND, M. M. and WHITMORE, G. F., 1967. The radiobiology of cultured mammalian cells. New York: Gordon and Breach

ELKIND, M. M., WITHERS, H. R. and BELLI, J. A., 1968. Intracellular repair and the oxygen effect in radiobiology and radiotherapy. Front. Radiat. Ther. Onc. 3:55-87

ELKIND, M. M. and KANO, E., 1971. Radiation-induced age-response changes in Chinese-hamster cells. Evidence for a new form of damage and its repair. Int. J. Radiat. Biol. 19:547-560

FABRIKANT, J. I., 1972. Radiobiology. Chicago: Year Book Medical Publishers

FISCHER, J. J., 1971a. Mathematical simulation of radiation therapy of solid tumors. I. Calculations. Acta Radiologica 10:73-85

FISCHER, J. J., 1971b. Mathematical simulation of radiation therapy of solid tumors. II. Fractionation. Acta Radiologica 10:267-277

FOLKMAN, J., 1971. Tumor angiogenesis: therapeutic implications. New Eng. J. Med. 285:1182-1186

FOLKMAN, J., 1972. Anti-angiogenesis: new concept for therapy of solid tumors. Ann. Surg. (in press)

FOSTER, C. J., MALONE, J., ORR, J. S. and MACFARLANE, D. E., 1971. The recovery of the survival curve shoulder after protracted hypoxia. Br. J. Radiol. 44:540-545

FROESE, G., 1962. The respiration of ascites tumour cells at low oxygen concentrations. Biochim. Biophys. Acta. 57:509-519

FROESE, G., 1967. An interaction between neighboring cells. Exptl. Cell Res. 47:285-301

GRAY, L. H., CONGER, A. D., EBERT, M., HORNSEY, S., and SCOTT, O. C. A., 1953. The concentration of oxygen dissolved in tissues at the time of irradiation as a factor in radiotherapy. Br. J. Radiol. 26:638-648

GRAY, L. H., 1957. Oxygenation in radiotherapy. Br. J. Radiol. 30:403-406

HAHN, G. M., STEWART, J. R., YONG, S. J. and PARKER, V., 1968. Chinese hamster cell monolayer cultures. I. Changes in cell dynamics and modifications of the cell cycle with the period of growth. Exptl. Cell Res. 49:285-292

HALL, E. J., BEDFORD, J. S. and OLIVER, R. A., 1966. Extreme hypoxia; its effect on the survival of mammalian cells irradiated at high and low dose-rates. Br. J. Radiol. 39:302-307

HALL, E. J., 1967. The oxygen effect: pertinent or irrelevant to clinical radiotherapy. Br. J. Radiol. 40:874

HALL, E. J., 1972. The effect of hypoxia on the repair of sublethal radiation damage in cultured mammalian cells. Radiat. Res. 49:405-415

HALPERN, B., PEJSACHOWICZ, B., FEBRE, H. L. and BARSKI, G., 1966. Differences in patterns of aggregation of malignant and non-malignant mammalian cells. Nature 209:157-159

HAM, A. W., 1970. Histology. Philadelphia: Lippincott

HAYNES, R. H., 1966. The interpretation of microbial inactivation and recovery phenomena. Radiat. Res. Suppl. 6:1-29

HERMENS, A. F. and BARENDSEN, G. W., 1969. Changes of cell proliferation characteristics in a rat rhabdomyosarcoma before and after X-irradiation. Eur. J. Cancer 5:173-189

HETZEL, F. W., KRUUV, J., and FREY, H., 1972. Effect of PNAP on radiation survival in an *in vitro* tumour model. Biophys. Soc. Abstract #FPM-B4, Toronto, Canada

HEWITT, H. B. and WILSON, C. W., 1959. A survival curve for mammalian leukaemia cells irradiated *in vivo*. (Implications for the treatment of mouse leukaemia by whole-body irradiation). Br. J. Cancer 13:69-75

HORNSEY, S., 1972a. The radiosensitivity of melanoma cells in culture. Br. J. Radiol. 45:158

HORNSEY, S., 1972b. The radiation response of human malignant melanoma cells *in vitro* and *in vivo*. Cancer Res. 32:650-651

HOWES, A. E., 1969. An estimation of changes in the proportion and absolute numbers of hypoxic cells after irradiation of transplanted C3H mouse mammary tumours. Br. J. Radiol. 42:441-447

INCH, W. R. and McCREDIE, J. A., 1968. Factors influencing radiosensitivity of animal tumors. Can. Medical Assoc. J. 99:337-342

INCH, W. R., McCREDIE, J. A. and SUTHERLAND, R. M., 1970. Growth of nodular carcinomas in rodents compared with multi-cell spheroids in tissue culture. Growth 34:271-282

KALLMAN, R. F., 1968. Repopulation and reoxygenation as factors contributing to the effectiveness of fractionated radiotherapy. Front. Radiation Ther. Onc. 3:96-108

KEMBER, N. F., 1967. Cell survival and radiation damage in growth cartilage. Br. J. Radiol. 40:496-504

KIEFER, J., 1969. The interpretation of split-dose survival data: recovery factor and 'pre-damage reversal fraction'. Int. J. Radiat. Biol. 16: 297-300

KIEFER, J., 1971. Target theory and survival curves. J. Theoret. Biol. 30:307-313

KOCH, C. J. and KRUUV, J., 1971. The effect of extreme hypoxia on recovery after radiation by synchronized mammalian cells. Radiat. Res. 48:74-85

KOCH, C. J., 1972. Effects of low partial pressures of oxygen on the radiation response, repair of radiation damage, and growth kinetics of mammalian fibroblasts. Doctoral dissertation, The University of Waterloo

KOLODNY, G. M., 1971. Evidence for transfer of macromolecular RNA between mammalian cells in culture. Exptl. Cell Res. 65:313-322

KRUUV, J., INCH, W. R. and McCREDIE, J. A., 1967a. Blood flow and oxygenation of tumours in mice. I. Effects of breathing gases containing carbon dioxide at atmospheric pressure. Cancer 20:51-59

KRUUV, J., INCH, W. R. and McCREDIE, J. A., 1967b. Blood flow and oxygenation of tumours in mice. II. Effect of vasodilator drugs. Cancer 20:60-65

KRUUV, J. and SINCLAIR, W. K., 1968. X-ray sensitivity of synchronized Chinese hamster cells irradiated during hypoxia. Radiat. Res. 36:45-54

LAJTHA, L. G. and OLIVER, R., 1961. Some radiobiological considerations in radiotherapy. Br. J. Radiol. 34:252-257

LAJTHA, L. G., 1968. Radiation effects on steady state cell populations. Radiat. Res. 33:659-669

LANGE, C. S., 1970. On the relative importance of repair and progression in Elkind recovery as measured in synchronous HeLa cells. Int. J. Radiat. Biol. 17:61-79

LAURIE, J., ORR, J. S. and FOSTER, C. J., 1972. Repair processes and cell survival. Br. J. Radiol. 45362-368

LEGRYS, G. A. and HALL, E. J., 1969. The oxygen effect and X-ray sensitivity in synchronously dividing cultures of Chinese hamster cells. Radiat. Res. 37:161-172

LINDOP, P., 1970. Tissue effects of radiation in relation to radiotherapy. Curr. Top. Radiat. Res. 6:293-324

LITTBRAND, B. and REVESZ, L., 1964. Recovery from X-ray injury and the effect of oxygen. Nature 203: 889-891

LITTBRAND, B. and REVESZ, L., 1969. The effect of oxygen on cellular survival and recovery after radiation. Br. J. Radiol. 42:914-924

LITTLE, J. B., 1969a. Repair of sub-lethal and potentially lethal radiation damage in plateau phase cultures of human cells. Nature 224:804-806

LITTLE, J. B., 1969b. Differential response of rapidly and slowly proliferating human cells to X-irradiation. Radiology 93:307-313

LITTLE, J. B., 1971. Repair of potentially-lethal radiation damage in mammalian cells: enhancement by conditioned medium from stationary cultures. Int. J. Radiat. Biol. 20:87-92

LITTLE, J. B., RICHARDSON, U. I. and TASHJIAN, A. H., 1972. Unexpected resistance to X-irradiation in a strain of hybrid mammalian cells. Proc. Nat. Acad. Sci. U.S. 69:1363-1365

LOEWENSTEIN, W. R., 1966. Permeability of membrane junctions. Ann. N. Y. Acad. Sci. 137:441-472

LOEWENSTEIN, W. R. and KANNO, Y., 1966a. Intercellular communication and the control of tissue growth: lack of communication between cancer cells. Nature 209:1248-1249

LOEWENSTEIN, W. R. and KANNO, Y., 1966b. Cell-to-cell passage of large molecules. Nature 212:629-630

LONGMUIR, I. S., 1966. In: Scientific basis of medicine. University of London: Athlone Press

MALONE, J. F., FOSTER, C. J., ORR, J. S. and SOLOMONIDES, E., 1971. The effects on the survival of HeLa S-3 cells of independent variations in the sizes of the first and the second X-ray doses in split dose experiments. Int. J. Radiat. Biol. 20: 225-231

MAURO, F. and LITTLE, J. B., 1970. Repair of potentially lethal radiation damage in plateau phase cultures of mammalian cells. Proc. Fourth International Congress Radiat. Res., Evian, France (in press)

MELAMED, M. R., ADAMS, L. R., ZIMRING, A., MURNICK, J. G. and MAYER, K., 1972. Preliminary evaluation of acridine orange as a vital stain for automated differential leukocyte counts. Am. J. Clin. Pathol. 57:95-102

MENDELSOHN, M. L., 1962a. Autoradiographic analysis of cell proliferation in spontaneous breast cancer of C3H mouse. III. The growth fraction. J. Natl. Cancer Inst. 28:1015-1029

MENDELSOHN, M. L., 1962b. Chronic infusion of tritiated thymidine into mice with tumors. Science 135:213-215

MITCHELL, J. S., 1968. Applied science and the development of radiotherapy--past, present and future. Br. J. Radiol. 41:729-748

MOSCONA, A., 1961. Rotation-mediated histogenetic aggregation of dissociated cells. Exptl. Cell Res. 22:455-459

MOSKOWITZ, M., 1963. Aggregation of cultured mammalian cells. Nature 200:854-856

MOSKOWITZ, M., 1964. Nutritional and physical factors affecting the aggregation of cultured mammalian cells. Nature 203:1236-1237

NIAS, A. W. H., GILBERT, C. W., LAJTHA, L. G. and LANGE, C. S., 1965. Clone-size analysis in the study of cell growth following single or during continuous irradiation. Int. J. Radiat. Biol. 9:275-290

OKADA, S., 1970. Radiation biochemistry, Vol. I. New York: Academic Press

OLIVER, R., and LAJTHA, L. G., 1961. Problems of radiosensitivity in mixed cell populations with particular reference to radiotherapy. Br. J. Radiol. 34:659-666

PHILLIPS, R. A. and TOLMACH, L. J., 1965. Anomalous X-ray survival kinetics in HeLa cell populations. Int. J. Radiat. Biol. 8:569-588

PHILLIPS, R. A. and TOLMACH, L. J., 1966. Repair of potentially lethal damage in X-irradiated HeLa cells. Radiat. Res. 29:413-432

PHILLIPS, T. L. and HANKS, G. E., 1968. Apparent absence of recovery in endogenous colony-forming cells after irradiation under hypoxic conditions. Radiat. Res. 33:517-532

POTTEN, C. S. and CHASE, H. B., 1970. Radiation depigmentation of mouse hair: Split-dose experiments and melanocyte precursors (amelanotic melanoblasts) in the resting hair follicle. Radiat. Res. 42: 305-319

POWERS, E. L., 1962. Considerations of survival curves and target theory. Phys. in Medicine and Biology 1:3-28

POWERS, W. E. and TOLMACH, L. J., 1963. A multicomponent X-ray survival curve for mouse lymphosarcoma cells irradiated in vivo. Nature 197: 710-711

POWERS, W. E. and TOLMACH, L. J., 1964. Demonstration of an anoxic component in a mouse tumor cell population by an in vivo assay of survival following irradiation. Radiobiology 83:328-336

PUCK, T. T. and MARCUS, P. I., 1956. Action of X-rays on mammalian cells. J. Exptl. Med. 103:653-666

REINHOLD, H. S. and DEBREE, C., 1968. Tumor cure rate and cell survival of a transplantable rat rhabdomyosarcoma following X-irradiation. Eur. J. Cancer 4:367-374

REVESZ, L. and LITTBRAND, B., 1964. Variation of the relative sensitivity of closely related neoplastic cell lines irradiated in culture in the presence or absence of oxygen. Nature 203:742-744

REVESZ, L., 1968. Medical radiation biology: basic research or applied science? Br. J. Radiol. 41: 12-19

ROSS, D. W. and SINCLAIR, W. K., 1972. Cell cycle compartment analysis of Chinese hamster cells in stationary phase cultures. Cell Tissue Kin. 5: 1-16

SHINOHARA, K. and OKADA, S., 1972. Radiosensitivities of murine lymphoma L5178Y cells in a multicellular colony system. J. Radiat. Res. (Japan) 13:109-114

SINCLAIR, W. K. and MORTON, R. A., 1964. Recovery following X-irradiation of synchronized Chinese hamster cells. Nature 203:247-250

SINCLAIR, W. K., 1965. Hydroxyurea: differential lethal effects on cultured mammalian cells during the cell cycle. Science 150:1729-1731

SINCLAIR, W. K. and MORTON, R. A., 1966. X-ray sensitivity during the cell generation cycle of cultured Chinese hamster cells. Radiat. Res. 29:450-474

SINCLAIR, W. K., 1967. Hydroxyurea: Effects on Chinese hamster cells grown in culture. Cancer Res. 27: 297-308

SINCLAIR, W. K., 1968. The combined effect of hydroxyurea and X-rays on Chinese hamster cells *in vitro*. Cancer Res. 28:198-206

SINCLAIR, W. K., 1968. Cyclic X-ray responses in mammalian cells *in vitro*. Radiat. Res. 33:620-643

STEWART, J. R., HAHN, G. M., YONG, S. J. and PARKER, V., 1968. Chinese hamster cell monolayer cultures. II. X-ray sensitivity and sensitization by 5-bromodeoxycytidine in the exponential and plateau periods of growth. Exptl. Cell Res. 49:293-299

SUBAK-SHARPE, H., BURK, R. R. and PITTS, J. D., 1969. Metabolic cooperation between biochemically marked mammalian cells in tissue culture. J. Cell Sci. 4:353-367

SUIT, H. and URANO, M., 1969. Repair of sublethal radiation injury in hypoxic cells of a C3H mouse mammary carcinoma. Radiat. Res. 37:423-434

SUTHERLAND, R. M., INCH, W. R., McCREDIE, J. A. and KRUUV, J., 1970. A multicomponent radiation survival curve using an in vitro tumor model. Int. J. Radiat. Biol. 18:491-495

SUTHERLAND, R. M., McCREDIE, J. A. and INCH, W. R., 1971. Growth of multicell spheroids in tissue culture as a model of nodular carcinomas. J. Natl. Cancer Inst. 46:113-120

SUTHERLAND, R. M. and DURAND, R. E., 1972a. Radiosensitization by nifuroxime of the hypoxic cells in an in vitro tumor model. Int. J. Radiat. Biol. (in press)

SUTHERLAND, R. M. and DURAND, R. E., 1972b. Hypoxic cells in an in vitro tumor model. Int. J. Radiat. Biol. (in press)

TANNOCK, I. F., 1968. The relation between cell proliferation and the vascular system in a transplanted mouse mammary tumor. Br. J. Radiol. 22:258-273

TANNOCK, I. F., 1970. Population kinetics of carcinoma cells, capillary endothelial cells, and fibroblasts in a transplanted mouse mammary tumor. Cancer Res. 30:2470-2476

TANNOCK, I. F., 1972. Oxygen diffusion and the distribution of cellular radiosensitivity in tumours. Br. J. Radiol. 45:515-524

TERASIMA, T. and TOLMACH, L. J., 1963. Variations in several responses of HeLa cells to X-irradiation during the division cycle. Biophys. J. 3:11-33

THOMLINSON, R. H. and GRAY, L. H., 1955. The histological structure of some human lung cancers and the possible implications for radiotherapy. Br. J. Cancer 9:539-549

THOMLINSON, R. H., 1968. Changes in oxygenation in tumours in relation to irradiation. Front. Radiat. Ther. Onc. 3:109-121

TILL, J. E. and McCULLOCH, E. A., 1961. A direct measurement of the radiation sensitivity of normal mouse bone marrow cells. Radiat. Res. 14:213-222

URTASUN, R. C. and MERZ, T., 1969. X-radiation damage to the hypoxic core and to the periphery of a tumor. An in vivo pilot study. Radiology 92:1089-1091

URTASUN, R. C. and MERZ, T., 1972. In vivo studies of X-irradiation damage and repair in mammalian tumor cells. Radiology 102:707-708

VAN DEN BRENK, H. A. S., 1969. The oxygen effect in radiation therapy. Curr. Top. Radiat. Res. 5: 199-252

VAN PUTTEN, L. M. and KALLMAN, R. F., 1968. Oxygenation status of a transplantable tumour during fractionated radiation therapy. J. Natl. Cancer Inst. 40:441-451

VASILIEV, Ju. M., GELFAND, I. M., GEULSTEIN, V. I. and MALENKOV, A. G., 1966. Interrelationships of contacting cells in the cell complexes of mouse ascites hepatoma. Int. J. Cancer 1:451-462

WIDEROE, R., 1971. Quantitative and qualitative aspects of radiobiology and their significance in radiation therapy. Acta Radiologica 10:605-624

WITHERS, H. R., 1966. The dose-relationship for epithelial cells of skin. Radiology 86:1110-1111

WITHERS, H. R. and ELKIND, M. M., 1969. Radiosensitivity and fractionation response of crypt cells of mouse jejunum. Radiat. Res. 38:598-613

WITHERS, H. R. and ELKIND, M. M., 1970. Microcolony survival assay for cells of mouse intestinal mucosa exposed to radiation. Int. J. Radiat. Biol. 17: 261-267

APPENDIX 1.

THE CONTINUOUS CULTURING APPARATUS

Intercomparison of results obtained with spheroids from different batches may not always be meaningful (compare figure 4.7 with figure 4.6), due to the differences already illustrated in growth patterns (figures 2.2 and 4.3). It was, however, very desirable to study the development of the different subpopulations in the spheroids, and this led to the design of the apparatus of figure A1.1 . The large volume of the flask and the ease of sampling allowed continuous study of growing spheroids, and ensured that at any given time, every spheroid remaining in the flask had an identical history. Thus, it was possible to accumulate data which represented one population of spheroids.

The culture system was 'continuous' in that the magnetic stirring bar did not need to be stopped to execute a medium change or to remove spheroids from the flask. There was thus much less chance of mechanical damage to the spheroids.

Before an experiment, the entire system was assembled and sterilized by autoclaving. Sterile water was then added aseptically to the reservoir (C), and medium introduced into the reservoir (D) by positive pressure sterile filtration. Air plus 3% CO_2 was used

FIGURE A1.1

Schematic diagram of the continuous culturing apparatus used for long-term or large volume experiments. The major components include .22 micron millipore filters (A), the culture vessel (B), sterile water reservoir (C), medium reservoir (D), medium equilibration bottle (E), medium flow regulator (F), three-way stopcock for sampling (G), sampling spout normally immersed in alcohol (H), and T-tubes interconnected to prevent airlocks in the lines during medium replacement (L). A water bath (J) was used to maintain the 37°C growth conditions, and the medium was refridgerated at 4°C in a cold room (N). Any desired atmosphere could be produced by gassing at (M), and the stirring speed was altered as required (see text) by the variable speed magnetic stirrer (K).

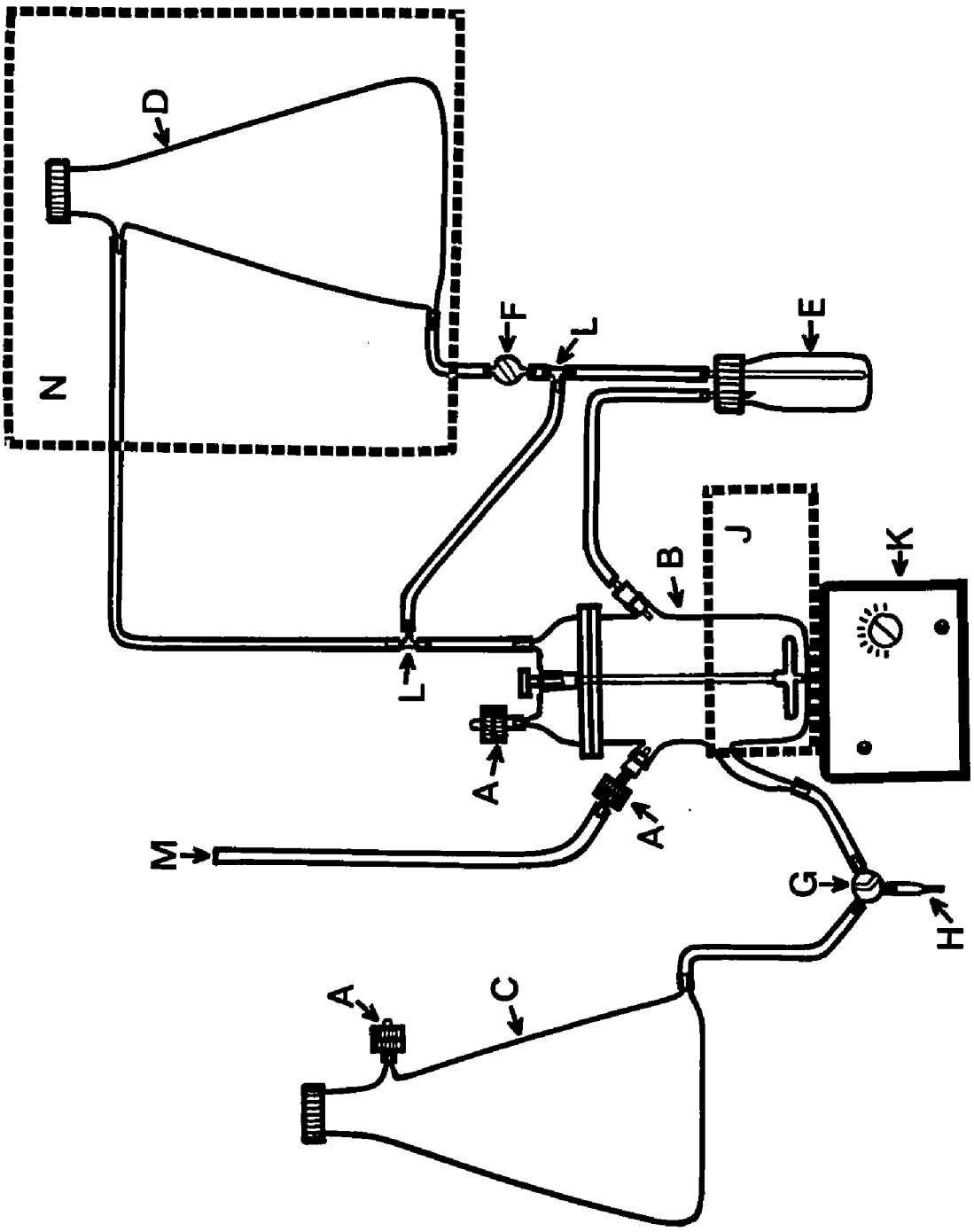
D
N
F
L
E
J
B
K
L'
A
A
M
G
H
A
C

to supply the positive pressure for the filtering process, thus assuring that the medium was maintained at an optimal pH. Single cells were harvested from exponential growth plates, and 5 X 10^6 cells added to 500 ml of BME containing 5% FCS in the culture vessel (B). The complete unit was then moved from the sterile preparation area to a convenient site in the laboratory, and the culture vessel was placed in the water bath (J) at 37°C. The medium reservoir (D) was placed in a refrigerated room (N) at 4°C, to prevent undue degradation of the constituents of the medium. All connections between the culture system and the non-sterile laboratory environment were made through .22 micron millipore filters (A).

The medium (D) and sterile water (C) reservoirs were placed at heights greater than the culture vessel (B) so that none of the operations required pumps to move the fluids. When valve (F) was opened, medium flowed from the reservoir into the equilibration vessel (E). This vessel was normally placed in the water bath (J) at 37°C, to allow the cold (4°C) medium to equilibrate to 37°C before being added to the culture flask. The actual addition of medium to the flask (B) was performed manually by lifting the equilibration vessel (E) out of the water bath and inverting it. The flow rate of the medium was

controlled simply by raising or lowering the vessel (E). The system was designed with a 'shunt' tube (L) so that the air displaced from the culture vessel (B) by the fresh medium would simply enter the equilibration vessel (E). Thus, airlocks were avoided in the system.

Sampling was accomplished by removing the sampling outlet (H) from a sterile alcohol container, flushing the line with sterile water (C) by means of the three-way stopcock (G), and then simply adding medium to the growth vessel from the equilibration vessel (E). The spheroids overflowed into a waiting sterile container. The sample line was then again rinsed with sterile water and the tip replaced in alcohol. Preliminary experiments established that satisfactory sampling was obtained, that is, that agitation found in the medium was sufficient to cause even large spheroids to overflow into the waiting container. Any desired atmosphere could be maintained in the culture vessel by introducing humidified gas at the point (M).

It should again be stressed that identical culture conditions between several batches of spheroids were no easier to obtain in the continuous apparatus; the advantage of this particular apparatus was instead the large volume which allowed analysis of one population of spheroids as they increased in size.

APPENDIX 2.

SURVIVAL CRITERIA AND SURVIVAL CURVE ANALYSIS

A2.1 Survival criteria

Among the more easily recognizable biological effects of ionizing radiations is cell killing, where killing refers specifically to the reproductive death or the loss of unlimited proliferative ability of the cell. In general, this is assayed *in vitro* by exposing the cells to radiation and then inoculating a known number of these cells into petri dishes to which they attach as they grow. After an appropriate interval of time, stainable, surface attached groups of cells visible to the naked eye form. These are termed 'colonies', though perhaps 'clones' would be more accurate since all cells within the colony generally are the progeny of a single cell that survived the initial treatment.

In the case of a dose-effect or survival curve after irradiation, the cells are generally given two treatments--they are separated into single cells with trypsin, and also exposed to various doses of radiation. Assuming that the treatments are independent, their order is unimportant. However, analysis of results requires recognition of both treatments, since usually not all trypsin-treated cells will reattach to dishes and form colonies. The fraction that do, or the number

that form colonies larger than an arbitrarily defined lower limit of size (in this work, the lower limit was taken as the number of cells which formed an easily identifiable colony visible to the naked eye, or about 50 cells), divided by the total number of cells plated is called the plating efficiency or PE. Survival following each dose of radiation is thus determined by counting the number of colonies formed on replicate plates, and dividing by the product of the PE and the number of cells plated. Occasionally, the experiment is not designed to use single cells, and another correction must be made for the multiplicity, or average number of cells per group that was plated or irradiated.

A2.2 Survival curve parameters

The meaning and relevance of several parameters used in the description of survival curves in this thesis are summarized in figure A2.1 where the natural logarithm of survival or the actual surviving fraction plotted on a $\log_{10}$ scale is plotted as a function of the radiation dose. In general, most survival curves start with a slightly negative slope, which becomes more negative with increasing dose. At high doses, the curve becomes linear, indicating that survival is exponentially related to the dose given. The following parameters can be defined:

FIGURE A2.1

Dose-effect or survival curve typically found for mammalian cells, where the logarithm of survival is plotted as a function of the dose. The parameters commonly used to describe such curves are indicated and explicitly defined.

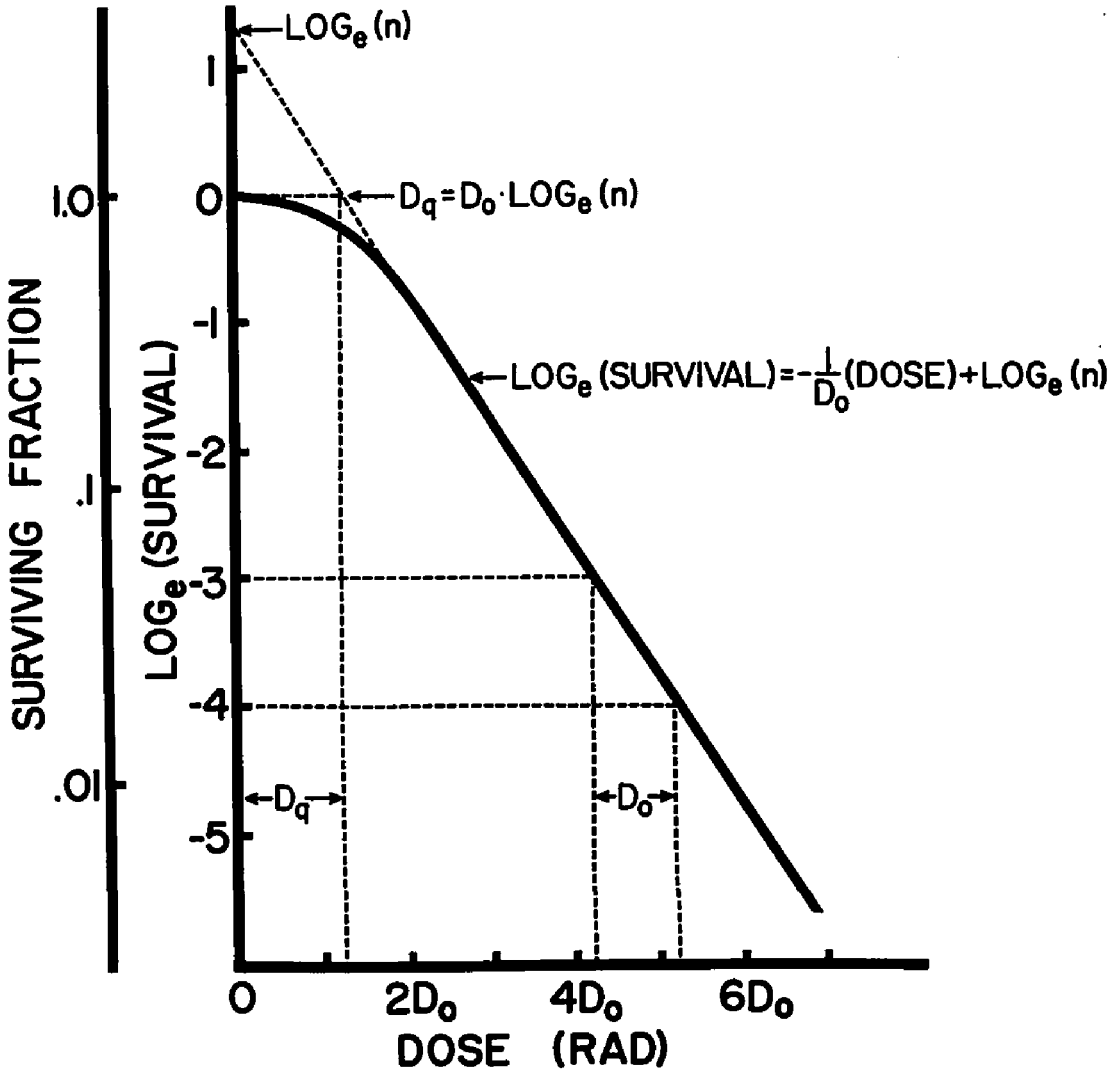
SURVIVING FRACTION
1.0
.1
.01
LOGe (SURVIVAL)
1
0
-1
-2
-3
-4
-5
LOGe (n)
Dq = Do · LOGe (n)
LOGe (SURVIVAL) = -1/Do (DOSE) + LOGe (n)
Dq
Do
0
2Do
4Do
6Do
DOSE (RAD)

(1) D_o: The negative reciprocal of the slope of the linear portion of the curve is generally called the mean lethal dose or D_o. Alternatively, this is the dose of radiation required to reduce survival by a factor 1/e. It is customary to use the slope $1/D_o$ as a measure of the 'radiosensitivity' of the cells, or D_o as a measure of the 'radioresistance'. Thus, treatments which alter the radiosensitivity (and only the radiosensitivity) of a population of cells produce survival curves differing only by a constant factor in the slope, the dose modifying factor or DMF.

(2) n: If the region of exponential survival is extrapolated back to the zero-dose axis, it intersects the ordinate at a value greater than 1.0, which is the natural logarithm of the extrapolation number n (or the actual value n on the $\log_{10}$ scale). The extrapolation number provides one means of quantitation of the capacity for accumulation of sublethal radiation damage, that is, curves with an extrapolation number > 1.0 indicate that damage must be accumulated before radiation kills the cell.

(3) D_q: The width of the shoulder of the survival curve can also be quantitated by the dose at which the extrapolation of the linear portion of the curve intersects the 100% survival axis. This dose is called the

quasi-threshold dose D_q (i.e. wasted radiation since damage is primarily sublethal), and is dependent on both the values D_o and n, i.e.:

$$D_q = D_o \log_e (n).$$

It is thus clear that most survival curves can be characterized simply by the two parameters n and D_o. Mathematical representation of survival curves has not been overly successful. The traditional interpretations of survival curves according to target theory (Powers 1962, Elkind and Whitmore 1967, Fabrikant 1972) have been succeeded by mathematical representations that specifically invoke the concept of repair of radiation damage (Haynes 1966, Calkins 1971, Fischer 1971a and 1971b, Kiefer 1971, Laurie et al 1972), or else suggest that different types of damage may arise (Wideroe 1971) during the irradiation procedure. None of the above models were found to be completely satisfactory in representing the experimental data presented in this thesis, so numerical analysis of the experimental curves had to be limited to determination of the values of n and D_o.

A2.3 Mixed cell populations

As a first approximation, the composite response of a population of cells can be defined by the independent responses of its individual components. Of course, due to

the possibilities of interplay in cells of organized tissue, there may be marked differences in the functional behavior of cells in the integrated, tissue-like environment and those in a single cell suspension. This would further complicate the evaluation or prediction of radiation damage at the population level.

For the purposes of interpretation of results in the present work, the assumption has been made that the complex survival response of the spheroid is due to the sum of the independent responses of the subpopulations. Numbering the subpopulations from 1 to N, and denoting the survival of the i^{th} fraction to be S_i leads to the expression for survival S of the entire population:

$$S = \sum_{i=1}^{N} S_i \ .$$

This interpretation carries the implicit assumption that the response of each subpopulation is adequately described by one survival curve. Using these criteria, figure A2.2 shows the expected survival curves when two populations of cells with survival characterized by curves A and H represent various fractions of the total population. The figure was produced with computer-generated survival curves of the multi target single hit type (Elkind and Whitmore 1967), with the output plotted directly by an x-y plotter unit.

In panel (a), both curves have a D_o of 160 rad, but

FIGURE A2.2

Computer-generated theoretical survival curves for mixed populations of cells. Curves A and H represent survival of each subpopulation alone, and curves B to G represent the curves obtained in mixed populations having type A cells reduced by a factor of 2 in each successive curve. Thus, curves C have the population being 25% type A cells and 75% type H cells, and so on.

Curve		D_o	n
(a)	A	160	128
	H	160	2
(b)	A	280	3.5
	H	140	3.5

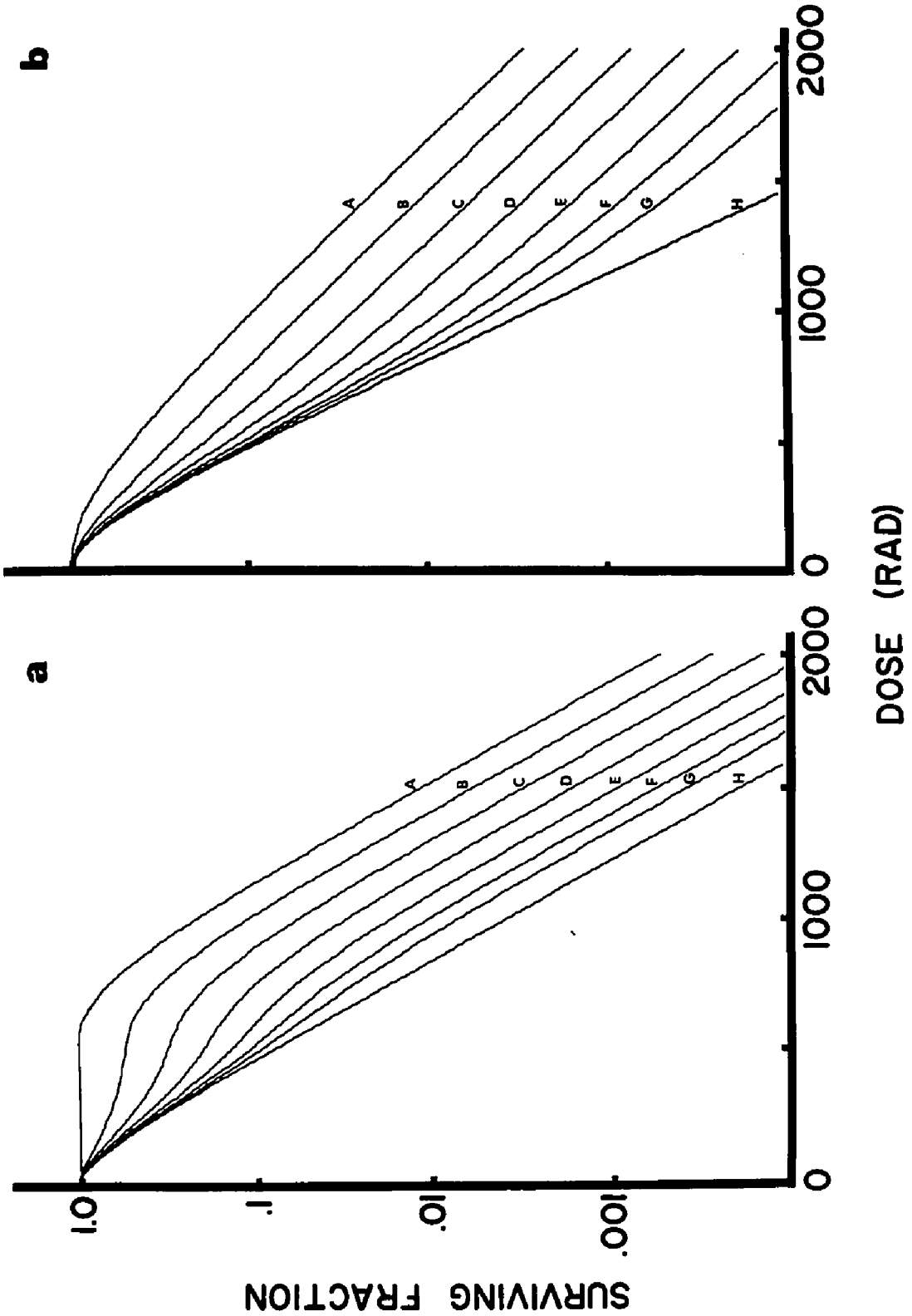
b
a
A
B
C
D
E
F
G
H
0
1000
2000
DOSE (RAD)
SURVIVING FRACTION
1.0
.1
.01
.001

curve A has n = 128, whereas curve H has n = 2.0 . Curve B shows the result if each cell type was 50% of the entire population. In curve C, the population is 25% type A cells; curve D shows the response for 12.5% type A cells, and so on with the fraction of type A cells reduced by a factor of 2 for each curve. For curves B and C, the type H cells contribute only slightly to the net response, so the fraction of cells of type A can immediately be determined from the ratio of the extrapolation numbers of curves B or C with curve A. When type H cells contribute to the final response, as in curves F and G, the ratio of extrapolation numbers does not immediately give the fraction of type A cells.

Figure A2.2b shows the expected radiation survival curves for two populations of cells having different radiosensitivities (D_o's). Both A and H cells have n = 3.5, but D_o = 140 rad for H and 280 rad for the more resistant type A cells. As in panel (a), the proportion of type A cells decreases from 100% by factors of two per curve in curves A to G. It is important to note that the curves diverge, so the contribution due to type H cells decreases with dose, and, at high enough doses, the final component will always determine the survival of only the most resistant (type A) cells. Curve B shows essentially only a reduced extrapolation number, where the type H cells

seemingly do not contribute to the final response. For large enough doses, the fraction of type A cells can always be found by extrapolation of the terminal portion of the curve back to the ordinate and finding the ratio of this extrapolation number to that of curve A.

These curves also reflect the difficulties in interpretation of results simply on the basis of survival curves. Resolution of data is often not adequate to show that curves reflect mixed populations (e.g. curves for asynchronous populations of cells). Thus, erroneous interpretations of capacity for accumulation and repair of sublethal damage may easily be made, unless other data is available to help define the population of cells observed. All survival curves presented in this thesis have thus been preceeded by morphological and cell kinetic studies that characterize the population of cells.

Another requirement in the analysis of survival curves for mixed cell populations is that PE's must be essentially equal for all populations. For example, consider curves B and H of figure A2.2b, with the PE of type A cells reduced to 50% while that of the type H cells remains at 100%. Of the viable cells, type A cells are then one third of the population, and the curve for the mixed population would simply be exponential with $n = 1.0$ and $D_o = 280$ rad. A more extreme case occurs when, for

some reason, the type A cells do not plate out. Then, despite the fact that the true survival curve for an equal mixture of each cell type is curve B, the observed curve would be identical to curve H. These considerations show the importance of characterizing both the population types and the PE's of each. In section 4.3.3, it was shown that different PE's in different regions of the spheroid could not be demonstrated experimentally. Even if viability were slightly less in the internal (hypoxic) regions, the only effect that would be noticed on the survival curves would be a slight survival increase at high doses.

APPENDIX 3.

CELLULAR RECOVERY FROM SUBLETHAL DAMAGE

A3.1 Recovery processes

The characteristics of radiation survival curves for most mammalian cells, with the shoulder region at low doses, suggests that radiation damage must be accumulated before it is expressed as cell killing. The ability of the cell to accumulate sublethal damage is thus related to the shoulder width (D_q). Another process, called 'repair' of sublethal damage, is observed for most cells that have this type of survival curve (Elkind and Whitmore 1967, Okada 1970).

The conceptual basis of 'repair' of sublethal damage is relatively simple, and follows immediately from examination of survival curves. When a cell is given a total dose of 2D rad, the survival found is generally much less than the square of the survival after only the first half the dose, D. This indicates that the second half of the 2D dose does more damage and reduces the survival more than does the first D rad, since during the first part of the exposure, the cells gradually lose the ability to accumulate sublethal damage. However, the cells that survive the first part of the exposure, say a total of D rad, might be expected to regain this capacity for accumulation of sublethal damage if some

recovery time were permitted between the doses. This can in fact be demonstrated experimentally, and represents the classical 'repair' of sublethal radiation damage (Elkind and Sutton 1960, Elkind et al 1961).

There is a question of semantics that must be resolved in any discussion about this process. 'Repair' may in fact be a misnomer, in that cells plated after the first dose of radiation do not increase their surviving fraction with time, i.e. the 'repair' is not in fact accompanied by a survival increase. The event that does occur is reflected in the cellular response to the second dose of radiation--that is, the cell regains the ability to accumulate sublethal damage. Thus, in the context of this thesis, 'recovery' explicitly refers to the renewed ability of the cell to accumulate sublethal damage on subsequent exposure to radiation. This concept is in agreement with the model proposed by Laurie et al (1972) as well as the previously-discussed concept of the functional energy pool of the cell introduced in this work.

A3.2 Experimental demonstration of recovery

Figure A3.1 shows the classical recovery curve obtained when exponentially growing, asynchronous V79-171b Chinese hamster cells were given two doses of 600 rad each

FIGURE A3.1

Survival of cells grown on petri dishes as a function of time between two doses of 600 rad each. Cells in panel (a) were metabolically active and proliferating at 37°C, whereas the cells of panel (b) were maintained at 24°C to prevent proliferation. Plating efficiencies of 88% and 92% respectively were found. The dose rate used was 121 rad/min.

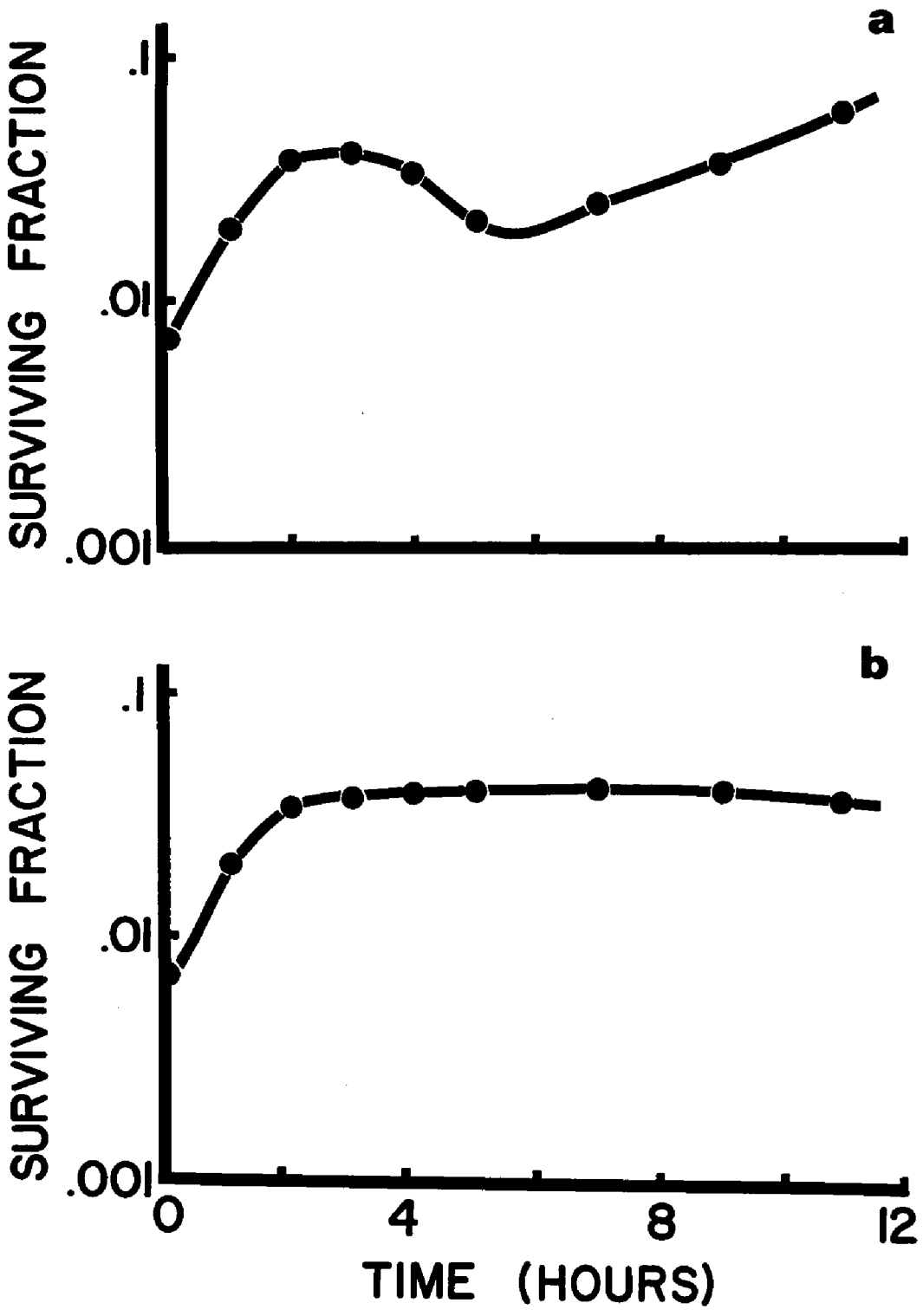
a
SURVIVING FRACTION
.1
.01
.001
b
SURVIVING FRACTION
.1
.01
.001
0
4
8
12
TIME (HOURS)

with various intervals between the doses. In panel (a), the cells were maintained at 37°C between doses. The initial increase in survival, usually attributed to repair of sublethal damage, can be more accurately interpreted as the return of the cellular ability to accumulate sublethal radiation damage. However, the first dose of radiation had a higher probability of killing the more sensitive cells, thus producing a partially synchronous population of the most resistant (late S phase) cells. As these surviving cells then progressed into more radiation sensitive parts of the cell cycle (G_2 and M) the net survival decreased, then increased again after mitosis due to progression and multiplication of the viable cells. Interpretation of these 'late' effects is thus more complicated due to this cellular progression and division.

It is, however, much easier to interpret results if cell progression is inhibited so that the cells do not progress through the cell cycle after the first dose of radiation. One method of inhibiting progression without affecting recovery (Elkind et al 1961, Belli and Bonte 1963, Elkind and Whitmore 1967, Arlett 1970), is the use of suboptimal growth temperatures. As shown in figure A3.1b, cells irradiated and held at room temperature between doses show an equal initial survival in-

crease, but no subsequent cellular progression. Again, the radiation produced a partial synchrony of the surviving cells.

A3.3 Quantitation of recovery

Repair of sublethal radiation damage has usually been quantitated by exposing cells to a 'conditioning' dose of radiation sufficiently large to reduce survival to the exponential region of the survival curve, and then obtaining the split dose survival ratio at various times after the initial dose. The enhanced capacity for accumulation of sublethal damage in the spheroids, reflected by the broad-shouldered survival curves, required prohibitively large conditioning doses to obtain survival in the exponential region. However, if a population of cells is synchronous, and if progression is inhibited so that the same cell cycle phase is maintained, the relative capacity for recovery of the ability to accumulate sublethal damage can easily be compared even for radiation doses on the shoulders of the survival curves.

As shown in figure A3.2, a dose D reduces survival to S_D. If the cells then totally regain the ability to accumulate sublethal damage, a subsequent dose D will again reduce the survivors to a fraction S_D, so the net

FIGURE A3.2

Theoretical derivation of the repair capacity or recovery. In short, the recovery is defined to be the ratio of the survival increase noted when doses are separated by a time T' ($S_{T'} - S_{2D}$) to the survival increase expected if the cells had completely regained the ability to accumulate sublethal damage ($S_D^2 - S_{2D}$). The base-line in each case is the survival measured after a prompt dose of 2D rad. A detailed explanation of the derivation of this expression is presented in the text.

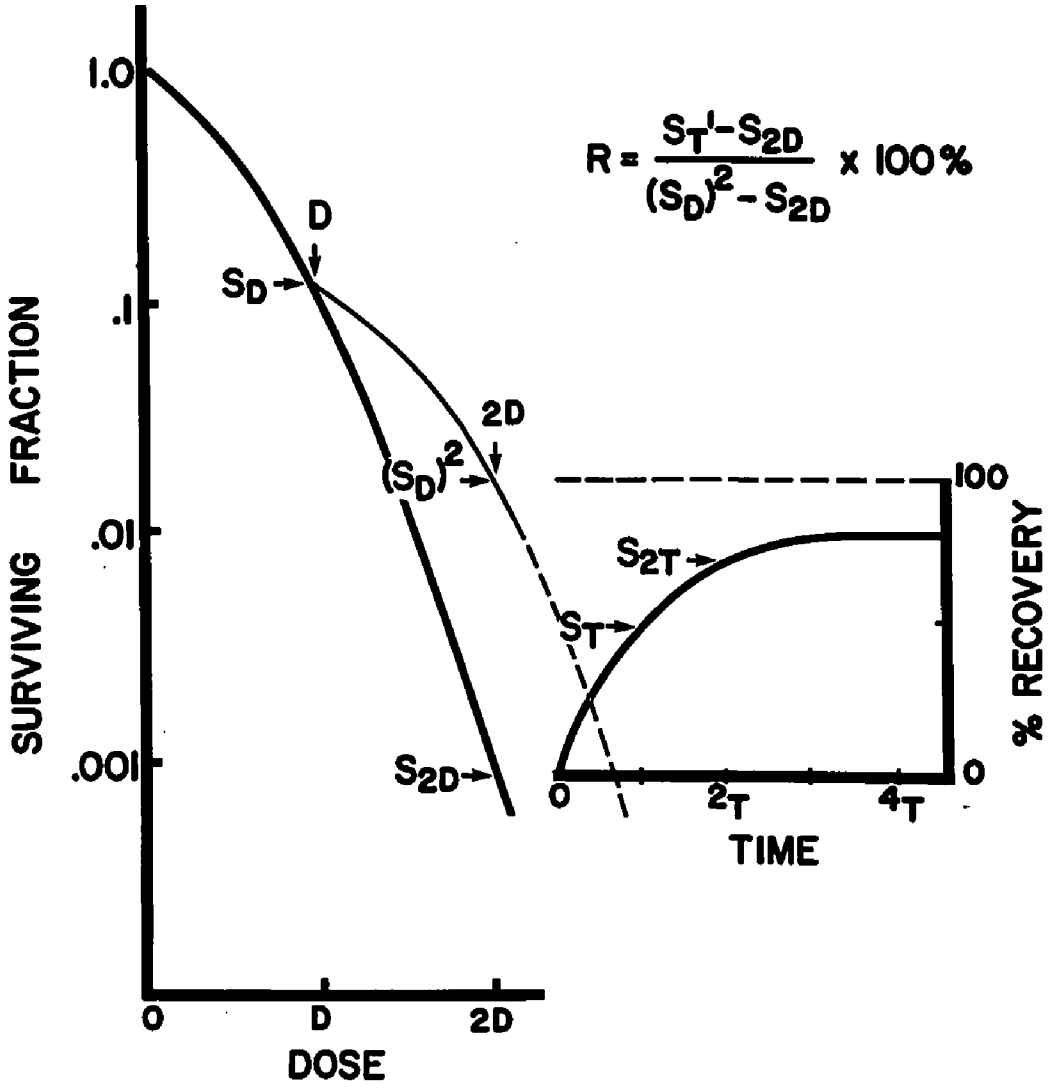
1.0
.1
.01
.001
SURVIVING FRACTION
D
S_D
2D
$(S_D)^2$
S_{2D}
$R = \frac{S_T^1 - S_{2D}}{(S_D)^2 - S_{2D}} \times 100\%$
100
S_{2T}
S_T
0
% RECOVERY
0
2_T
4_T
TIME
0
D
2D
DOSE

survival is $(S_D)^2$. However, if the dose 2D is given in a single increment, the measured survival is S_{2D}. In practise, the survival after two increments of dose D separated by a time T will be measured as S_T. Knowing S_D, S_{2D} and $S_{T'}$, it follows that repair capacity of the cells, or recovery (R), is given at any time T' by:

$$R = \frac{S_{T'} - S_{2D}}{(S_D)^2 - S_{2D}} \quad .$$

More simply, this is a comparison of the survival following two exposures to the survival expected if full recovery had occurred. This normalizing procedure is more meaningful than the usual split dose ratio which is usually dose dependent (see Malone et al 1971), and may depend on the type of damage induced (Elkind and Kano 1971). A similar derivation (Lange 1970) can also be extended to allow for subsequent cell progression through the cell cycle.

It must be noted that the information given by the recovery capacity or R value defined in this way is not the same information that is given by the complete two-dose curve. The recovery curve shows only the relative return of the shoulder of the survival curve with time, and does not indicate any information about the absolute size of that shoulder. Thus, it is very conceivable that cells with a high capacity for accumulation

of sublethal damage may only partially recover after irradiation according to this criteria, but may still have a much wider survival curve shoulder than would completely-recovered cells which initially had only a small capacity for accumulation of sublethal damage.

APPENDIX 4.

OXYGEN IN SPHEROIDS

A4.1 Introduction

The importance of molecular oxygen in modifying the radiosensitivity of mammalian cells has been of interest for many years, and has recently been reviewed in several books (Elkind and Whitmore 1967, Okada 1970, Fabrikant 1972). Chapter IV of this thesis indicated the significance of oxygen in determining the radiation response of cells in the spheroid model. A more detailed study of the influence of oxygen on growth characteristics of the spheroid, and particularly the role of oxygen in the development of central necrosis has already been published (Sutherland and Durand 1972b).

In that study, it was demonstrated that oxygen was probably the critical metabolite which, when unavailable to the internal cells, led to the formation of central necrosis. This was determined on the basis of two results: oxygen deprivation resulted in a more rapid development of central necrosis than did deprivation of other nutrients, and secondly, the necrotic volume was found to vary inversely with oxygen concentration in the growth medium. Specifically, under otherwise identical and optimal growth conditions, a reduction of the available oxygen by a factor of four (20% O_2 in air to 5% O_2

in N_2) resulted in a decrease of the viable rim of spheroid cells by a factor of two (see section 4.2 and Sutherland and Durand 1972b).

A4.2 Diffusion theory

Diffusion of a solute is such that the concentration of that solute (C) is defined by:

$$\nabla^2 C = 0 \qquad (1)$$

However, with diffusion coefficient D and with the solute consumed at the rate K, the equation becomes:

$$\nabla^2 C = K/D \qquad (2)$$

It is thus possible to solve the diffusion equation (2) to determine whether the observed morphological and radiation survival characteristics of the spheroid model could be predicted theoretically. Two questions were of particular concern: did development of central necrosis agree theoretically with oxygen diffusion calculations, and was the anoxic population likely to be altered by the irradiation procedure?

A4.3 Calculation of hypoxic fraction

Using the symbols and units shown in Table 3, the diffusion equation (2) can be solved in spherical coordinates for concentration C as a function of the radius r. The oxygen concentration is thus defined to be 0 for $r \leq b$ and to be C_o for $r \geq a$. Then:

TABLE 3.

Symbols and units for oxygen diffusion calculations.

	Symbol	Value[1]	Units
Diffusion coefficient	D	2.0×10^{-5}	$cm^2\ sec^{-1}$
Concentration of oxygen	C	-	$mole\ cm^{-3}$
In air-saturated water	C_o	2.5×10^{-7}	$mole\ cm^{-3}$
Consumption of oxygen	K	-	$mole\ sec^{-1}$
Cellular	K_c	6.55×10^{-17} [2]	$mole\ cm^{-3}\ sec^{-1}\ cell^{-1}$
Radiochemical	K_r	5.0×10^{-11} [3]	$mole\ cm^{-3}\ rad^{-1}$
Spheroid radius	a	2.0×10^{-2}	cm
Spheroid necrosis radius	b	2.0×10^{-3}	cm
Medium depth	h	-	cm
Flow of oxygen (planar)	Q	-	$mole\ cm^{-2}\ sec^{-1}$

[1] Numerical value of constants used in calculations

[2] Dependent on cell density; multiply by number of cells/cm^3

[3] Dependent on dose rate; multiply by number of rad/sec

$$\frac{1}{R^2}\frac{d}{dR}\left(R^2\frac{dC}{dR}\right) = \frac{K}{D} \qquad (3)$$

or $$\frac{d^2C}{dr^2} + \frac{2}{r}\frac{dC}{dr} = \frac{K}{D}$$

letting $p = \frac{1}{r}\frac{dC}{dr}$; then $\frac{dC}{dr} = rp$

and $$\frac{d^2C}{dr^2} = r\frac{dp}{dr} + p$$

for r = b, dC/dr = 0

so $$r\frac{dp}{dr} = \frac{K}{D} - 3p$$

$$\int_{p=0}^{p}\frac{dp}{K/D - 3p} = \int_{r=b}^{r}\frac{dr}{r} \qquad (4)$$

$$-\frac{1}{3}\log\left(\frac{K/D - 3p}{K/D}\right)_0^p = \log\left(\frac{r}{b}\right)_b^r \qquad (5)$$

so $$\frac{K}{D} - 3p = \frac{K}{D}\frac{b^3}{r^3} \qquad (6)$$

then $$p = \frac{K}{3D}\left(1 - \frac{b^3}{r^3}\right)$$

$$\frac{1}{r}\frac{dC}{dr} = \frac{K}{3D}\left(1 - \frac{b^3}{r^3}\right) \qquad (7)$$

$$\frac{dC}{dr} = \frac{K}{3D}\left(r - \frac{b^3}{r^2}\right) \qquad (8)$$

$$\int_{C}^{C_o} dC = \frac{K}{3D} \int_{r}^{a} \left(r - \frac{b^3}{r^2} \right) dr \qquad (9)$$

$$\text{and} \qquad C_o - C = \frac{K}{3D} \left(\frac{a^2 - r^2}{2} + \frac{b^3}{a} - \frac{b^3}{r} \right) \qquad (10)$$

Thus, expression (10) gives the concentration C at any radius r. This can be simplified by applying appropriate boundary conditions:

$$\text{for } r = b \; ; \quad C = 0$$

$$\text{then} \qquad C_o = \frac{K}{3D} \left(\frac{a^2 - b^2}{2} + \frac{b^3}{a} - \frac{b^3}{b} \right) \qquad (11)$$

$$= \frac{K}{3D} \left(\frac{a^2}{2} - \frac{3b^2}{2} + \frac{b^3}{a} \right) \qquad (12)$$

$$= \frac{K}{6aD} \left(a^3 - 3ab^2 + 2b^3 \right) \qquad (13)$$

$$= \frac{K \left(a + 2b \right)}{6aD} \left(a - b \right)^2 \qquad (14)$$

$$\text{and} \quad (a - b) = \sqrt{\frac{6aDC_o}{K \left(a + 2b \right)}} \qquad (15)$$

Equation (15) thus relates the thickness of the viable rim (a - b) to the external oxygen concentration C_o and the consumption K. For b = 0, that is, the spheroid radius at which necrosis first appears, the equation reduces to:

$$a_n = \sqrt{\frac{6DC_o}{K}} \qquad (16)$$

For very large spheroids, where the value of b approaches that of a, then:

$$(a - b)_1 = \sqrt{\frac{2DC_o}{K}} \qquad (17)$$

Note that the limiting diffusion radius of (17) in fact is the diffusion depth into a planar region of tissue.

The last two equations indicate that the viable rim thickness decreases as the spheroids enlarge, and thus cannot simply be expected to reflect changes in oxygenation status. However, for small necrotic radii, that is, when b tends to zero, it follows that the rim $a_n \propto \sqrt{C_o}$ as found experimentally (Section 4.2.3 and Sutherland and Durand 1972b).

Further evidence for oxygen being the critical metabolite can be found by solving equation (16) for the oxygen consumption K, knowing that necrosis was first observed under optimal growth conditions for spheroids of 365 micron diameter (see Table 1). Solution of (16) gives $K = 6.55 \times 10^{-17}$ mole sec^{-1} per cell. Numerous experiments on cell respiration have been reported (Froese 1962, Longmuir 1966, Boag 1969), and probably the most accurate work by Froese showed that ascites tumor cells had an oxygen consumption of 2.5×10^{-17} mole sec^{-1}

per cell. Other results vary as much as an order of magnitude. Since Froese's cells were smaller (5 micron radius) than the Chinese hamster cells (6-7 micron radius), and since oxygen consumption varies approximately linearly with cell volume, the theoretically calculated value may be in excellent agreement with experimental results.

A4.4 Radiation studies

Several potential problems are introduced in the radiation procedures. The spheroids were irradiated in a thin layer of unstirred medium on the lower surface of glass vessels. Although air was vigorously flushed through the vessels, the high cell density of the spheroids and the thickness of the covering medium suggested that additional hypoxia might be induced during the irradiation procedure. This possibility was investigated theoretically by assuming the worst possible irradiation conditions, and calculating oxygen profiles in the spheroids based on these assumptions.

Oxygen was thus required to diffuse from the surface of the liquid down to the spheroid (in the presence and absence of radiation-induced binding of free oxygen), and then to diffuse into the spheroid. The radiochemical elimination of oxygen was assumed to occur at the rate shown in Table 3, as calculated and measured by Boag (1969).

The oxygen concentration C at any position d beneath the surface of the liquid is easily found by solving (1):

$$C = C_o - \frac{Qd}{D} \qquad (18)$$

The solute flow Q must be adequate to supply the spheroids at the bottom of the vessel, and hence is dependent upon the spheroid size (number of cells) as well as the density of the spheroids (number per cm^2 on the surface of the radiation vessel). In addition, radiation-induced binding of oxygen required a larger net flux of O_2 to ensure that adequate quantities of oxygen reached the spheroids. To simplify the calculation, no concentration gradients were postulated in the horizontal direction, that is, only vertical concentration gradients were permitted.

The oxygen profiles through any spheroids were then calculated by a computer, using equation (18) to define the oxygen concentration at the spheroid surface in equation (10). Several conditions of spheroid crowding, depth of medium, spheroid sizes and radiation dose rates were investigated for equilibrium conditions, and typical results for some of these conditions are shown in figures A4.1 to A4.3 . Necrotic cells, as observed by histological techniques, are indicated by Ø. Other numbers represent the upper limit of oxygen available in a given

FIGURE A4.1

Theoretical prediction of oxygen tensions in 400 micron diameter spheroids resting on a planar surface and with unstirred medium of the indicated depth in the vessel. Observed central necrosis is shown by Ø; actual oxygen concentration in parts per million is $_2^{N-1}$ X 1000 ppm, where N is the plotted number. Effects of high spheroid density are seen by comparison of (b) with (a). All cells without more than 1000 ppm oxygen would be expected to show a hypoxic radiation response (i.e. those cells in the regions labelled 1 in the spheroids).

a

MEDIUM DEPTH: .400IMM
SPHEROID DENSITY: 1/CM^2
DOSE RATE: 0 RAD/MIN

HYPOXIC FRACTION: 8.8%

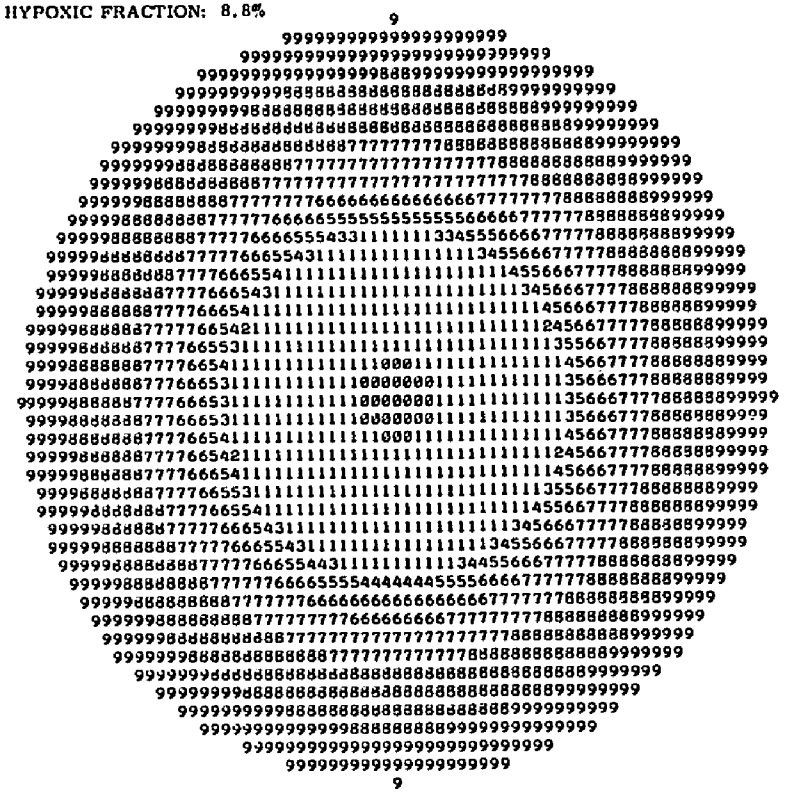

b

MEDIUM DEPTH: .400IMM
SPHEROID DENSITY: 100/CM^2
DOSE RATE: 0 RAD/MIN

HYPOXIC FRACTION: 64%

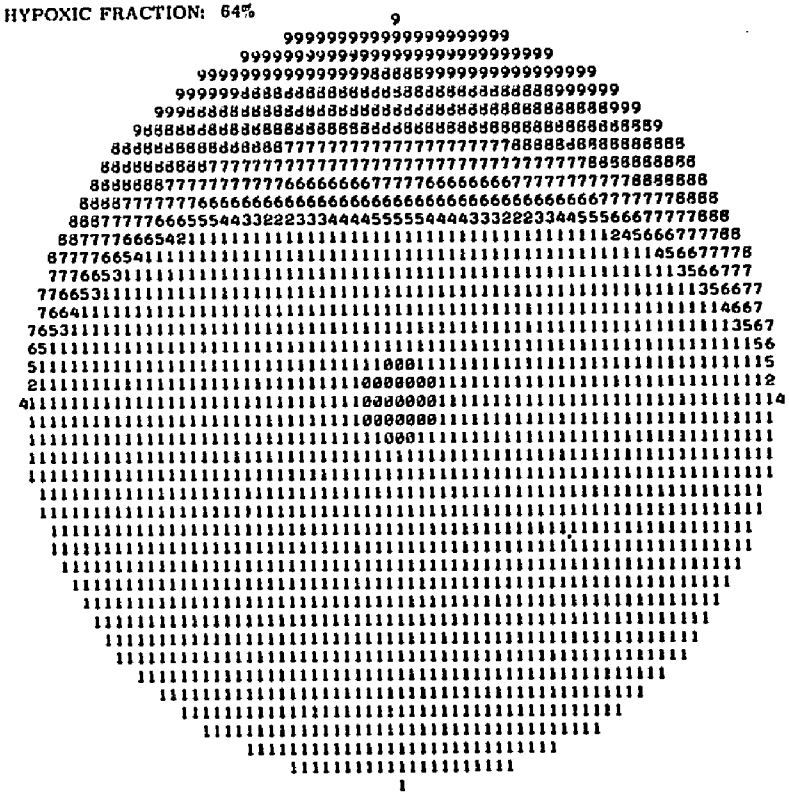

region, where oxygen concentration can be read directly as $_2^{N-1}$ X 1000 ppm. The lower limit of oxygenation shown was chosen to be 1000 ppm, as cells were expected to respond to radiation as though completely anoxic for this and lower oxygen concentrations (Elkind and Whitmore 1967, Okada 1970, Koch 1972). These cells were referred to as hypoxic.

Under optimal conditions of only one spheroid per square cm in the vessel and the medium layer only .1 micron thicker than the spheroids (spheroid diameter was 400 micron, as this included enough cells that central necrosis was well defined and yet was expected to have only a small hypoxic fraction), a hypoxic fraction of about 8% was computed as in figure A4.1a. However, merely increasing the spheroid density to 100 per cm^2 with the same depth of medium resulted in almost all cells in the spheroid becoming severely hypoxic as a hypoxic fraction of 65% was found in figure A4.1b.

Oxygen profiles under typical radiation conditions are shown in figure A4.2, where 5 spheroids per cm^2 were placed in a layer of medium 1.0 mm deep. Comparing the hypoxic fraction of the spheroid in figure A4.2a with optimal conditions (figure A4.1a) shows that the increased spheroid density, as well as the deeper layer of medium reduces the oxygen available to the spheroids, and in turn

FIGURE A4.2

Theoretical prediction of oxygen tensions in spheroids as in figure A4.1 . Panel (a) indicates the additional hypoxia present at a higher density in a greater depth of fluid (compare with figure A4.1a). The effects of irradiation at the usual dose rate of 150 rad/min are shown in panel (b).

a

MEDIUM DEPTH: 1. MM
SPHEROID DENSITY: 5/CM^2
DOSE RATE: 0 RAD/MIN

HYPOXIC FRACTION: 20%

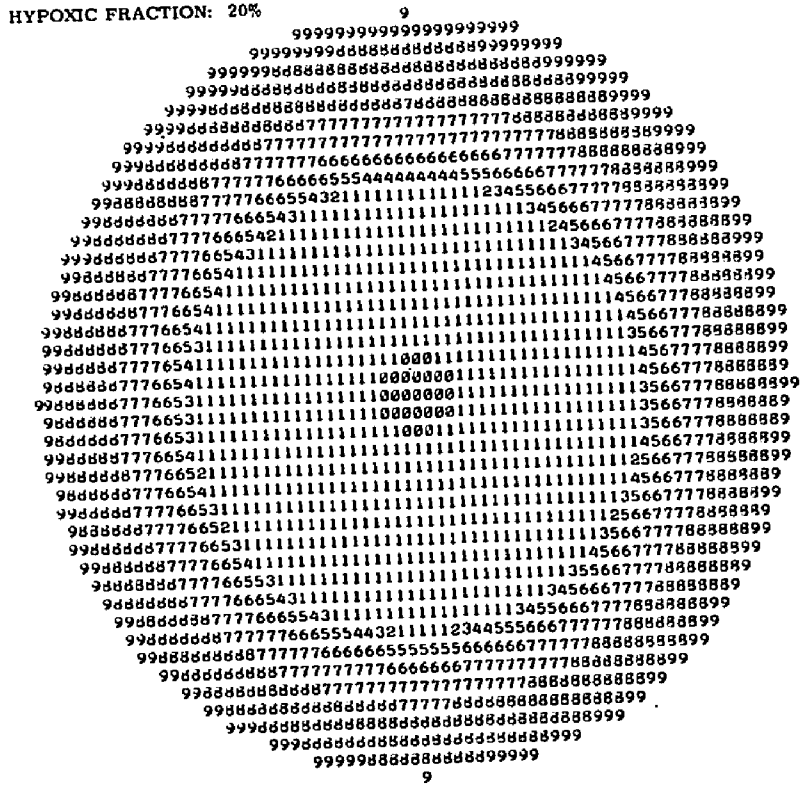

b

MEDIUM DEPTH: 1. MM
SPHEROID DENSITY: 5/CM^2
DOSE RATE: 150 RAD/MIN

HYPOXIC FRACTION: 22%

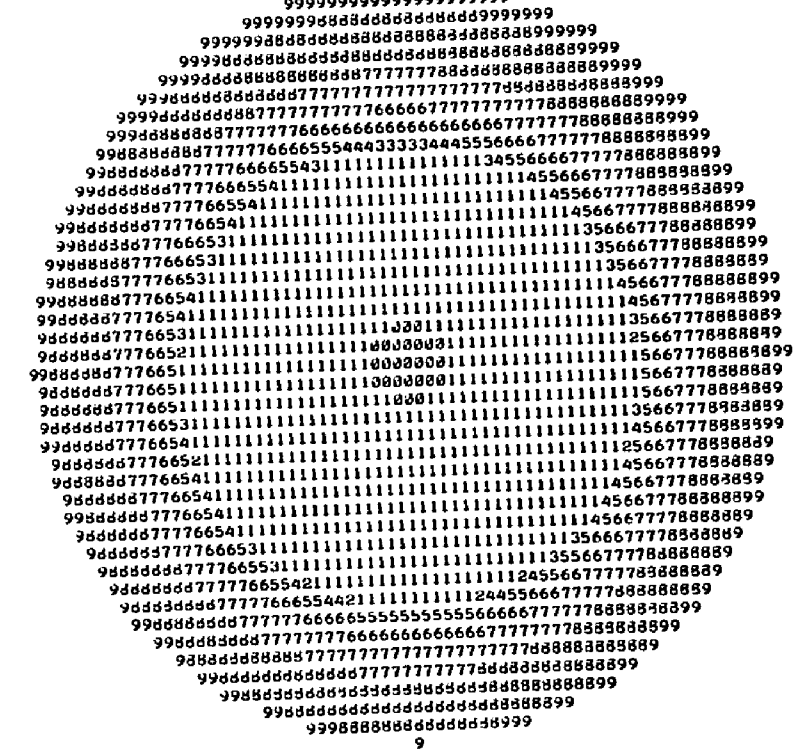

increases the hypoxic fraction to about 20%. The typical radiation dose rate of 150 rad/min had little additional effect on the spheroids, increasing the hypoxic fraction by only 2% (figure A4.2b). Thus, under typical irradiation conditions, very little hypoxia was induced by the irradiation.

In contrast, increasing the number of spheroids to 15 cm^{-2} in 1.0 mm of medium led to a hypoxic fraction of about 55% when the spheroids were irradiated at the same dose rate (figure A4.3a). The effect of higher dose rates is shown in figure A4.3b, where a dose rate of 10 times higher was used. Under these conditions, and a spheroid density comparable to the usual conditions, a hypoxic fraction of only 34% was found. These figures thus suggested that spheroid density was much more important than radiation dose rate in increasing the yield of hypoxic cells in the spheroid.

Comparison of figures A4.2a and A4.1a, that is, oxygen concentration profiles in spheroids under optimal conditions as compared to the more crowded conditions generally used for radiation experiments may indicate that some problems were introduced. In fact, the irradiation conditions probably were much better than in the theoretical calculations for a number of reasons. The vigorous flushing of the vessels with humidified gas pro-

FIGURE A4.3

Theoretical prediction of oxygen tensions in spheroids as in figure A4.1 . Panel (a) indicates the additional hypoxia present when spheroids are irradiated at a higher density (compare with figure A4.2b). The effects of even a ten-fold increase in radiation dose rate are seen to be small in panel (b) in comparison to cell crowding effects.

a

MEDIUM DEPTH: 1. MM
SPHEROID DENSITY: 15/CM^2
DOSE RATE: 150 RAD/MIN

HYPOXIC FRACTION: 55%

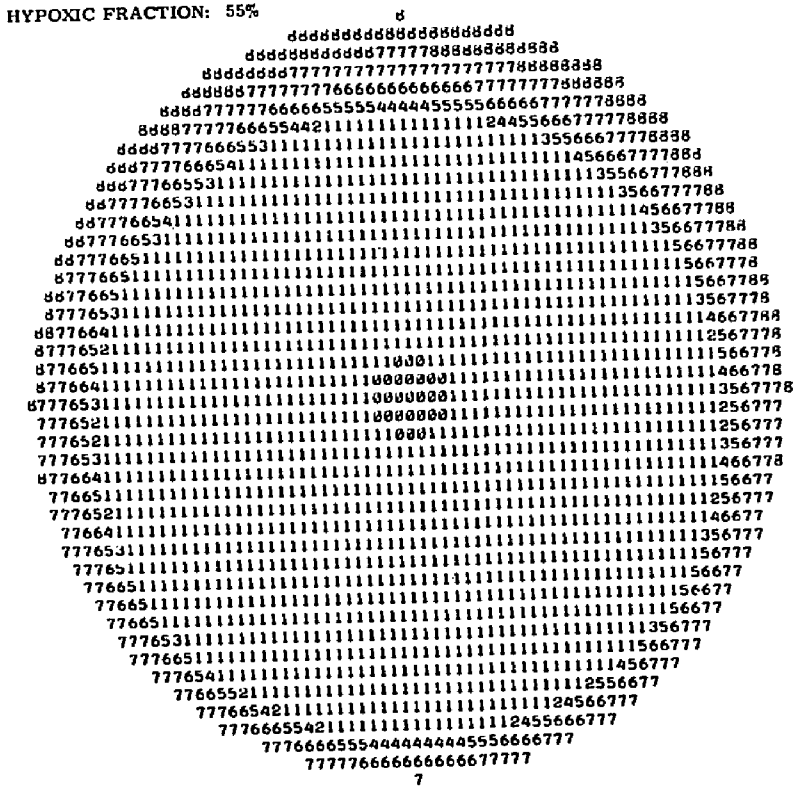

b

MEDIUM DEPTH: 1. MM
SPHEROID DENSITY: 5/CM^2
DOSE RATE: 1500 RAD/MIN

HYPOXIC FRACTION: 34%

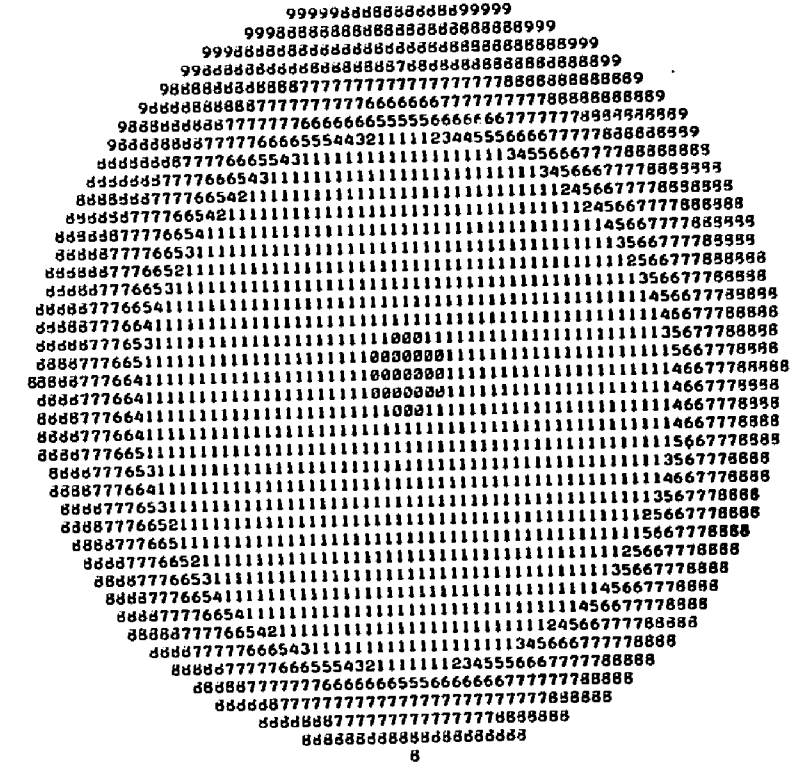

duced turbulence in the medium, which would facilitate transfer of oxygen, and would reduce diffusion gradients. Spheroids were generally used at sizes smaller than in the calculations shown, so total oxygen consumption would have been less. It was assumed that all cells were using oxygen at the same rate, despite the fact that the internal, oxygen-starved cells were obviously not consuming it. In addition, as cells become hypoxic, oxygen consumption decreases, adding a degree of self-regulation to the system. All calculations were for equilibrium conditions, which would develop only slowly during the actual radiation procedure, and would be a factor only in relatively long irradiations. Control experiments did in fact show that reduction of the volume of medium did not increase survival, again suggesting that the medium was agitated sufficiently to maintain equilibration with the appropriate atmosphere, and thus that no additional hypoxia was introduced in the irradiation procedure.

A4.5 Discussion

The relevance of this theoretical discussion is twofold. One important result can be seen from examination of figure A4.1a, where it can be seen that there is a very rapid transition from relatively good oxygenation (5-6 in figure) to very poor oxygenation (1). Thus, in terms of radiosensitivities, only a very small number of

cells would be expected to behave as a 'partially' hypoxic population, due to the well known, critical dependence of survival on oxygen tension (Elkind and Whitmore 1967, Koch 1972). Secondly, consideration of the worst possible conditions shows emphatically that growth and irradiation conditions must be monitored and designed to maintain equilibration of all parts of the growth medium with the appropriate external atmosphere. In general, these considerations indicate that the influence of oxygen on spheroid cell hypoxia is modified much more by cellular respiration that accompanies the high cell densities in the spheroids than by radiation-induced removal of the oxygen.